Development of bio-analytical methods for the quantitative and qualitative analysis of labelled peptides and proteins via hyphenation of chromatography and mass spectrometry

Dissertation

zur Erlangung des Doktorgrades
der Mathematisch-Naturwissenschaftlichen Fakultät
der Christian-Albrechts-Universität zu Kiel

in einem binationalen Promotionsverfahren mit der
Université de Pau et des Pays de l'Adour
in Pau, Frankreich

Vorgelegt von

Angela Sarah Holste

Kiel, 2013

Erster Gutachter	Prof. Dr. Andreas Tholey
Zweiter Gutachter	Prof. Dr. Dirk Schaumlöffel

Tag der mündlichen Prüfung: 24. Februar 2014

Zum Druck genehmigt :

Gez. (Prof. Dr. Wolfgang J. Duschl), Dekan

Ich versichere hiermit, dass diese Abhandlung, abgesehen von der Beratung durch die Betreuer, nach Inhalt und Form meine eigene Arbeit darstellt. Sie wurde weder ganz, noch zum Teil schon einmal an anderer Stelle im Rahmen eines Prüfungsverfahrens vorgelegt. Ausgewiesene Teile der Arbeit wurden in einem internationalen Wissenschaftsmagazin veröffentlicht. Diese Arbeit ist unter Einhaltung der Regeln guter wissenschaftlicher Praxis der Deutschen Forschungsgemeinschaft entstanden.

Kiel, den 18.12.2013

Angela Holste

Table of contents

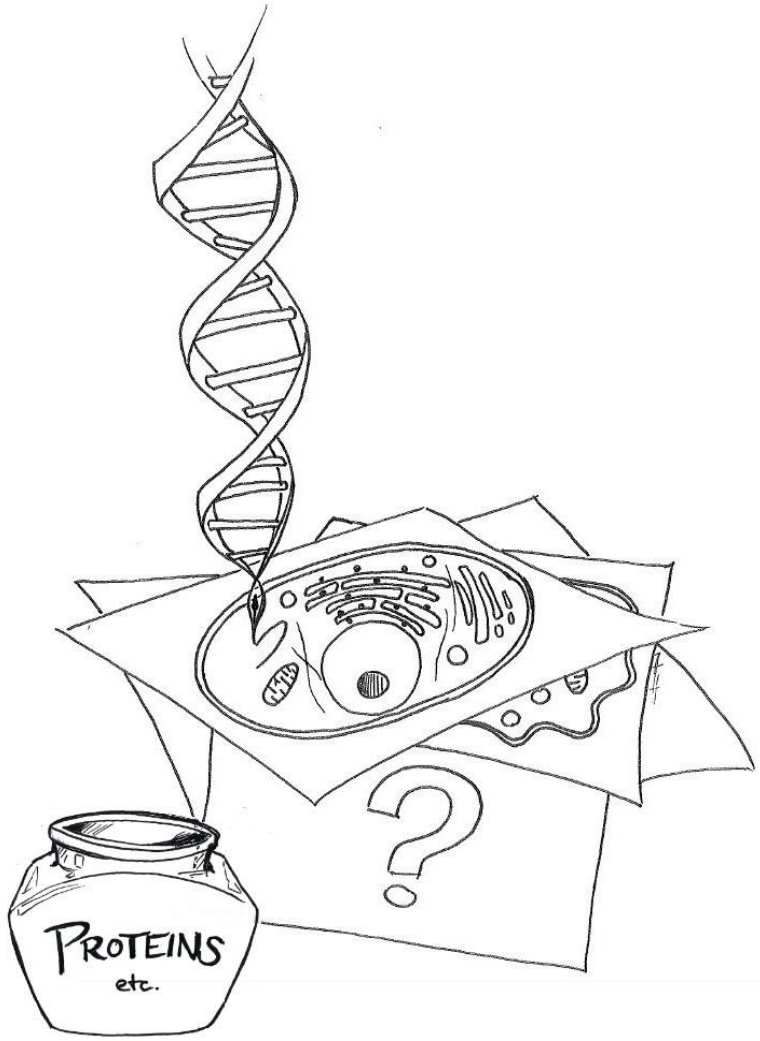

"Proteins embody the active life of cells,
while nucleic acids represent only plans.

There is more to paella than the recipe,
more to Bach than ink on paper,
and more to a society than its code of laws."

Anderson & Anderson 1998

Zusammenfassung

Diese Dissertation entstand im Rahmen einer Cotutelle zwischen der Université de Pau et des Pays de l'Adour (UPPA) in Pau, Frankreich und der Christian-Albrechts Universität zu Kiel (CAU), Deutschland. Während dieser internationalen Zusammenarbeit wurden bioanalytische Methoden für die quantitative wie qualitative Analyse markierter Peptide und Proteine erarbeitet. Die Arbeiten basierten auf der Kopplung von Chromatographie und Massenspektrometrie.

Peptide und Proteinverdaue wurden nach einem optimierten Protokoll mit DOTA-basierten Verbindungen lanthanid-markiert. Die Separation auf Peptidebene wurde mittels IP-RP-nanoHPLC durchgeführt. Komplementäre Datensätze wurden mittels MALDI-MS zur Peptidindentifizierung und mittels ICP-MS zur Quantifizierung erstellt. In diesem Rahmen wurde ein online Aufreinigungsschritt zur effektiven Entfernung von Reagenzüberschüssen entwickelt und in die nanoHPLC Trennungsmethode implementiert. Dies führte zu niedrigeren Metallhintergrundwertem in nanoHPLC-ICP-MS Messungen und einer besseren Interpretierbarkeit der Daten, gleichzeitig konnten die Peptidausbeuten auf höchstem Niveau erhalten bleiben. Alternative offline Reinigung mittels Festphasenextraktion (SPE) verursachte beträchtliche Verluste in den Peptidausbeuten und konnte für quantitative Analysen als ungeeignet erachtet werden. Die Zumischung verschiedener Substanzen, wie HFBA und EDTA zu den Eluenten der nanoHPLC wurde untersucht und für die Analyse normaler Peptidproben als wenig nutzbringend befunden. HFBA kann dennoch eventuell für Spezialanwendungen auf besonders hydrophile Peptide in Betracht gezogen werden.

Ein Satz markierter Peptide wurde zusammengestellt, welcher durch Verwendung bekannter Mengen für eine schnelle und einfache Quantifizierung einer wenig komplexen Probe eingesetzt werden konnte. Zudem konnten diese Peptide dazu verwendet werden, eine zuverlässige Überlagerung von Chromatogrammen zu erwirken und damit die Probenvergleichbarkeit speziell zwischen ICP-MS und MALDI-MS sicher zu stellen.

Versuche zur Anwendung von fsLA-ICP-MS auf MALDI-Stahlplatten wurden durchgeführt und zeigten vielversprechende Ergebnisse. Hierzu sollten bereits mit MALDI-MS identifizierte Proben, erneut mittels fsLA-ICP-MS gemessen werden. Erste

Quantifizierungsversuche auf modifizierten MALDI-Platten waren erfolgreich. Angepasste MALDI-MS Parameter ermöglichten eine eindeutige Peptididentifikation.

Schlüsselwörter

Molekulare Massenspektrometrie und Elementmassenspektrometrie, MALDI-MS, ICP-MS, fsLA-ICP-MS

Lanthanid Markierung, NHS-DOTA, maleimido-monoamide-DOTA,

Peptide, Proteinverdaue

nanoHPLC, online Vorreinigung, Festphasenextraktion, HFBA, EDTA

Abgleichen von Daten, Identifizierung, Quantifizierung

Résumé

Cette thèse est le résultat d'une cotutelle entre l'Université de Pau et des Pays de l'Adour (UPPA) à Pau, en France et l'Université Christian Albrecht (CAU) à Kiel, en Allemagne. Dans le cadre de cette collaboration internationale, des méthodes bio-analytiques sont développées pour analyser quantitativement et qualitativement des peptides et protéines marquées par le couplage de la chromatographie avec la spectrométrie de masse.

Les peptides et les digestats des protéines sont marquées selon un protocole optimisé par des lanthanides en utilisant des composés à base de DOTA. La séparation des peptides est réalisée par IP-RP-nanoHPLC. Des données complémentaires sont acquises par MALDI-MS pour l'identification et par ICP-MS pour la quantification. Dans ce contexte, une étape de pré-nettoyage en ligne est développée et mise en œuvre dans le protocole de séparation par nanoHPLC. Cette étape permet l'élimination efficace des réactifs appliqués en excès et ainsi la diminution du bruit de fond lié à la présence de métaux lors des analyses par ICP-MS. Les données obtenues sont alors plus facile à interpréter, la sensibilité des signaux des peptides n'étant par ailleurs pas modifié. L'extraction en phase solide (SPE) appliquée comme alternative entraîne des pertes importantes de peptides et peut être considérée comme inadaptée pour l'analyse quantitative. Des additifs pour éluants de nanoHPLC, tels que l'EDTA et le HFBA sont testés et jugés non bénéfiques pour l'analyse des échantillons peptidiques normaux. HFBA peut être reconsidéré pour une application spéciale sur des peptides très hydrophiles.

Des peptides marqués sont développés. Leur utilisation en quantité connue pourrait permettre la quantification rapide et simple d'un échantillon de digestat à faible complexité. De plus, cet ensemble de peptides permet la superposition fiable des chromatogrammes, et ainsi de comparer des données complémentaires obtenues par l'analyse d'échantillon par ICP-MS et MALDI-MS.

Expériences d'application avec le couplage laser femtoseconde avec ICP-MS sont effectuées sur des plaques métalliques de MALDI-MS et montrent des résultats très prometteurs. Pour cela, les échantillons préalablement identifiés par MALDI-MS sont analysés par fsLA-ICP-MS. Les premières tentatives de quantification sur la plaque en

acier modifiée sont satisfaisantes et donnent des résultats répondant aux attentes. L'optimisation des paramètres de MALDI-MS facilite l'identification des peptides.

Mots Clés

Spectrométrie de masse moléculaire et élémentaire, MALDI-MS, ICP-MS, fsLA-ICP-MS
Marquage avec des lanthanides, NHS-DOTA, maleimido-monoamide-DOTA,
peptides, digestats de protéines
nanoHPLC, purification en ligne, extraction en phase solide, HFBA, EDTA
Superposition des chromatogrammes, identification, quantification

Abstract

This PhD thesis was a Cotutelle between the Université de Pau et des Pays de l'Adour (UPPA) in Pau, France and the Christian-Albrechts University (CAU) in Kiel, Germany. In the course of this international collaboration, bio-analytical methods for the quantitative and qualitative analysis of labelled peptides and proteins were developed, which were based on the hyphenation of chromatography with mass spectrometry.

Peptides and protein digests were lanthanide labelled using DOTA-based compounds according to an optimised protocol. Separation on the peptide level was performed using IP-RP-nanoHPLC. Complementary data sets were acquired using MALDI-MS for identification and ICP-MS for quantification. In this context, an online precleaning step was developed and implemented in the nanoHPLC separation routine, which allowed for effective removal of excess reagents. This lead to lowered metal backgrounds during ICP-MS measurements and thus better data interpretability, while guarding peptide recovery at a maximum level.

An alternative offline purification using solid phase extraction (SPE) resulted in important peptide losses and can be considered unsuitable for quantitative analysis. Additives to the nanoHPLC eluents, such as HFBA and EDTA were tested and not deemed beneficial for the analysis of normal peptide samples. HFBA can be reconsidered for special application on very hydrophilic peptide species.

A set of labelled peptides was developed, which due to application of known quantities could be employed for quick and simple quantification of a low complexity digest sample. In addition this peptide set allowed for the reliable superposition of chromatograms, enabling sample comparability especially for complementary ICP-MS and MALDI-MS data.

Experiments for application of fsLA-ICP-MS on MALDI-MS target plates were conducted and showed very promising results. For this purpose, samples that were already identified using MALDI-MS were supposed to be remeasured using fsLA-ICP-MS. First quantification attempts on the modified steel target plate were successful and in the range of expectance. Adjusted parameters for MALDI-MS allowed for proper peptide identifications.

Key Words

Molecular and elemental mass spectrometry, MALDI-MS, ICP-MS, fsLA-ICP-MS

Lanthanide labelling, NHS-DOTA, maleimido-monoamide-DOTA,

Model peptides, protein digests

nanoHPLC, online precleaning, Solid Phase Extraction, HFBA, EDTA

Data alignment, identification, quantification

I Introduction

Proteins are the building blocks of life: Structural proteins give cells stability, enzymes conduct chemical reactions, transport proteins are regulating supply and removal of substances to and from cells and their compartments. Life is a complex interplay and proteins play a vital role in it.

In order to understand these interactions, now the involved proteins need to be characterised. This is where the field of proteomics comes into play, which concerns itself with the analysis of proteins in a large scale, elucidating questions about functions and structure and thus helping to map out biological pathways. The most powerful tool in proteomics is molecular mass spectrometry (MS), which can be utilised to determine the molecular weight of proteins and their sequence. Proteomics goes hand-in-hand with genomics and bioinformatics in form of sequence databases and tools for data interpretation.

But not only is it important to know which proteins are present and where, their quantities are of equal importance. Therefore a growing interest is held in quantitative proteomics, as can be seen by taking a look at the rising number of publications in the field. Unfortunately molecular MS is limited in regard to quantitative applications. Recent developments therefore try to implement elemental MS into protein analysis.

Elemental MS, e.g. inductively coupled plasma MS (ICP-MS) is a highly sensitive analytical method providing matrix independent analysis of elements. It has an unrivalled dynamic range of commonly 9 orders of magnitude, which means that certain metals can still be detected at attomole levels. ICP-MS is already commonly applied for protein analysis based on elements such as S, Se or P which are occurring naturally in the proteins of interest. Such approaches quickly reach their limitations, since these elements show low ionisation efficiencies and require quite high protein concentrations. An alternative are labelling approaches, which introduce a detectable element into the molecule of interest. Labels employing chelators, such as DOTA and DTPA are especially interesting, since the introduced element can be chosen quite freely, allowing for multiplex analysis. DOTA is commercially available in form of bifunctional reagents with different reactive groups enabling targeted derivatisations.

Two of these very versatile DOTA-based reagents were employed during this PhD thesis. NHS-DOTA targets amino groups in both N-termini and lysine residues, whereas maleimido-monoamide DOTA can be used to tag sulfhydryl groups in cysteines. They were applied in combination with five mostly monoisotopic lanthanides, forming extremely stable complexes and enabling multiplex analysis. In addition, lanthanides are among the elements with the best ionisation efficiencies in ICP-MS, enabling sensitive and accurate detection of peptides labelled with these tags.
The destructive nature of the ICP process causes a complete loss of the structural info, causing a need for complementary identification by e.g. molecular MS.

1.1 Aim of the Thesis

The general aim of the thesis was the development of bio-analytical methods that contribute to the analysis of peptides, proteins and proteomes both in a qualitative and quantitative manner. A combination of separation techniques was supposed to be employed alongside mass spectrometry. The main basis for the experiments were the labelling approaches using DOTA-reagents and their detection with molecular MS, represented by MALDI-MS on the one hand and the application of elemental MS in form of ICP-MS on the other. For separation purposes classical approaches, such as gel separations and nanoHPLC were employed.

Being a cotutelle between two universities, the experiments were conducted at both sites, namely at the '*Laboratoire de Chimie Analytique, Bio-inorganique et Environnement*' (LCABIE) of the '*Institut des Sciences Analytiques et de Physico-Chimie pour l'Environnement et les Matériaux*' (IPREM) at the UPPA in Pau and at the facility for *Systematic Proteomics and Bioanalytics* of the *Institute for Experimental Medicine* (IEM) as a part of the CAU in Kiel.
The experiments in both laboratories were not separated per se; they rather were conducted in conjunction, since the equipment of both laboratories was of complementary nature. This posed an additional challenge to the thesis, through the geographical distance. The laboratory in Pau provided access to a nanoHPLC system and several ICP-MS instruments. A fraction collector was provided for the facilities in Pau by the laboratory in Kiel as an item on loan. Thereby samples could be analysed via

nanoHPLC ICP-MS for quantification and in a second analysis they could be spotted on MALDI-target plates using the fraction collector. Like this, the measured samples could be transported to Kiel for the complementary MALDI-MS analysis.

The implementation of this 'in-between laboratories routine' was part of the aims of the thesis. It should thereby be shown, that it is possible to conduct experiments of this kind, without the need of having all necessary instruments in the same locality.

Regarding the experimental part, firstly the DOTA-labellings were supposed to be optimised and evaluated for the use with nanoHPLC ICP-MS based quantification. Therefore special attention was given to the excess reagents employed during derivatisation. Several options should be enquired for the reliable removal of the excess metal prior to ICP-MS analysis, in order to facilitate data interpretability. This included online purification approaches implemented in the nanoHPLC routine, as well as offline purification attempts. Another challenge lay in the baseline separation of peaks in ICP-MS chromatograms, which is a vital prerequisite for quantification approaches.

Furthermore the general comparability of ICP-MS based data sets to data sets from complementary techniques, such as MALDI-MS should be ensured. This was especially important in regard to the experiments conducted on different equipment at both laboratories. The peptide identifications from MALDI-MS generally needed to be attributed to the respective peaks in the ICP-MS chromatograms. For this purpose data superposition in form of chromatograms should be conducted, including the development of a reliable tool to resolve possible difficulties with such overlays.

Concepts for lanthanide-DOTA based quantification of peptides and protein digests should be developed and tested for their applicability. Aim was the development of an assay which would in the best of cases be applicable on any kind of protein and peptide sample, thus suitable for proteome analysis. Therefore the capabilities of labelled standard peptides should be evaluated and analysed according to their comparability with the unrelated labelled peptide samples.

Lastly, novel combinations of different complementary analysis techniques should be investigated, such as the use of consecutive MALDI- and laser ablation (LA) ICP-MS.

II Scientific Background

2.1 From Genes to Proteins – a Short Historic Overview

In the 1990s, the world's attention was drawn to the human genome project. During the rapid development in the genomics sector, the interest in the proteins linked to those sequences grew again and in 1996 the term *proteome* finally appeared[5] and gave a modern name to this complementary piece of the biology puzzle. Especially the introduction of soft ionization methods for mass spectrometry enabled a great leap in protein studies. It was thereby possible to determine the molecular weights of proteins and peptides in a fast and accurate manner.[6, 7]

It was then clear pretty quickly that mRNA measurements cannot substitute direct protein analysis. Not only was it merely impossible to reliably predict protein abundance on a cellular level, just by looking at mRNA copy numbers. Also the correlation between the mRNA and protein abundance was shown to be somewhere in the middle between perfect and no correlation at all, suggesting that post-transcriptional regulation plays a great role in gene expression in higher organisms.[8]

Currently scientists are trying to develop a map of the human proteome, to further investigate signalling pathways, protein families and interactions. To date, proteomics is a large and indispensable research field, contributing to the web of knowledge trying to enlighten biological pathways. Many other 'omics' followed since: Metabolomics, lipidomics, transcriptomics, metallomics or metallothiolomics, just to name some.[9-12]

2.2 Proteins – Structure and General Properties

Proteins are made of AA chains which can have fairly large dimensions (e.g. titin[13] isoforms with up to 3.000kDa). The AAs incorporated are linked by peptide bonds and consist mainly of a set of 20 proteinogenic α-AAs. This set is universal and can be found in all organisms likewise, from bacteria to mammals. Depending on the type of organism, sometimes other proteinogenic AA can be incorporated, such as selenocysteine or pyrrolysine which are indirectly coded on the DNA, as special cases of stop codons.[14, 15] The combination of all those amino acids leads to hundreds of thousands of protein sequences, each protein afterwards unique in its structure and

function. The sequence of the AA in the polypeptide chain is called *primary structure*. Interactions between adjacent side chains cause the strands to fold characteristically, the most prominent *secondary structures* being α-helices, β-pleated sheets and β-turns. The *tertiary structure* comprises the complete three-dimensional configuration of the protein, also including side chain interactions between AA residues that are farther away from each other and intra-molecular disulfide bonds. Subareas of the protein often fold in independent structures, which are then called domains. When several folded polypeptide chains assemble to form a bigger complex, we speak of the *quaternary structure*, with the separate polypeptide chains being the subunits.

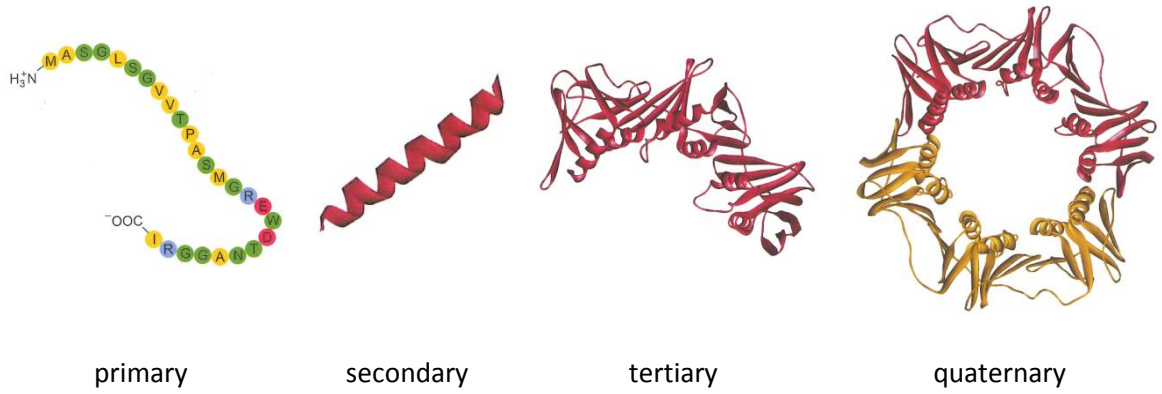

Figure 1. Structure of proteins[16]

To add even more to the protein diversity, post translational modifications (PTMs) can occur which give certain properties to the proteins. To name only some examples: hydroxyproline helps building out the triple helix of the structural protein collagen; phosphorylations (e.g. on Ser, Thr or Tyr) can induce conformation changes and thereby activate and deactivate certain enzymes; carboxylation of glutamic acid in blood factors can start the coagulation cascade and glycosylation on e.g. Asp, Ser or Thr, can add to protein stability and plays roles in cell-cell adhesion, interaction and recognition, thus playing a major role in immune system recognition reactions.[16]

2.2.1 Functions

The real importance of proteins becomes quite clear when looking at the vast amount of tasks taken over by them. In fact most functions in living organisms are taken on by proteins.

It already starts with the static stability of cells and tissues, where proteins such as collagen, keratin or actin and tubulin are giving structural support. Proteins also play key roles in biochemical cascades or in signal transmission in form of neurotransmitters. They regulate the reproduction of cells and the replication of DNA, as well as the production of the proteins themselves in the ribosomes. Trophic factors are influencing the development and growth of tissues. The immune response is taken on by immunoglobulins.

Proteins are also in charge of storage and transport of substances (e.g. transport of oxygen by haemoglobin). Enzymes conduct chemical reactions that would not be possible in the normal surrounding of the cell. Also they catalyse the reactions in a way that they are much faster than it would ever be possible in a laboratory.[16]

2.3 Sample Preparation for Protein Analysis

Before being able to analyse the proteins, they have to be made accessible. When working with biological samples, like cells or tissue, it starts with homogenisation and cell disruption. In order to not destroy or inactivate the proteins of interest, several precautions should be taken, such as the use of suitable buffers, protection from proteolysis by addition of protease inhibitors and sample preparation at low temperatures (≤4°C). Depending on the protein of interest and its location in the cell or the cell compartments, even fractionation by ultracentrifugation can be utilised.

A very essential problem is to keep the proteins in solution: an inadequate pH can cause certain proteins to precipitate because of their IP. Also protein structure (secondary and tertiary) can hinder solubilisation. Denaturing agents, such as urea, can be employed to convert the native proteins to more soluble denatured monomers. Detergents (SDS, CHAPS) further improve solubilisation, reducing agents (DTT, TCEP, β-mercaptoethanol) can be utilised to break disulfide bridges. Reducing agents also prevent unwanted oxidations.

In order to keep the free thiol groups from reacting with each other, alkylation is applied (e.g. with iodoacetamide or methyl methanethiosulfonate).

Cell disruption itself can be carried out in different ways: osmotic shock lysis (in hypotonic solutions), mechanic (sonication, pressing, grinding with glass beads) or chemical (alkali or enzymatic treatment). After the disruption, the sample contains cell

debris that needs to be removed by centrifugation or microfiltration. The supernatant is supposed to be transparent and contains a multitude of compounds: proteins, added chemicals for the lysis, lipids, salts, nucleic acids, amino acids, peptides and metabolites. For removal of lipids, extraction with an organic solvent (e.g. chloroform) can be performed. Nucleic acids can be broken down to nucleotides by RNAse and DNAse.
While, back in the days, it was interesting to just isolate and purify single proteins, for modern protein analysis it is necessary to avoid changes in the protein composition of the sample. Unfortunately, classical protein purification methods like e.g. precipitation, tend to favour certain protein species and lose others, making quantitative whole proteome analysis impossible.[17, 18]

2.3.1 Separation and Purification

In order to remove proteins from their matrix after cell lysis and in order to separate them from each other, different separation and purification techniques can be employed. They can e.g. be separated according to physical properties, such as size, isoelectric point, hydrophobicity or charge state.

Precipitation. For removal of interfering species in the matrix of a protein mixture, protein precipitation can be used. One option is the use of organic solvents, such as ethanol, methanol or acetone. Proteins can also be salted out, using anti-chaotropic salts from the Hofmeister-series.[19, 20] The precipitate can then be removed from the supernatant and be washed and reconstituted in a suitable buffer. Precipitation is commonly used prior to gel electrophoresis and isoelectric focussing.[21] **Dialysis** enables protein purification through diffusion processes by application of a semi-permeable membrane. The driving force for the process is a concentration difference between the sample inside the membrane and the dialysate solution outside of it. The membrane pores only let the low molecular weight compounds pass through, leaving behind the purified proteins. This method does not lower the sample volume, but provides high recoveries and enables purification of proteins in their native form.[22] **Ultrafiltration** (UF) can also be used on native proteins. It employs membranes with pore sizes that retain particles with more than 10-200 Å, which makes it ideal for macromolecules between 1 and 500 kDa. For small scale applications, centrifugal filters can be applied, leading to a purification and concentration of the sample in the filter by removal of low

molecular weight impurities and solvents. The choice of adequate pore sizes (molecular weight cut-off) also allows for fractionation of proteins according to their size.[22] **Solid Phase Extraction** (SPE) can be utilised to extract compounds from a solution by binding them reversibly to a stationary phase. Different materials can be employed (further discussed in section 2.3.3): ion exchange, reverse and normal phase materials. The sample is loaded onto an extraction cartridge under specific conditions that allow for the binding of the analyte. In the following the cartridge can be washed to remove impurities and the analyte then be eluted from the cartridge. By variation of elution solution composition, fractionation is possible.

2.3.2 Electrophoresis

Gel Electrophoresis (GE) is based on the migration of macromolecule ions through a gel by application of an electric field. In protein analysis SDS-PAGE (sodium dodecyl sulphate poly acrylamide gel electrophoresis) is one of the methods of choice for protein separation. SDS inhibits protein-protein interaction, keeping the proteins in solution, by shielding direct protein-protein interactions. All proteins are negatively charged in the same way, so that the charge state does not play a role in the separation. In the electric field the proteins are therefore separated according to their size (Stoke's radius), while they migrate though the pores of the gel with different velocities. The polymerisation grade of the gel can be manipulated by the percentage of acrylamide in the gel mixture. After the separation, proteins have to be made visible with staining (coomassie, silver).[23] **Isoelectric Focussing** (IEF) separates proteins according to their isoelectric point (pI). The pI of a protein is the pH where the protein reaches a global charge state of zero. For IEF a pH gradient is immobilised in form of a gel. Proteins are applied and migrate in the electrical field until they reach the pH where their net charge is zero and thus stop migrating. IEF is commonly used together with SDS-PAGE in **2D-GE** (two-dimensional gel electrophoresis). The IEF strip as a first dimension is applied on a SDS-PAGE gel and the pI separated protein groups are separated in a second dimension according to their molecular weight. Separations of up to 5 000 proteins in one gel are possible.[24] **Capillary Electrophoresis** (CE) is based on the separation of ions in an electrically conductive liquid within an applied electrical field. In the most basic setup, a fused silica capillary (I.D. 25-100 µm) is linking two buffer reservoirs which contain one

electrode each. All ions, both positive and negative, as well as neutral species are pulled in the same direction because of the electro-osmotic flow in the capillary. This leads to a separation according to charge state, shape and size of the analyte. Variations of CE are capillary zone electrophoresis (CZE), capillary electro chromatography (CEC), capillary gel electrophoresis (CGE), micellar electro kinetic chromatography (MEKC), capillary isotachophoresis (CITP) and capillary array electrophoresis (CAE).[25]

2.3.3 Chromatography

Basically, chromatography is the separation of a mixture dissolved in a mobile phase through interaction with a stationary phase. The categories in chromatography are numerous and it already starts with the mobile phase: it can be a liquid – as in liquid chromatography (LC), a gas – as in gas chromatography (GC) or a supercritical fluid (SFC). Another possibility of differentiation is into column and planar chromatography (e.g. TLC, thin layer chromatography). Depending on the capacity of the chromatography system, it can further be distinguished between analytical and preparative application or into miniaturised formats like micro or nanoLC.

In column based chromatography the pressure that is applied by the pump during analysis is another parameter for categorisation: LC runs at low pressure, high performance liquid chromatography (HPLC) applies pressures between approx. 50 and 350 bar, ultra high performance liquid chromatography (uHPLC) has a pressure limit of approx. 3600 bar.

The choice of the stationary phase material is the parameter which determines through which physical or chemical property the analytes are going to be separated:

Size-Exclusion Chromatography (SEC) also referred to as gel filtration, separates proteins according to their size. In contrary to SDS-PAGE big molecules move faster and elute first, since small molecules interact more intensively with the porous structure of the stationary phase. SEC can be used to remove low molecular species from the mixture and since mobile phases with the physiological pH of 7.4 can be applied, it is valid for separation of native proteins. Limitations are its applicability on water-soluble proteins, since hydrophobic proteins can precipitate on-column.[26] **Ion Exchange Chromatography** (IEX) is based on the separation of ions and polar molecules according

to their charge. The stationary phase carries either positively (anion exchange, AEX) or negatively charged groups (cation exchange, CEX). AEX and CEX both exist as strong or weak ion exchange. The interaction between the ion exchange material and the analyte is mainly depending on the pI of the protein and the pH and ionic strength of the employed buffer. IEX-purification is usually more efficient than with SEC and the sample is concentrated in a smaller volume after elution.[23] **Affinity Chromatography** is based on highly specific interactions and allows a selective purification of proteins or protein groups of interest. It can be used to deplete highly abundant proteins or isolate a protein of interest, which is especially interesting for less abundant protein species. Depending on the application different functional groups are immobilised on the stationary phase to reversibly bind the target structures: Antibodies (ABs) can be utilised for specific application, biotin-tags can be used with immobilised streptavidin, lectins can be employed to bind glycoproteins, Ni or Co can be used to bind hexahistidine tagged proteins.[23, 27] **Reverse Phase** (RP) is one of the most commonly used column materials in peptide and protein analysis. It relies on hydrophobic interactions between the analyte and alkyl hydrocarbon chains which are often bound on a silicagel surface as support. Column material which contains unmodified SiOH or other polar moieties is called 'normal phase'(NP). The most popular RP material is C18, which is applicable for analytes with MWs up to 5 kDa (peptides and small proteins). For proteins larger than 5 kDa, C4 columns are recommended (see Figure 2).[28]

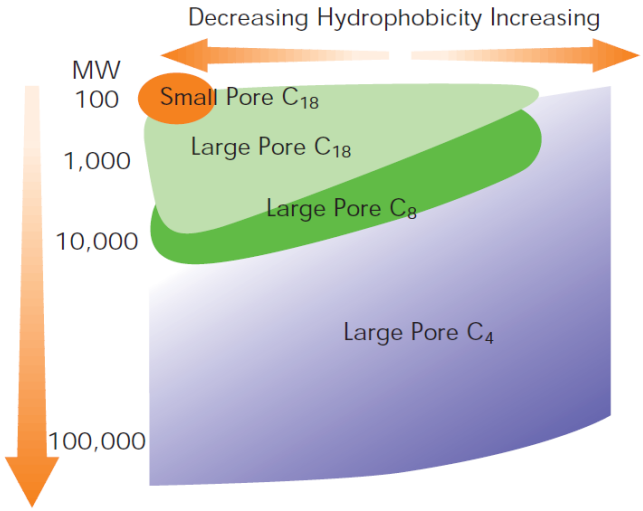

Figure 2: Pore size and RP materials recommended for various MWs and hydrophobicities. Reproduced from Carr.[28]

Ion Pairing (IP) reagents such as TFA can be added to the mobile phase in order to enhance the interaction between hydrophilic species and the hydrophobic surface of the RP material. **Hydroxylapatite** (HA) is a calcium phosphate based material which interacts with both carboxyl and amino groups in native proteins. Low molecular weight compounds or denatured proteins do not bind. It can be regarded as a mixed-mode ion exchange chromatography and its outcome is usually hard to predict in advance. Analytes can be eluted with a rising phosphate buffer gradient.[23] **HIC and HILIC.** Hydrophobic Interaction Chromatography (HIC) is based on interactions between hydrophobic parts of the analyte and the hydrophobic surface of the stationary phase, while hydrophilic interaction liquid chromatography (HILIC) is pretty much the same with hydrophilic moieties. It is another mode which can be used with e.g. RP and NP materials and only differs in the composition of the mobile phase. While in RP chromatography, the most commonly used eluents are mixtures of organic solvents and water, in HIC mode, the elution is done with a decreasing salt gradient (e.g. NH_4SO_4).[23, 29] **Two-dimensional LC** (2D-LC) is referring to the consecutive combination of two orthogonal LC separation techniques. It can be conducted by direct elution from the first column onto the second (online) or by e.g. fraction collection from the first column and reinjection of the fractions onto the next column (offline). Orthogonal techniques which were reported are: high pH RP and low pH IP-RP,[30] IEX and RP, RP and CEC, SEC and RP, AC and RP.[31]

2.4 Mass Spectrometry

Figure 3: General scheme of a mass spectrometer

Mass spectrometry in the broadest sense, can also be seen as a separation technique. It concerns itself with the determination of the mass to charge (m/z) ratio of atoms or molecules. As a first step, analytes need to be converted into ionized species and brought into a gaseous state. The sample is therefore vaporised and ionised in an ion source. The ions are then transferred into a mass analyser, which separates them according to their m/z ratios, prior to their arrival at the detector. The resulting spectra,

in general, show abundance in form of signal intensity over m/z. The most accurate mass spectrometers can determine ion masses with errors smaller than 1ppm.[32] Mass spectrometry, including tandem MS is one of the most important and powerful analytical tools in life science, chemistry and industrial applications.

2.4.1 Ionisation Techniques

As mentioned above, the analyte has to be brought into a gaseous state before it can be analysed. Depending on the analyte there is a multitude of ionisation techniques, distinguished between soft and hard ionisation methods. The soft ionisation methods for biomolecules comprise among others: Matrix Assisted Desorption/Ionisation (MALDI), Electrospray Ionisation (ESI), Surface Enhanced Laser Desorption/Ionisation (SELDI) and Fast Atom Bombardment (FAB). They enable ionisation of macromolecules, without destroying them prior to their analysis. Those soft ionization techniques are utilised in molecular MS. A hard ionisation method is inductively coupled plasma (ICP), where the analytes are broken down to their atoms, due to the high thermal energy. It is used for elemental MS.

2.4.1.1 Inductively Coupled Plasma

ICP-MS is a highly sensitive analytical method and is widely used in trace element and environmental analysis. The ionisation takes place in an argon plasma flame at 5.000-10.000 K, leading to a complete loss in structural information of the sample. The scheme for the ion generation in the plasma is shown in Figure 4. The sample is usually introduced as a liquid aerosol using a nebuliser, which is adapted to the experimental needs. Due to the different heat zones of the plasma, the aerosol is dried, vaporised, atomised and then ionised. The plasma itself is generated by induction of a high frequency current into ionised argon.

The extent to which an element is ionised depends on its first ionisation energy. The available energy of the argon plasma is approximately 15.8 eV, whereas the majority of the elements have first ionisation potentials between 4 and 12 eV.[33]

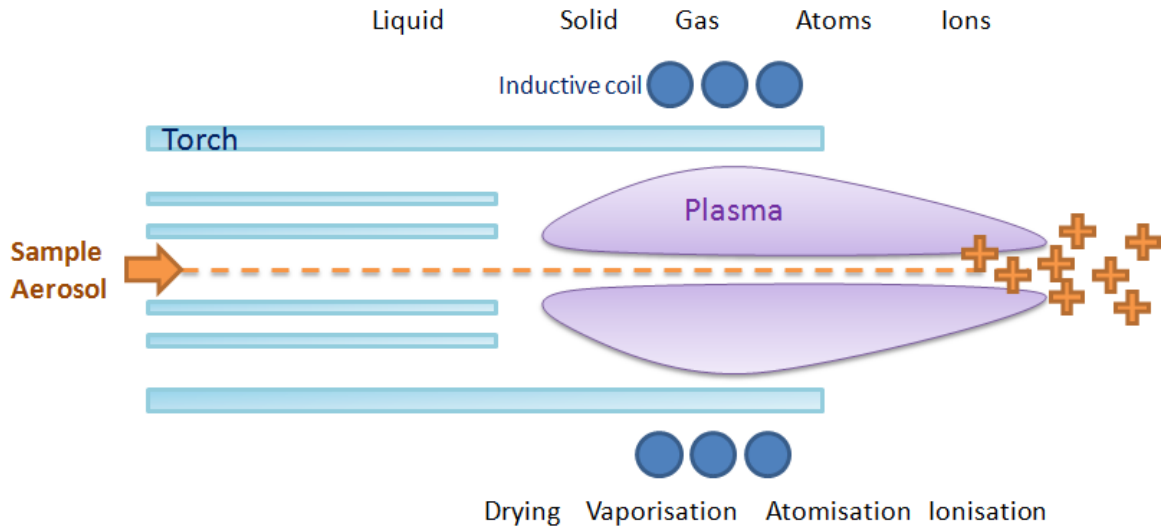

Figure 4: Generation of positively charged ions in the plasma, adapted from Thomas [33]

As shown in Figure 5, the required ionisation energies rise from bottom to top and left to right in the periodic table. Metals in general, except for platinum, gold and mercury, show good to excellent ionisation efficiencies. It has been shown that even attomole amounts of certain metals can still be detected using ICP-MS.[34] Apart from its remarkable sensitivity, ICP-MS also shows a very high dynamic range, which cannot be rivalled by any other method. Usually nine orders of magnitude are possible,[35, 36] but also twelve orders of magnitude were reported for metal-salt solutions.[34] Since ionisation is virtually matrix and molecule independent, external calibration can be used for quantification.[37]

Table 1: Polyatomic interferences for selected lanthanides [38, 39]

Element	m/z values	Interference	Required resolution R for peak separation[39]
Erbium	166	$^{150}Sm^{16}O$	
	167	$^{151}Eu^{16}O^{+}$	
	168	$^{152}Sm^{16}O$	9470
Holmium	165	$^{149}Sm^{16}O$	
Lutetium	175	$^{159}Tb^{16}O$	8520
Terbium	159	$^{142}Nd^{16}O^{+}$	
Thulium	169	$^{154}Eu^{16}O$	9342

Depending on the analyte species, interferences can occur: elemental isobaric interferences can be caused by isotopes of an element which have the same mass to charge as the analyte, e.g. ^{114}Cd and ^{114}Sn. Also doubly charged ions can interfere, which is the case for $^{150}Sm^{++}$ and $^{75}As^{+}$. The most commonly occurring interferences are

polyatomic, where molecular species with the same m/z as the analyte hamper with the analysis. Especially reaction products of argon, atmospheric gases, salts and acids pose problems. For example, ArO^+ can interfere with $^{56}Fe^+$, $^{52}Cr^+$.[38]

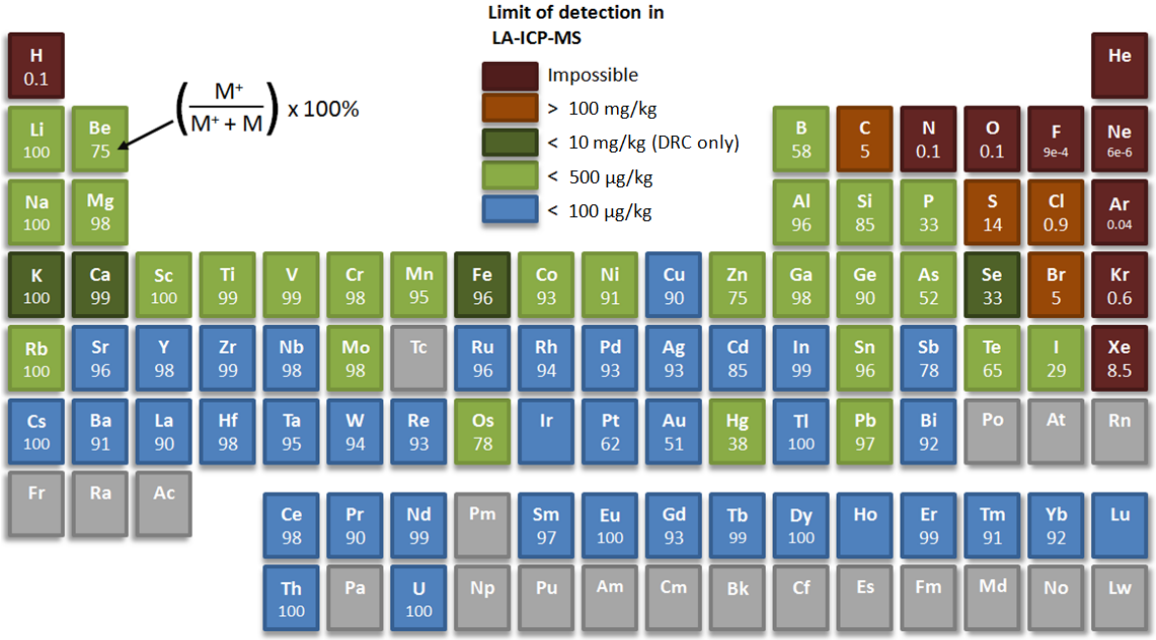

Figure 5: Periodic table of elements with calculated values of the degree of ionisation of M^+ (T = 7500K n_e = $1x10^{15}cm^{-3}$)[40] and limits of detection in LA-ICP-MS[41]

A collision/reaction cell can remove those interferences by kinetic energy discrimination through collision with an inert gas or by shifting their m/z by reaction with a gas in a way that it won't interfere anymore. Commonly used gases are ammonia, methane, oxygen or hydrogen. As an example, the instrument used in this thesis from Agilent's 7500 series uses an octopole reaction system (ORS) which runs with helium or hydrogen. In collision mode, pure Helium is used to remove unwanted molecules: it collides more frequently with the larger ionised molecules than it does with ionised atoms, causing the molecules to lose more of their kinetic energy. The needed collision energy is characteristic for each ion species, allowing the application of a kinetic energy filter using the octopole. Being inert, Helium does not form new interferences. The reaction mode is mostly used for analytes which show plasma based interferences (e.g. Se). Hydrogen reacts quickly with the Ar-based interfering species, but reacts only slowly or not at all with the analyte.[42]

2.4.1.2 Laser Ablation

For analysis of solid samples with ICP-MS, a hyphenation with laser ablation (LA) became the method of choice, ever since it was introduced in 1985.[43] Ablation is the removal of material by heating, by e.g. a laser or through atmospheric friction. In LA, small amounts of solid sample (or rarely liquids) are removed by short but intense laser pulses. Depending on the laser fluence, the sample is either evaporated by heat (low fluence) or directly converted into a micro plasma (high fluence). The ablation takes place in an air-tight ablation cell. The particle/vapour mixture created through LA is then transported by a vector gas from the cell to the plasma of the ICP-MS. Ideally, the LA should result in a quantitatively transportable aerosol, which is representative for the sample in its composition.

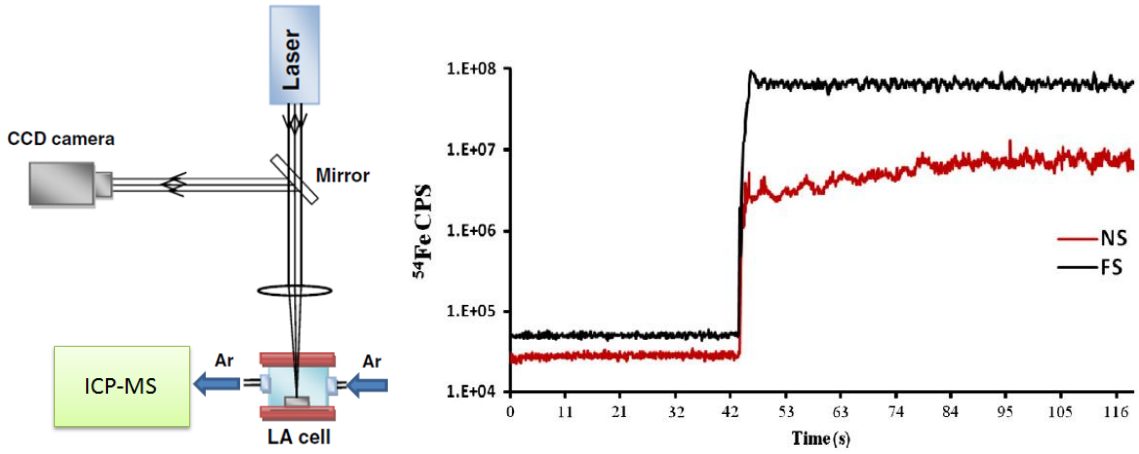

Figure 6, left: Simple scheme of a fsLA-ICP-MS system. Right: ICP-MS signal obtained by femtosecond (785 nm, 130 fs) and nanosecond (266 nm, 8 ns) LA-ICP-MS of steel. Adapted from Shaheen et al.[44]

The analytical performance is influenced by a large variety of parameters, which makes it hard to implement laser ablation as a routine analysis tool. Laser related parameters comprise: wavelength (IR, UV, deep UV), pulse width, fluence, pulse repetition rate, beam profile and focus. Apart from ICP and MS related parameters, the geometry and volume of the ablation cell, as well as the type or composition of the vector gas, also play a role in the performance. Lastly, physical properties of the sample itself can also have an influence.[44]

Classification of the laser system is usually based on the laser pulse width, which ranges from nanoseconds (ns), down to femtoseconds (fs). Ablation quality of fsLA-systems is shown to be better than longer wavelength ns-LA, which is due to the interaction of the

ultra short laser pulses with the matter: the energy transfer of a fs pulse is too short to leave the material enough time to melt, resulting in more uniform ablation behaviour of materials with different physic-chemical properties. The generated particles (size in nanometre range) are more efficient to transport and ionise, than the ones resulting from a ns pulse.[44-47]

The most evident advantage of this technique is the possibility to analyse solids without having to put them in solution via mineralisation with strong acids. This is avoiding further contamination and loss of sample. Another advantage is the possibility of spatially resolved analysis, either on a plane or in depth.

LA-ICP-MS is used on various materials and has applications in chemical analysis (alloys, crude oils),[48, 49] geochemistry (soils, sediments),[50] industry (semiconductors, coatings)[51, 52] and biology (tissue imaging, blotted membranes and IEF-strips/2D-gels).[53-55]

2.4.1.3 Matrix Assisted Laser Desorption/Ionisation

The MALDI process was discovered by Karas and Hillenkamp in 1985 as a way of ionising small organic compounds[6] and it was published for the application on proteins in October 1988.[56] Shortly before their report, Koichi Tanaka succeeded in applying 'Soft Laser Desorption' for the ionisation of macromolecules without losing their structure in the process.[57] Tanaka was therefore awarded the Nobel Prize in chemistry in 2002. Today MALDI is the technique that remained present in laboratories, since Tanaka's approach has poorer ionisation efficiencies.

CHCA: α-Cyano-4-hydroxycinnamic acid
(for proteins and peptides < 10 kDa)

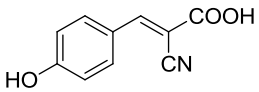

THAP: 2,4,6-Trihydroxy acetophenone
(for RNA, glycoproteins, glycolipids)

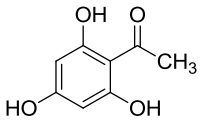

Sinapinic acid, SA:
Trans-3,5-dimethoxy-4-hydroxy cinnamic acid
(for proteins, polymers >10 kDa)

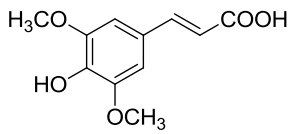

DHB: 2,5-Dihydroxybenzoic acid
(for carbohydrates, glycopeptides,
proteins, peptides < 10 kDa)

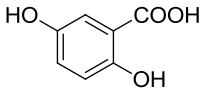

Figure 7: Commonly used MALDI matrices

MALDI stands for Matrix Assisted Laser Desorption/Ionisation, meaning that the desorption and ionisation process of analytes with the laser is aided by a matrix. Properties of this matrix must comprise a good ability at absorbing photons from the laser and converting the thereby absorbed energy into heat, as well as the potential for charge transfer reactions. Therefore, most UV-MALDI matrices are organic acids with aromatic structures, such as CHCA, DHB, SA or THAP (Figure 7). The analyte is usually embedded in a huge molar excess of matrix molecules due to co-crystallisation, e.g. as a dried droplet on a ground steel target. Under vacuum conditions, the matrix/analyte spot is then shot with a pulsed UV laser, commonly N_2 (337nm, up to 60 Hz) or Nd:YAG (frequency tripled: 355nm, up to 1 kHz). Lasers of other wavelengths are seldom found in commercial MALDI systems.

The π-electrons in the aromatic structures of the matrix are excited by the laser photons, which leads to an energy and heat transfer into the volume of the crystal and a phase explosion due to the rise in temperature and pressure. The high excess in matrix molecules prevents most of the thermal decomposition of the analytes. [58]

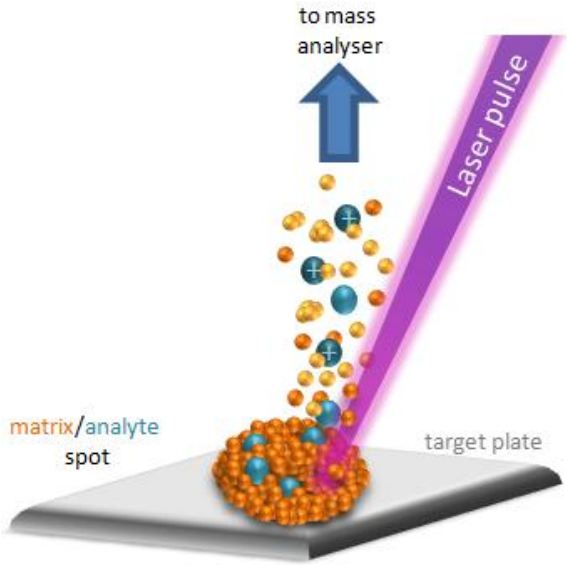

Figure 8: Scheme of ionisation via MALDI. The laser beam is ablating the matrix/analyte spot; neutral species as well as ions of both matrix and analytes are released into the gas phase and accelerated in direction of the mass analyser using an acceleration electrode/extraction grid.

There was a controversy going on about the mechanism of the ionisation process, between the 'gas phase protonation model' and the 'lucky survivor model' (unified mechanism in Figure 9). The first model postulates that neutral analytes collide with protonated $ma+H^+$ or deprotonated $[ma-H]^-$ matrix molecules in the gas phase, thus leading to the transfer of a proton, either from or to the analyte molecule *A*, thus leaving positive AH^+ and negatively charged $[A-H]^-$ analyte species respectively.[59-61] In the lucky survivor scenario it is stated that the analyte molecules already have their charge state prior to incorporation in the matrix crystal. After ablation and during matrix cluster dissociation, a portion of the analytes are either still paired with a counter ion *X* (no net

charge) or they get re-neutralised, due to photoelectrons or electrons from the metallic target. The 'lucky survivors' which still carry a charge can then be detected.[62, 63] Both models were proven to be valid using deuterated matrix esters.[64] The complete mechanism is still being debated.

MALDI creates mostly singly charged ions, which makes the spectra quite easy to interpret, contrary to e.g. ESI-MS with its series of multiply charged ions.

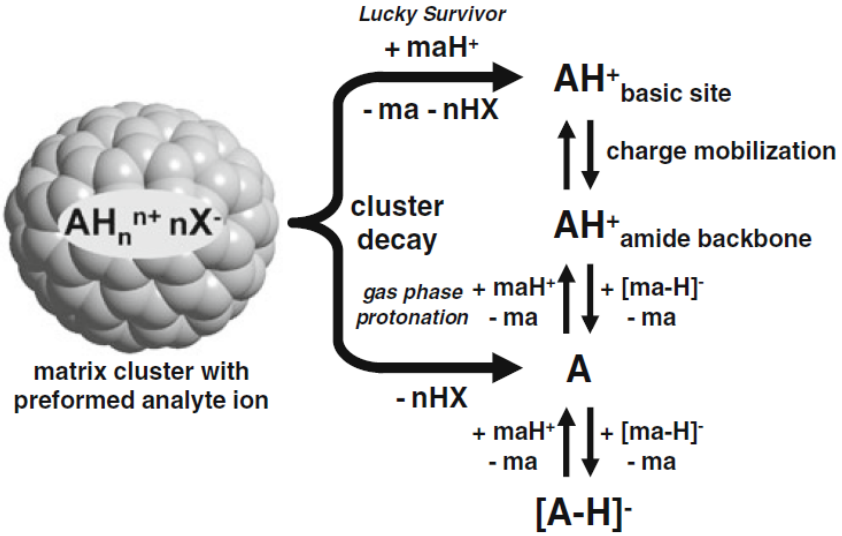

Figure 9: Unified MALDI analyte protonation mechanism. Combination and connection between the lucky survivor and the gas phase protonation model by Jaskolla and Karas.[64]

2.4.1.4 Electrospray ionisation

Electrospray ionisation (ESI) is, like MALDI, a soft ionisation method commonly used for macromolecules. Unlike MALDI which has to be hyphenated to HPLC in an offline manner, ESI can be coupled directly to an HPLC System.

The analyte solution is introduced into a metallic capillary/needle on whose tip a high voltage is applied. An electrical field is formed between the capillary and its counter electrode which leads to the formation of a Taylor cone at the tip of the capillary. A jet of liquid leaves the cone end which dissociates to a fine spray of charged droplets. Evaporation of the solvent reduces the droplet size until the repulsion of the charges causes a coulomb explosion of the aerosol droplets. Before entering the high vacuum of the mass spectrometer the analyte is completely desolvated and can carry multiple charges.

The multiple charges enable the analysis of very large molecules (up to 150kDa). The low m/z ratios make ESI-sources compatible with all types of mass analysers. Unfortunately the signal for an analyte is distributed over several charge states, thus elevating its limit of detection and causing elaborate interpretation of the spectra.

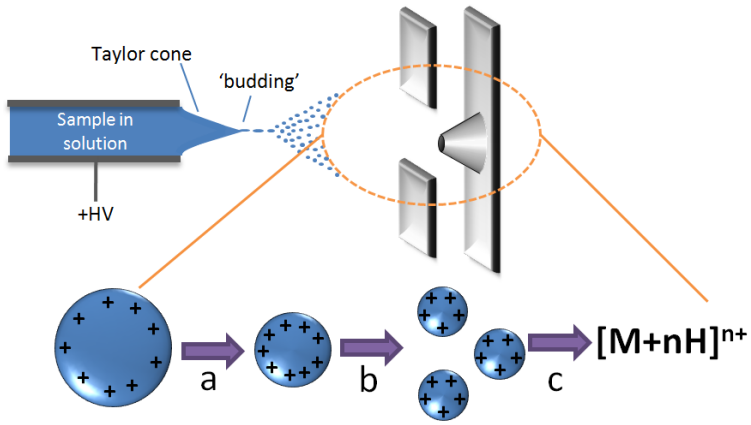

Figure 10: Scheme of ionisation via ESI and essential features of the experimental arrangement. Analyte ion formation: (a) solvent evaporation, (b) droplet fission at Rayleigh limit, (c) formation of desolvated ions by further droplet fission and /or ion evaporation. Adapted from Gaskell. [65]

2.4.2 Mass Analysers

After ionisation of the analyte molecules, their molecular weight (m/z ratio) needs to be determined. Using ICP as a mean for ionisation, it is usually paired with quadrupole mass analysers, whereas MALDI is mostly coupled with a time-of-flight (TOF) or TOF-reflectron mass analysis system.

Other mass analysers comprise sector field mass analysers, with electrostatic and/or magnetic sectors (e.g. used in multi-collector MS), 3D- and linear ion traps, orbitrap and Fourier transform ion cyclotron resonance. Resolution power and other figures regarding the mass analysers are shown in Table 2.[32]

Table 2: Typical figures of merit for different mass analysers. Adapted from Hart-Smith and Blanksby[32]

Mass analyzer	Double focusing sector field	Quadrupole	Linear ion trap	TOF	FT-ICR	Orbitrap
Mass resolving power	100 000	100 – 1 000	1 000 – 10 000	1 000 – 40 000	10 000 – 1 000 000	10 000 – 150 000
Mass accuracy	<1 ppm	100ppm	50 – 100 ppm	5-50 ppm	1-5 ppm	2 – 5 ppm
Mass range	10 000	4 000	4 000	> 100 000	> 10 000	6 000
Linear dynamic range	$1x10^9$	$1x10^7$	$1x10^3 – 1x10^4$	$1x10^6$	$1x10^3 – 1x10^4$	$1x10^3 – 1x10^4$
Abundance sensitivity	$1x10^6 – 1x10^9$	$1x10^4$ – $1x10^6$	$1x10^3 – 1x10^4$	$1x10^6$	$1x10^3 – 1x10^4$	$1x10^4$

2.4.2.1 Quadrupole

A quadrupole (Figure 11) consists of four metallic rods through which the ions have to make their way. The application of radio frequency and direct current voltages determine the trajectories of the ions. Depending on the way those voltages are combined, only ions with a given m/z can achieve a stable trajectory in the mass filter and pass through to the detector, all others will hit the electrodes and be neutralised.

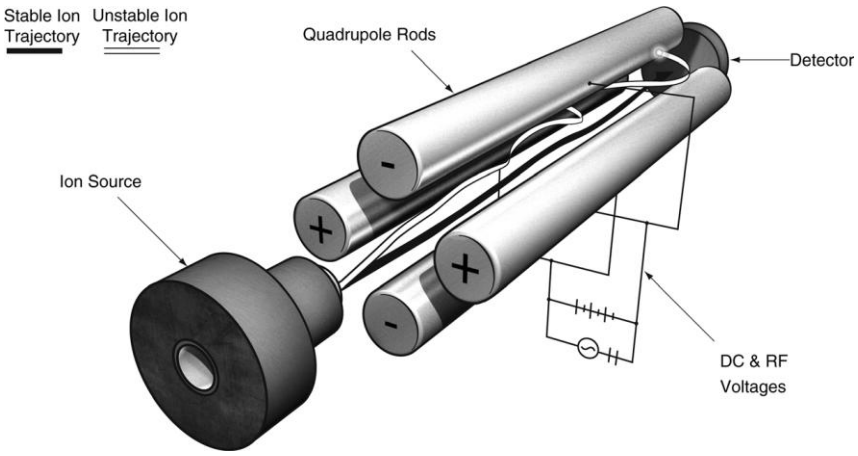

Figure 11: Quadrupole mass analyser. Reproduced from Hart-Smith and Blanksby. [32]

2.4.2.2 Time of Flight

With the development of MALDI in the 1980s, the time of flight (TOF) analyser gained more importance, since it is ideal to be interfaced with this ionisation technique. In order to function reliably, TOF requires discrete packages of ions with the same start time. They are provided by the pulsed ionisation via the laser in MALDI.

Figure 12 shows an orthogonal TOF analyser. Even though in the instrument used during the thesis, the flight tube is arranged on-axis with the laser, the principle stays the same. The sample is ionised in the source, ions are accelerated through a fixed potential and enter a field-free drift zone of defined length. The velocity of the ions is dependent on their m/z ratio: all ions with the same charge obtain the same kinetic energy, resulting in a higher velocity of small molecules and a lower velocity of heavier analytes. In consequence, small molecules need less time to pass through the drift region and hit the detector than the bigger ones with the same charge state. The analytes are thereby separated according to their m/z.

Small differences in kinetic energies between analytes of the same m/z, which can be a result of the ionisation process, are usually ruled out by the use of an ion mirror. The enlarged flight distance also improves resolution and mass accuracy, without the need of a larger instrument. The problem of different kinetic energies can also be taken on by a delayed extraction. For this technique, the MALDI process is conducted without an electric field and the ions then accelerated using a high voltage pulse after a defined delay of time. [32, 58]

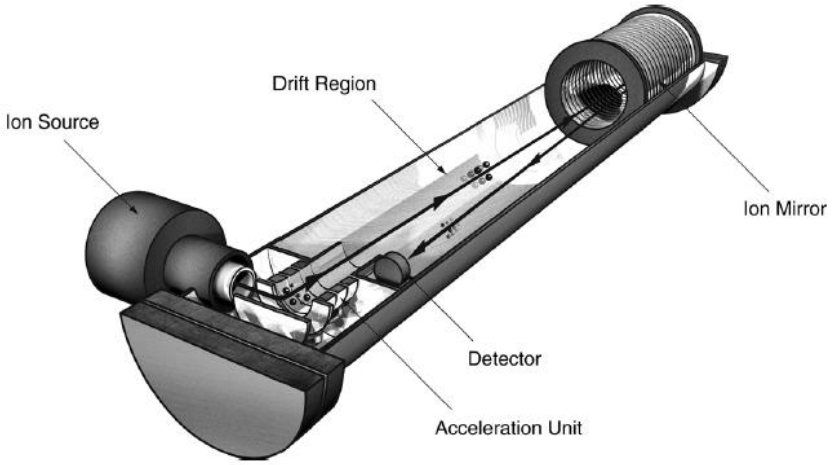

Figure 12: Orthogonal TOF mass analyser with an ion mirror. Reproduced from Hart-Smith and Blanksby. [32]

2.4.3 Tandem Mass Spectrometry

Tandem MS (also: MS/MS or MS^2) is a technique for structure determination. Big molecules are broken apart to smaller characteristic fragments, which are then mass analysed and thus enable the identification of the parent molecule. The acquired fragment spectra provide highly credible, qualitative information. In the case of proteins or peptides, their sequence can be determined with this technique, making it the first choice for fast peptide/protein identification. For the purpose of fragmentation, a collision cell is built into the mass spectrometer, usually situated between two mass analysers. One of the simplest arrangements of a tandem mass spectrometer is a triple quadrupole (QqQ), with the first quadrupole (Q_1) conducting parent ion selection, the second one (q_2) acting as a collision cell for fragmentation and transport and the third one (Q_3) scanning the product ions. Alternatively an ion trap can be used, where the parent ion can be trapped and fragmented through collision with a gas. The product ions will then be released to the detector in order of their m/z. Depending on the setup, even

MS^n experiments can be performed in such a way, which is especially interesting for intact proteins. Fragment ions from MS^2 can be selected and fragmented again, resulting in MS^3, MS^4, ... , MS^n.

There are many scan modes that make use of tandem MS. Their utility depends entirely on the problem that needs to be resolved. **Product ion scan.** In this scan mode, a precursor ion is selected and subjected to fragmentation. All resulting product ions are then being recorded. **Precursor ion scan.** This method is not possible with time based MS, like TOF or ion traps. In a triple quadrupole for example, the product ion is selected in Q_3, while Q_1 is scanning the mass spectrum for possible parent ions. Only those precursors that result in the product ion are recorded. **Neutral loss scan.** Since many classes of molecules tend to lose a neutral moiety during fragmentation, this neutral loss can be monitored using this scan mode. The two analysers scan both precursor and product ions for a constant mass offset. This scan mode is interesting to determine the presence of certain modifications, like for example phosphorylations, with a mass offset of 98 Da for the loss of phosphoric acid. **Selected reaction monitoring (SRM)** In order to achieve increased sensitivity for a certain compound, the mass analyzers (e.g. Q1 and Q2) can be programmed with predetermined masses for precursor and product ions to let only the ions of interest pass. If more than one precursor is monitored, it is called **Multiple reaction monitoring (MRM)**.[66]

2.4.3.1 Post Source Fragmentation Techniques

The type of product ions in MS^2 largely depends on the used fragmentation technique and the underlying mechanism. Most commonly used is the collision induced dissociation (**CID**), also referred to as collision aided or activated dissociation (CAD): The parent ions are fragmented by collision with an inert gas, a neutral molecule or a surface. The kinetic energy is then converted into internal energy and after its accumulation, the parent ion breaks apart. This usually happens at the peptide bond between CO and NH, resulting in b- and y-ion series (Figure 13). For the generation of c- and z-ion series (Figure 13), the ion trap exclusive technique **ETD** (electron transfer dissociation) can be used. It is based on ion-ion interactions, where specially generated anions react with the multiply charged parent cation, promoting fragmentation by electron transfer. Also based on electron transfer is **ECD**, electron capture dissociation. It

has the advantage of leaving most PTMs intact. In this method, the parent ion reacts with low energy electrons, building radicals, resulting in reduction of its charge state and generation of c- and z-ions. It is optional in FTMS and Orbitrap mass spectrometers. The fragmentation techniques are often combined for complementary information.[66]

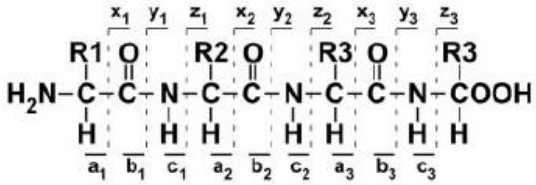

Figure 13: Fragmentation pattern in tandem-MS, with a-/x-, b-/y- and c-/z-ion series. Reproduced from Khalsa-Moyers and McDonald.[67]

There are also several types of fragmentation which are only indirectly induced by the user and can be used for interpretation. **In source fragmentation** occurs directly in the ion source, because of the high amount of energy of the ionisation process. It is not tandem MS per se, but it can be used for fragment analysis in a similar way. Especially in combination with an additional post source fragmentation, a pseudo MS^3 can be performed. **Post source decay** is a phenomenon commonly used in MALDI-TOF/TOF analysis. Some of the parent ions fall apart in the flight tube of the analyser. This can be utilised for a special type of analysis because the parent ions and their matching fragments both have the same velocities, but different kinetic energies. In linear mode they hit the detector at the same time because of their velocities, but in reflector mode they are separated according to their kinetic energies, resulting in product-ion spectra.[66]

2.5 Proteomics

The term proteome was introduced as the protein counterpart to the genome[68] – a quite misleading definition, since the genome is a rather static construct, while the proteome is very dynamic in its nature. During the lifetime of an organism, the genome does not alter (except for mutations), whereas the proteome is always changing. Therefore the definition was changed shortly after by Jungblut:

'The proteome of an individual is defined by the sum and the time dynamics of all protein species occurring during the life-time of this individual' [69]

With these definitions, it is not very surprising to find, that it is merely impossible to draw direct conclusions regarding protein expressions from translational data: One gene can be easily translated into several proteins with different functions.[70, 71] Many metabolic and regulatory processes are involved on the way to protein formation: splicing, post-translational modification, proteolytic processing, etc. Genomic techniques alone, like the determination of mRNA concentrations, cannot provide information on the final appearance of a protein species, including its PTMs or its function and destination in the organism.[72]

Already the qualitative analysis of the proteome is a challenge, since no method ever comprises all proteins likewise. There is always a loss when analysing acidic or basic, very large or very small proteins. Also concentrations of proteins in natural samples can easily differ by up to 12 orders of magnitude (see e.g. the millimolar range for albumin versus an attomolar range for cytokines in plasma)[73], leading to the necessity of higher sample amounts for the detection of low abundant proteins. Unfortunately, unlike PCR for nucleic acids, there is no generic amplification method for proteins.[23]

The most powerful tool in proteomics is mass spectrometry and it enabled a giant leap in protein analysis since its introduction.

2.5.1 Classical Proteomic Approaches

The two main strategies in MS based proteomics are the top-down and the bottom-up approach.

Top-Down. In this approach, intact proteins are separated by e.g. multidimensional chromatography and then subjected to MS^n fragmentation, typically by CID, ECD, ETD or IRMPD. Interpretation of the resulting spectra is fairly complicated though and identification of the parent ion needs special algorithms for data processing prior to database search. This is why top-down is rarely applied and still not well established.

Bottom-up. For the bottom-up approach the proteins are digested, and the peptide mixture can then be separated and analysed. Complex protein mixtures can first be separated by e.g. 1D- or 2D-gel electrophoresis. After tandem MS the spectra are compared with published protein databases to find the most likely match for the parent protein. Bottom-up approaches starting with the direct digestion of a crude protein mixture are referred to as ‘shotgun’ protein sequencing. The resulting complex peptide

mixture can then be separated using 1D or 2D HPLC and analysed using tandem MS. Database searches then help the reconstruction of protein mixture composition. [66]

2.5.1.1 Protein Identification

Thanks to genomic research, the sequences of many organisms are fully or at least partly known. Those sequences are available in databases, such as UniProtKB/Swiss-Prot and TrEMBL, on open access servers, free for everyone to use.[74] With the help of special software, the data obtained from MS and MS^2 experiments can be compared with the sequence data from those databases. This way the analysed proteins can be identified and the reliability of the result assessed, e.g. by taking a look at the score given out by software such as Mascot.[75] Identification can almost be fully automated for shotgun and bottom-up approaches, using e.g. proteomic grade trypsin for selective cleavage. The database search parameters can be set according to the experimental setup.

2.5.2 Quantitative Proteomics

It already is a challenge to identify the complete set of proteins in a given sample, because of their different properties, sizes, abundances, etc. But only having the information about a protein species' presence in a sample does not help much elucidating its role in the cell or organism. Knowledge about its amounts is equally important for the understanding of the fundamental processes in biological pathways.[76] Quantitative protein analysis though, is a far more difficult task than 'only' identification; it is likely the most challenging part of proteomic research. As seen in Figure 14, only a fraction of peptides present in a sample can be quantified.

Traditional quantitative approaches are based on differential analysis of 2D-gels and blots, stained with dyes, fluorophores or radioactivity: two or more gels are dyed differentially and the corresponding spots/bands are then compared with each other, allowing relative quantification through their intensities. Even though the methods show good sensitivity, linearity and dynamic range, they are only applicable on abundant and soluble protein species. Also they do not provide data on the identities and they are unfortunately quite user subjective. [1, 2]

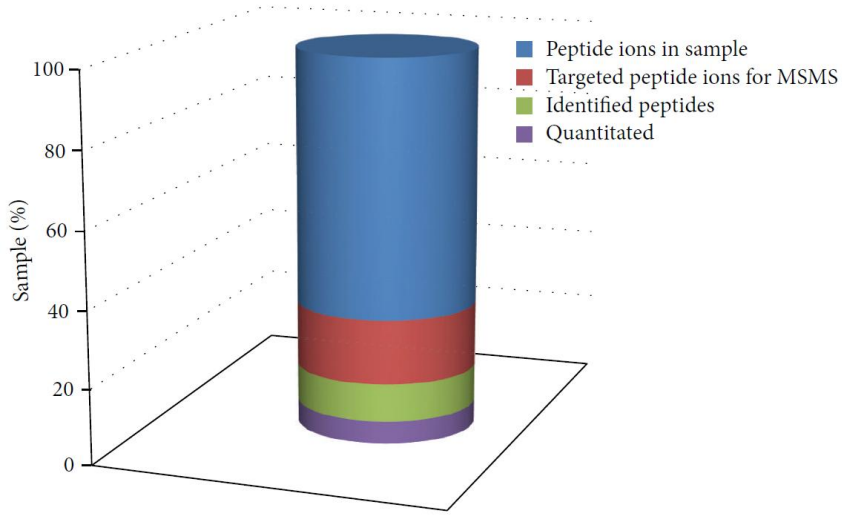

Figure 14: In general only a small fraction of peptide ions resulting from a sample can really be identified and quantified. Reproduced from Wasinger et al.[1]

Relative quantification can also be achieved with label free MS, where several experiments are directly compared with regard to the MS ion intensity of peptides or spectral counts, giving data on relative quantities in form of fold-changes.[2, 77]

The field of absolute quantification is increasingly popular, which is mirrored by the rising amount of approaches and publications. Figure 15 on the next page shows the rising number of publications on quantitative proteomics. Currently 45% of the publications on quantitative proteomics also contain the keyword 'labeling', whereas approximately 20% are on absolute quantification – with a rising tendency.

Absolute quantification can give exact amounts of proteins in e.g. ng/mL or copies/cell. Quantitative information is interesting for various fields in life science. Especially clinical applications such as biomarker discovery are a popular topic.[78, 79] In medical science, the interest often lies in the discovery of differences between two states e.g. healthy and diseased. Comparing those states, the only difference to be seen might be in the presence and change in abundance of proteins or their posttranslationally modified forms.[80] Being able to monitor the protein expression in an organism, like eukaryotic cells or bacteria, also facilitates a more reliable manipulation of the mechanisms of synthesis in those organisms, potentially resulting in a sustainable bio-production of a compound of interest in cell culture. Many potentially interesting pharmaceuticals are protein or peptide based compounds with posttranslational modifications that cannot

be synthesised reliably by chemical means. Especially the glycosylation is a challenge, which is important for compatibility of those compounds when applied on patients.[81] To date already plenty of products in healthcare, such as vaccines, hormones, antibodies or coagulation factors are synthesised by cell culture and thus made commercially available.[82]

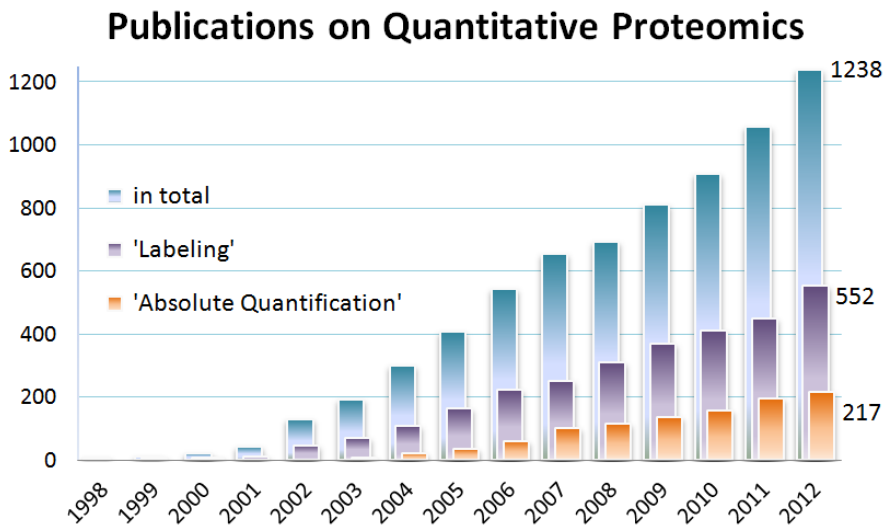

Figure 15: Number of publications per year, listed in Scopus[83] for the keyword 'Quantitative Proteomics', +/- the keywords 'Labeling' or 'Absolute Quantification'

Table 3 gives a brief overview on the main approaches used in quantitative proteomics. It can be seen, that most approaches are only applicable for relative quantification. Another way of absolute peptide/protein quantification are approaches using metal labels together with a combination of molecular and elemental MS. Therefore a comparison of the characteristics of ICP-MS and molecular MS is shown in Table 4, which emphasises the complementary nature of both techniques. Metal labelings are discussed in a separate paragraph, because of their special importance for this thesis.

Table 3: Overview of main approaches in quantitative proteomics. Adapted from Wasinger et al. and Bantscheff et al.[1, 2]

Method	Application	Dynamic Range (orders of magnitude)	Quant. Proteome Coverage	Accuracy (Process)	Throughput	Quantitation type	Publications
Label-free							
2D gels	**Simple biochemical workflows; Whole proteome analysis**	1-4, stain dependent	++	++	+	Relative, needs ID by MS	[83, 84]
Ion Intensities MS		3	+++	++	++ / +++	Relative, LC dependent	[85, 86]
Spectrum count MS^2		3, Inaccurate for low abundance	+++	+	++ / +++	Relative, LC dependent	[87]
APEX, emPAI		3 or 4	+++	+	+++	Relative, within sample only	[88, 89]
Metabolic Labelling	**Complex biochemical workflows; Cell culture systems only**						
^{15}N		1-2	++	+++	+	Relative, between 2 conditions	[90, 91]
SILAC		1-2	++	+++	+	Relative, between 2 and 3 samples	[92, 93]
Isotopic Labelling							
ICAT ^{18}O ICPL	**Medium complexity biochemical workflows**	1-2	+	+++	+	Relative, between 2 conditions	[94, 95] [96, 97] [98, 99]
Isobaric Labelling							
iTRAQ	**Medium complexity biochemical workflows**	2	++	++	+	Relative or Absolute, between 2 and 8 conditions	[100-102]
TMT		3					[103, 104]
Targeted							
MRM	**Medium complexity biochemical workflows; Targeted analysis of few proteins**	5	+	+++	+++	Relative or Absolute, requires intensive method development	[114, 115]
Isotope dilution +/- heavy label		Attomolar detection					

Table 4: Comparison of characteristics of molecular (MALDI/ESI) and ICP-MS. Reproduced from Tholey and Schaumlöffel.[3]

	Molecular (MALDI/ESI)-MS	ICP-MS
Atomic information	Impossible	Metals + heteroelements: (C), S, Se, P, Cl, Br, I
Isotopic Information	Possible	Method of choice
Structural information; Identification of peptides, proteins	Method(s) of choice	Impossible
Characterization of peptides, protein, e.g. PTMs	Method(s) of choice	Only answer: yes/no (e.g. via P detection); no identification or characterization
Quantification (absolute)	Restricted, low dynamic range	High potential
Quantification (relative)	Restricted, low dynamic range	High potential
Sensitivity (quantification)	Medium	High
Precision (quantification)	Low/medium	High
Parallelization or multiplexing capacity (e.g. for quantification)	Low, restricted availability of standard labeling reagents (e.g. SILAC – about 5 channels; iTRAQ – 4 or 8 channels)	High number of metal atoms available (e.g. 14 lanthanides; isotopes, other metals)
Coupling with high resolution separation techniques	ESI-MS: on-line and off-line MALDI MS: only offline	On-line and off-line

2.5.3 Labelling

Using ICP-MS for quantification, the molecule of interest needs to contain a detectable element, such as heteroelements (S, P or Se) or metals (Zn, Fe). Unfortunately, only about one third of the whole proteome contains metals (mostly in form of protein cofactors)[106] and the ionisation efficiencies for heteroelements are usually very low, which makes them unsuitable for the quantification of less abundant proteins. An alternative approach is the introduction of a label into the biomolecule.

In the past decade, researchers have come up with quite a few strategies on how to modify biomolecules – especially proteins, in such a way that they are accessible for quantification.[107]

2.5.3.1 Target Groups for Chemical Modification Reactions

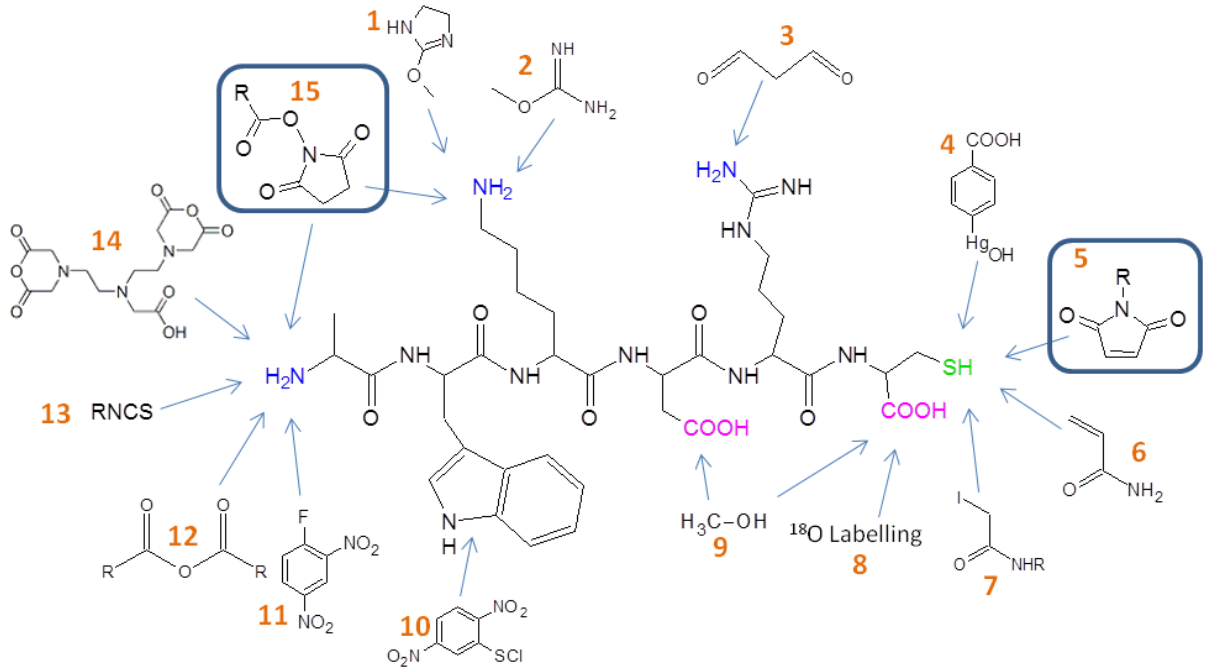

Figure 16: Chemical modification reactions in peptides and proteins. All reactions occurring on the N-terminal α-amino group also occur on the ε-amino group of lysine; adapted from Pieper, Julka and Regnier.[39, 108]
(1) 2-Methoxy-4,5-dihydroxy-1H-Imidazol[109] (2) O-methylisourea[110] (3) malondialdehyde[111] (4) p-hydroxymercuribenzoic acid[112] (5) alkyl-maleimide[113] (6) acrylamide[114] (7) iodoacetamide[95] (8) ^{18}O labelling [115] (9) methanol[116] (10) 2,4-Dinitrobenzylsulfenylchlorid[117] (11) Sanger's reagent[118] (12) carbonic acid anhydride[119] (13) phenylisothiocyanate[120] (14) DTPA-anhydride[121] (15) NHS-ester [122]

Figure 16 lists a number of chemical reactions for derivatisation of reactive groups in peptides and proteins. Most commonly used chemistries for commercially available derivatisation agents are based on maleimido-derivatives (5) or NHS-esters (15). Maleimido-compounds target sulphhydryl-groups, whereas NHS-esters can be used to

modify free amino-groups. Iodoacetamides (7) are usually used to block sulphhydryl-groups in order to keep them from interfering with the following reactions, but they can also be used for modification reactions on cysteine residues. O-methylisourea (2) enhances ionisation efficiencies of lysine-containing peptides through conversion of lysine to homoarginine by guanidination. This can also be utilised to block ε-amino-groups in lysine side chains selectively, so that α-amino-groups are still available for derivatisation. This is due to their different pK_a-values.

Reactions 1-3 were reported to be beneficial for the quality of MS and MS^2 data in terms of fragmentation behaviour and ion intensity of the labelled peptides. Reactions 1, 6 and 8 to 13 can be used for isotopic labelling with either deuterium or ^{13}C-variants of the reagents, enabling relative quantification through differential labelling of two different samples.

2.5.3.2 Isotope Labels

In **SILAC** (stable isotope labelling by amino acids in cell culture), two cell populations are grown in cell culture, incorporating light or heavy AAs in their protein synthesis. The heavy AAs are labelled using ^2H, ^{13}C or ^{15}N. After a few cell divisions with only the heavy AA present, the labelling is close to 100%. Using the fact, that there is virtually no chemical difference between the heavy and light AAs, the samples can be compared directly for differences in expression.[93] The **AQUA** (absolute quantification) approach uses stable isotope labelled standard peptides which can be added in known amounts to the sample prior to MS. Absolute quantification is done using the peak ratios of both the native and the labelled peptides. It can be seen as a variation of isotope dilution analysis (IDA).[123] **ICAT** (Isotope-coded affinity tag) utilises chemical labelling of target side chains in peptides with isotopically marked probes (^3H, ^{13}C). Using light and heavy probes, two samples can be compared to each other. Additionally the probes contain a biotin group which can then be used for avidin affinity chromatography. [95, 96] **ICPL** (isotope-coded protein label) is a similar approach, targeting intact proteins.[100] **Labelling with ^{18}O**: Alternatively a digestion in $H_2{}^{18}O$ can be used to introduce an isotopic label by enzymatic proteolysis (Figure 16-8). The oxygen is incorporated in the C-terminus of the peptide during the cleavage with the proteolytic enzyme. The thereby obtained 'heavy' sample

can be directly compared with a 'light' sample, obtained from a digest in normal water.[97, 98] The approaches in this section are all used with molecular MS.

2.5.3.3 Isobaric Labelling

Another technique applied in molecular MS is based on the introduction of isobaric tags into the analytes. This approach is especially interesting because of its multiplexing capabilities. Several samples can be labelled differentially and then be analysed altogether. The tags have nominally the same mass, ensuring the same chromatographic or MS behaviour for the differentially labelled peptides of the same type. In the course of fragmentation the tags release reporter ions of different masses, which can then be quantified according to their signal intensities, which are directly proportional to the peptide amounts.

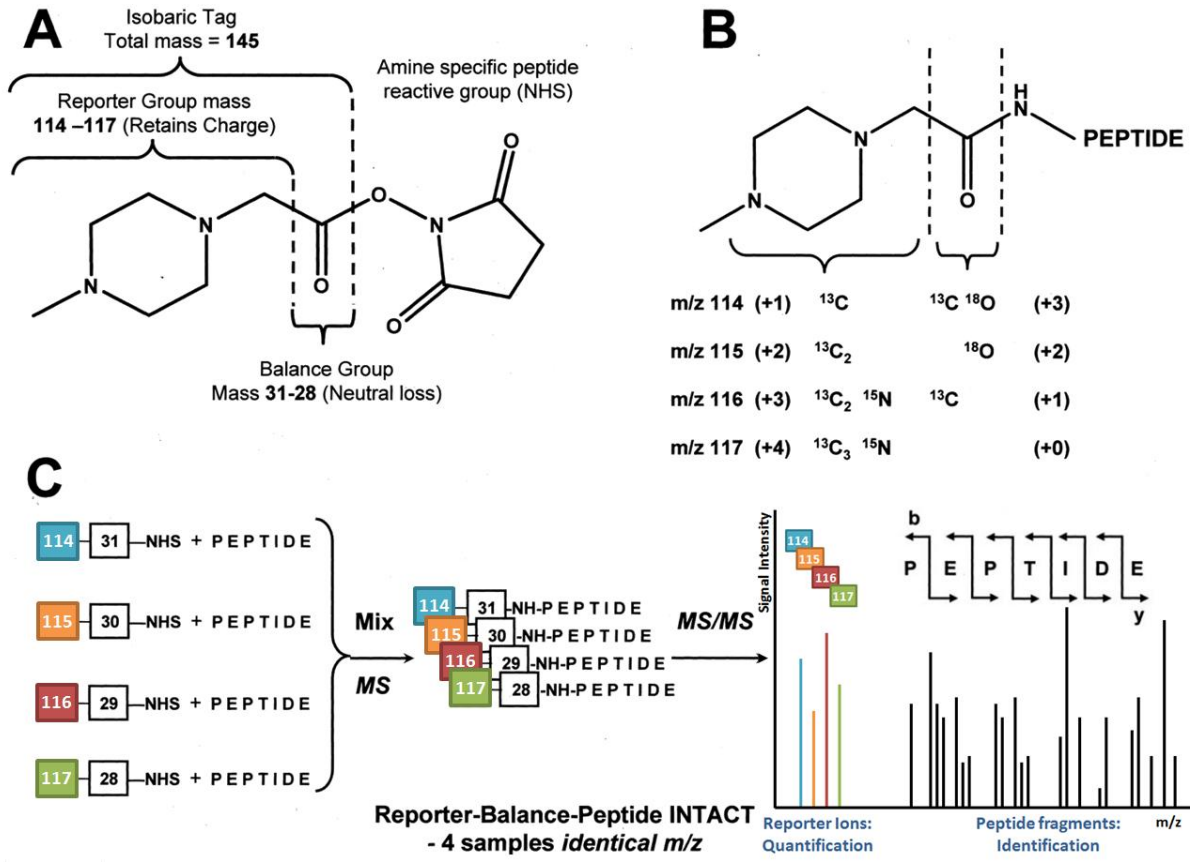

Figure 17: iTRAQ reagent (A), Isobaric variations (B), Reaction, MS and MS^2 Scheme (C), adapted from Ross et al.[101]

Another type of isobaric labels are tandem mass tags (**TMT**), which function in the same way as iTRAQ. The TMT reagents consist of four regions: reporter region, cleavable linker, a mass normalisation region and a protein reactive group. Reporter and mass

normalisation region are balanced by isotopes and upon MS^2 of the precursor of interest, the reporter ions give quantifiable signal intensities.[104]

TMT is currently available up to 10-plex,[124] iTRAQ up to 8-plex.[125]

2.5.3.4 Metal Labels

Making use of ICP-MS for quantification, metal labels offer a good sensitivity due to their high ionisation efficiency (see Figure 5). **Mercury** has a lower ionisation efficiency than most other metals (~50%), but it is known to react readily with sulphur. This is why it reacts easily with the sulphhydryl groups in proteins, which also happens to be one of the reasons for the element's toxicity.[126] The compound used for labelling is *p*-hydroxymercuribenzoate (Figure 16-4).[112, 127, 128] Far less hazardous is the labelling approach using **ferrocene** compounds, where the ICP-MS detectable iron atom is sandwiched in a stable complex between two cyclopentadienyl rings. Together with a linker and a reactive group, such as iodoacetamide[129], maleimide[130] or NHS[131], free amino- or sulfhydryl-groups in proteins and peptides can be targeted. A back draw for ferrocene labelling is the relatively high iron background in biological samples. Another alternative is the attachment of a chelating moiety to the analyte and its combination with a metal of choice: The anhydride of **DTPA** (diethylenetriamine pentaacetic acid, Figure 16-14), can be used for specific derivatization of amino groups. After reaction with the protein or peptide, DTPA can form a stable complex with triple positively charged metal ions, such as lanthanides (complex stabilities in Table 5).[132, 133] DTPA anhydride does not require the introduction of a linker and a reactive group, since it already reacts readily with amino groups.

2.5.3.5 DOTA

Another chelator used for labelling is **DOTA** (1,4,7,10-tetraazacyclododecane-1,4,7,10-tetraacetic acid) which also forms complexes with triple positively charged metals. DOTA-lanthanide complexes are even more stable than the ones formed by DTPA (Table 5) and reagents for peptide and protein labelling can be synthesised/purchased with different linkers and reactive groups, making application possibilities more variable and specific than with DTPA anhydride.

Table 5: Stabilities of lanthanide complexes formed by DOTA, DTPA and EDTA, K being the thermodynamic stability constant[134] adapted from Byegard et al.

Cation	DOTA log K	DTPA log K	EDTA log K
Nd^{3+}	23.3	21.7	16.6
Eu^{3+}	23.5	22.5	17.4
Gd^{3+}	24.7	22.6	17.4
Tb^{3+}	24.2	22.8	17.9
Yb^{3+}	25.0	22.7	19.5
Lu^{3+}	25.4	22.6	19.8

For labelling of amino groups, DOTA-N-hydroxysuccinimide ester (**NHS-DOTA**)[135] and 2-(4-isothiocyanatobenzyl)-DOTA (SCN-DOTA)[136] reagents are available, whereas for sulfhydryl-groups, maleimido-monoamide (**Mal-DOTA**) and iodoacetamide derivatives can be applied. Together with the 14 lanthanides from the periodic table, this provides a large number of potential labels for multiplex analysis in ICP-MS. Additionally it was shown by Gregorius et al. that the DOTA-label enhances peptide detection in MALDI-MS, in particular for Cys-containing peptides.[137] A commercially available labelling kit, using metal-coded affinity tags (**MeCAT**) is adding an affinity tag to the DOTA chemistry mentioned above.[138-141] The affinity tag is attached to the linker between DOTA and the reactive group and it brings ICAT back to mind, where the tagged peptides can also be isolated with biotin-avidin affinity chromatography.

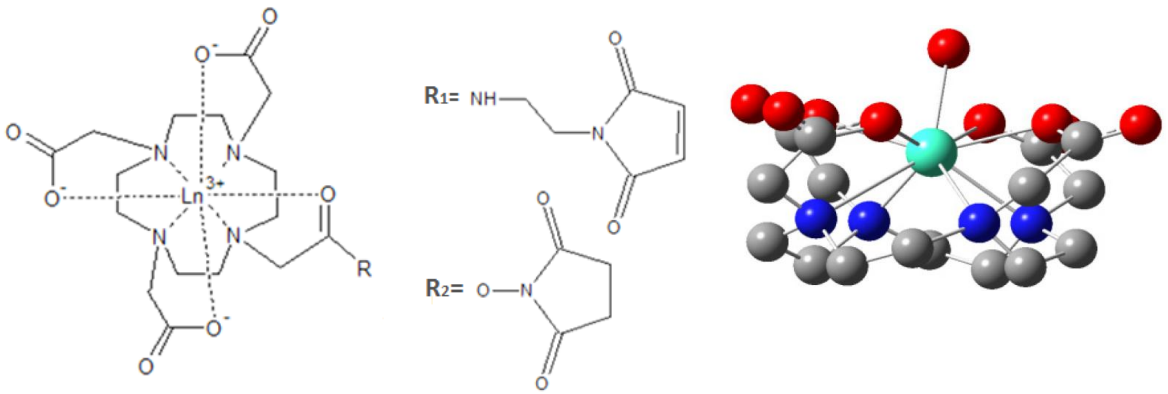

Figure 18 left: Structures of Mal-DOTA (R_1) and NHS-DOTA (R_2), including complexed Ln^{3+} ion. Right: 3-dimensional structure of $Gd[(DOTA)H_2O]^-$. Adapted from Gregorius et al. and Pieper.[39, 137]

2.5.3.6 Lanthanides

Lanthanides are also referred to as rare earths. Even though this name implements that they are indeed rare elements, they are still relatively abundant in the Earth's crust. Taking a look at the least abundant element of the series, thulium, it can be seen that is still nearly 200-times more common than the precious metal gold. As for the most abundant lanthanides such as lanthanum, cerium and neodymium they can be found in a similar abundance to the common industrial metals nickel, copper or lead (Figure 19). Mining and isolation of lanthanides is a very environmentally destructive process, with the demand by the industry for those elements rising continuously. Unlike ordinary metals, lanthanides have very little tendency to concentrate themselves into ore which makes it more complicated to access them.

Lanthanides are commercially used in many everyday products, such as magnets which can be found in electronic devices like computers and loud speakers. Even the lasers used in the ABSCIEX MALDI-MS and the LA-ICP-MS system utilised during this thesis are based on lanthanide doted crystals, such as Nd:YAG.

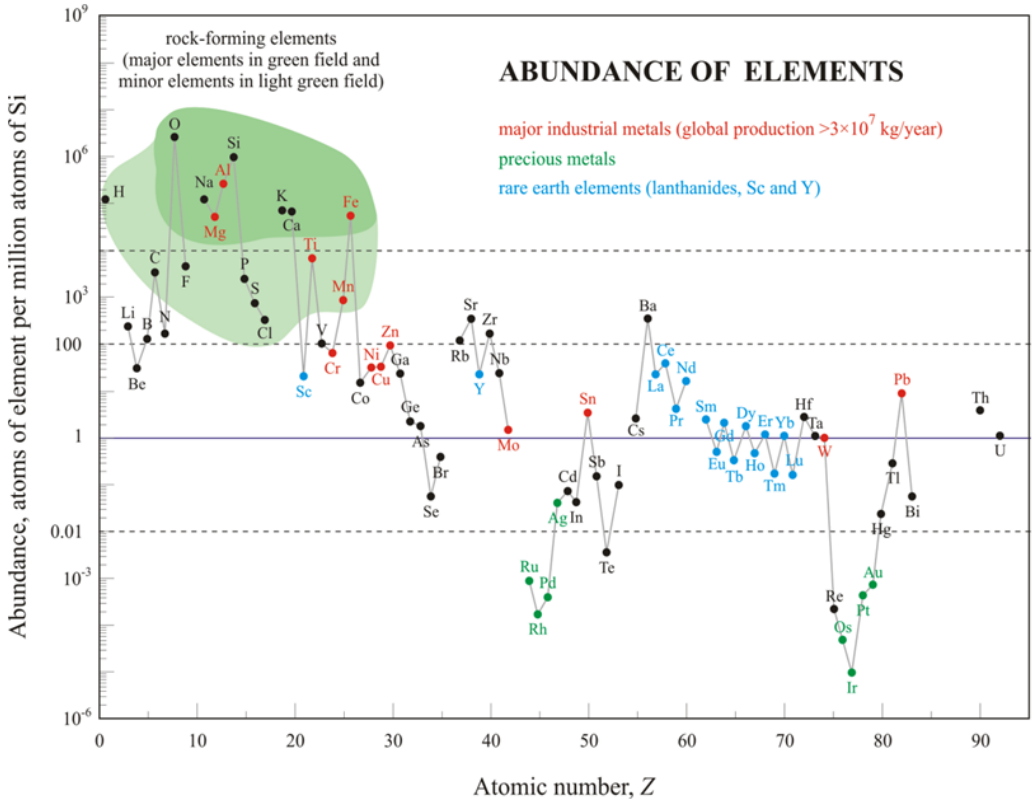

Figure 19: Abundance of the chemical elements in Earth's upper continental crust as a function of atomic number. Lanthanides, La–Lu, and Y are labelled in blue. Adapted from the US geological survey 2002 [142]

Lanthanides are very uncommon to be found in biological samples, which makes them an ideal choice for labelling approaches using chelators. There is virtually no background to be monitored in protein samples, so that the acquired lanthanide signals can be exclusively attributed to the labelling procedure. Another big advantage is the complete ionisation of the lanthanides in the ICP process and the absence of important polyatomic interferences, because of their high molecular mass.

2.5.4 Hyphenated Systems used with ICP-MS and Molecular MS Detection

Figure 20 shows a simplified overview of hyphenated techniques used together with ICP-MS and molecular MS. In this thesis, one major particularity is the uncommon online hyphenation of RP-IP-nanoHPLC to ICP-MS and its combination with MALDI-MS in an offline approach by coupling the same nanoHPLC to a fraction collector. Hyphenations of HPLC with ICP-MS are very common, but need special precautions, since the high amounts of organic solvent employed in RP-LC can hamper with the stability of the plasma. Very often a compromise needs to be found between separation efficiency and plasma stability, leading to limitations of the HPLC flow rate, the use of flow-splits or restriction to isocratic gradients.[143] Alternatively the plasma gas can be modified by mixing e.g. 20 % oxygen into argon. This way the organic solvents can be introduced into the plasma directly. Platinum cones are required with this approach.[144]

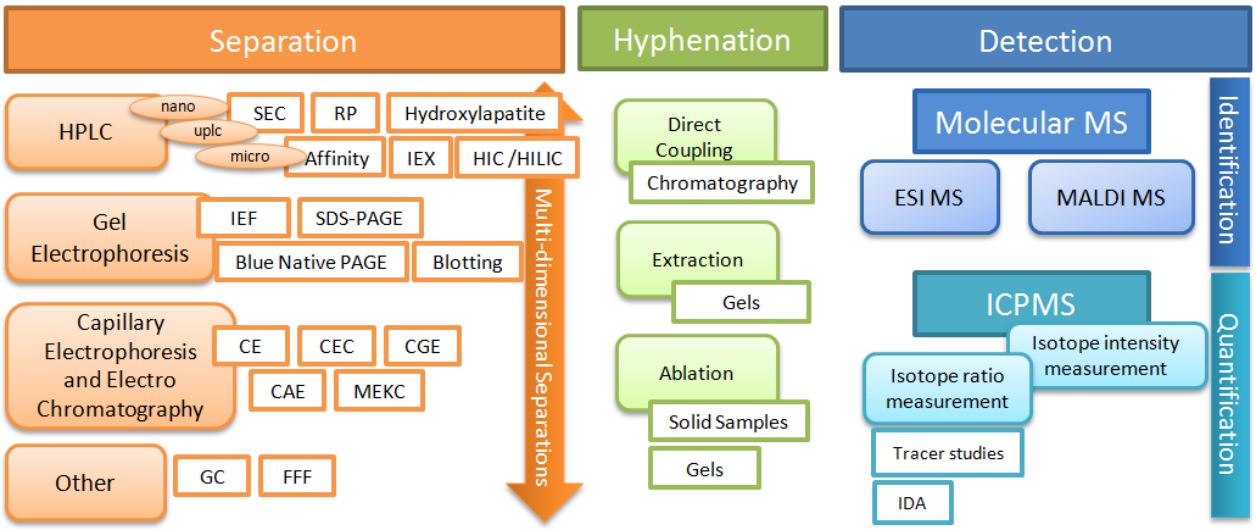

Figure 20: Hyphenated systems used with ICP-MS and molecular MS

These limitations are only one of the reasons why nanoHPLC represents such an attractive option for hyphenation with ICP-MS: one of them is the possibility to apply extremely low sample amounts in nanoHPLC (pmol range), which is a perfect match with the high sensitivity detection of ICP-MS. Also, the flow rates of the nanoHPLC are directly compatible with ICP-MS. For this purpose a custom made total consumption nebuliser was employed during the PhD thesis.[145-148] The outlet capillary of the nanoHPLC (Figure 21-a1) was directly joint with the nebuliser needle (a2) without dead-volume. Like this, the eluting separation can be introduced completely and be nebulised in the nebulisation chamber using argon. The chamber is connected directly to the torch where the sample is ionised in the plasma. The low amounts of solvent do not have an influence on the plasma stability.

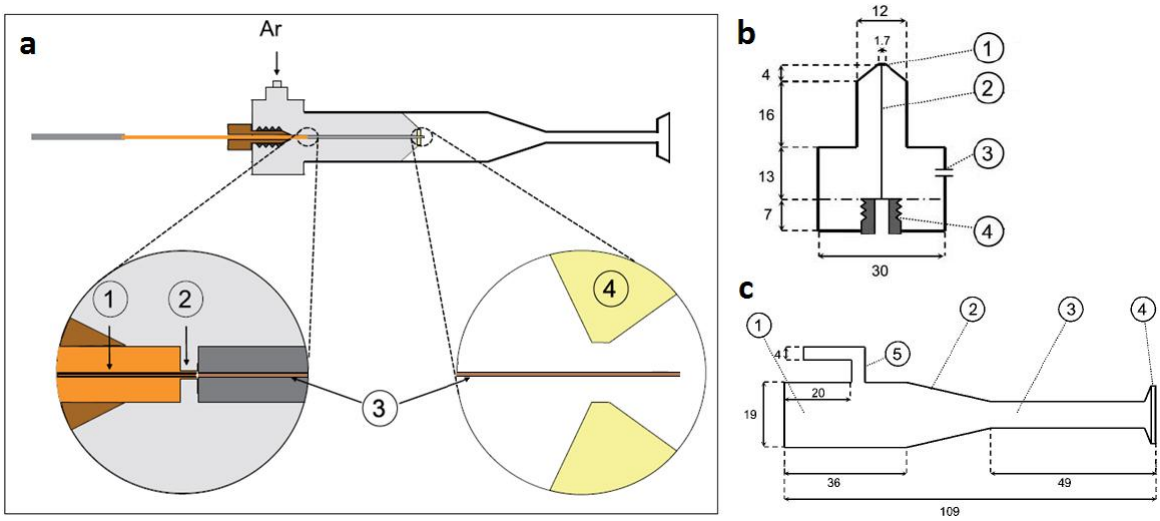

Figure 21: nano-nebuliser for hyphenation of nanoHPLC and ICP-MS. (a) nebuliser scheme with magnifications of (1) the outlet capillary from the nanoHPLC and (2) the dead-volume free connection to the (3) nebuliser capillary and (4) the orifice made of industrial sapphire. (b) Short nebuliser type T1 with (1) orifice, (2) nebuliser capillary, (3) argon inlet and (4) liquid inlet with screw for adjustment of the capillary position. (c) Spray chamber type S2 (12.5 cm^3) with (1) connection to nebuliser, (2) transition, (3) tube, (4) connection with ICP-MS torch and (5) make-up gas inlet.
Adapted from Giusti et al., Rappel and Schaumlöffel. [146, 148]

The downside of HPLC/ICP-MS couplings is the necessity of baseline separation of the analytes, due to the destructive nature of ICP-MS and the loss in structural information. Only by baseline separation, the accurate quantification in ICP-MS can be attributed to the identified analyte species (in e.g. MALDI-MS) without doubt.

In order to acquire the complementary identification data, molecular MS in form of ESI-MS and MALDI-MS can be employed. While for ESI-MS, online coupling to the nanoHPLC is possible, for MALDI-MS, only offline couplings are applicable. This can be both seen as advantage and disadvantage. Advantageous is the fact that the fraction

collection in form of dried droplets prior to MALDI-MS, allows sample preservation. This enables a thorough analysis without time limitation. Also re-measurements of the same spot/sample can be conducted. Another advantage is the fact that the instruments do not need to be in the same laboratory. MALDI-targets are easier to be transported than a whole LC-system. In comparison to e.g. online coupling of HPLC with ESI-MS, one disadvantage lies in the higher time requirements of MALDI-MS based approaches, due to the disconnectedness of the separation and measurement.

2.6 Scientific Context of the Thesis

Table 6 gives a brief overview on current developments in the field of labelling approaches for quantification in combination with detection via ICP-MS. Some of the publications were already mentioned in the sections above. The table starts with publications from 2010, as a follow up to the review by Tholey and Schaumlöffel from the same year.[3]

There are also several other reviews related to the topic which can be recommended for reading, by Pröfrock [149], Wasinger et al. [1] and Sanz-Medel et al.[150]

Even with the rising number of publications in quantitative proteomics, recent developments still mainly concern themselves with relative quantification, mapping out the differences between two or more samples. This also counts for quantitative approaches in protein and peptide analysis, which employ labelling and ICP-MS. Only a fraction of the publications concerns themselves with absolute quantification approaches, comparing the sample to an independent standard and thus providing information on absolute quantities. For absolute quantification, mainly isotope dilution analysis (IDA) is employed. The simplest setup for IDA is the application of an isotopically enriched standard of known concentration which is analysed together with the sample. Using the signal ratios of both isotopes the sample concentration can be determined.[151]

Taking a look at Table 6, it can be seen that most samples consist of purified proteins or synthetic peptides. More complex samples, e.g. tissue samples, cells and groups of proteins were analysed mostly with imaging techniques, employing LA-ICP-MS. For chromatography based analysis, the higher complexity samples consist of purified proteins, most of which are commercially available. This shows that the methods are still

on a ‘proof-of-principle’ stage, mainly working with standard material. None of the techniques has been reported to be valid for application of absolute quantification on complex protein samples or for proteome analysis. This is most likely also due to the separation difficulties which were discussed in the section before.

In this prospect, the global aim of the thesis is the development of new methods that facilitate the analysis of labelled protein and peptide samples on the basis of hyphenations of chromatography with mass spectrometry. For labelling, the versatile DOTA-based compounds were chosen, in combination with mostly mono-isotopic lanthanides. The different labels should be characterised regarding their applicability and behaviour during the separations and detection in both molecular and elemental MS. Different means of separation and purification techniques for the labelled analytes should be inquired.

General obstacles, such as the baseline separation of the analytes, data interpretability or comparability and limitations of sample complexity should be addressed.

A method for absolute sample quantification should be developed, that in the best case is not only applicable on peptide and low complexity protein digests, but also on biological samples and for proteome analysis.

Table 6: Overview –selected publications on labelling approaches in combination with detection via ICP-MS since 2010.

Author	Year	Label	Sample	Separation/other	Detection	Reference
Liu et al.	2010	Au-nanoparticles	Albumin	CE	ICP-MS	[152]
Bräutigam et al.	2010	Ferrocenecarboxylic acid (2-maleimidoyl)ethylamide	Phytochelatins; standard peptides	LC	ICP-MS; ICP-OES; ESI-MS	[129]
Giesen et al.	2011	Iodine	cells and cell nuclei	Imaging	LA-ICP-MS	[153]
Giesen et al.	2011	Ln labelled ABs	breastcancer tissue	Immunohistochemistry; Imaging	LA-ICP-MS	[154]
Jahn et al.	2011	succinimidyl-3-ferrocenylproprionate	Glutathione	LC; EC-LC	ICP-MS; NMR; LC-ESI-MS	[131]
Peng et al.	2011	mercury	carcinoembryonic antigen	SEC; magnetic immunoassay	ICP-MS	[155]
Schwarz et al.	2011	Ho MeCAT-IA, MeCAT-Mal	BSA; β-Lactoglobulin	nano-HPLC	ICP-MS; ESI-MS	[141]
Tang et al.	2011	CdTe quantum dots	urinary proteins	-	ICP-MS	[156]
Waentig et al.	2011	Ln SCN-DOTA labelled ABs	rat liver cytochromes	SDS-PAGE, western blot	LA-ICP-MS	[157]
Waentig et al.	2011	Iodine; IODO-Beads	proteins, proteomes, ABs		LA-ICP-MS	[158]
Zhang et al.	2011	dual label: Eu-Mal-DOTA, fluorescein-SCN	standard peptide	HPLC; CE-LIF	UV, ESI-MS, IDA-ICP-MS	[159]
Zheng et al.	2011	DTPAA with Ce and Sm	standard protein	cation exchange HPLC	ICP-MS	[121]
Esteban-Fernandez et al.	2011	Eu-MeCAT-Mal	lysozyme, BSA	RP-HPLC (fractions); LC	IDA-ICP-MS; ESI-MS	[160]
Bergmann et al.	2012	MeCAT-NHS	standard peptides; E.coli total protein	SDS-PAGE (dissolved); nanoHPLC	FIA-ICP-MS; ESI-MS	[139]

Table 6, continued.

Author	Year	Label	Sample	Separation	Detection	Reference
El-Khatib et al.	2012	dual label: Ln NHS-DOTA; MeCAT-IA	BSA and HSA peptides; standard peptides	LC	ICP-MS	[122]
Esteban-Fernandez et al.	2012	MeCAT	standard peptides; BSA, Lysozyme, Transferrin	2D-LC (SCX; RP)	IDA-ICP-MS; ESI-MS	[138]
Liu et al.	2012	Ru-NHS ester	3 standard proteins	SEC	IDA-ICP-MS	[161]
Moreno-Gordaliza et al.	2012	cis-platin	protein complexes	nanoHPLC; 2D-GE	ESI-MS; LA-ICP-MS	[162]
Waentig et al.	2012	Ln-chelate, MeCAT, MAXPAR	ABs	western blot	LA-ICP-MS	[136]
Yang et al.	2012	Eu-DTPAA	β-casomorphins	CE	ICP-MS	[163]
Yoon et al.	2012	Y, Gd p-aminobenzyl-DOTA	IgG	SPE; PDMS microarray	LA-ICP-MS	[164]
Christopher et al.	2012	microwave assisted NHS-DOTA, Ho Tm Tb	standard peptides	SPE	MALDI-MS; ESI-MS; ICP-MS	[165]
de Bang et al.	2013	Ln labelled ABs	Plant thylakoid proteins; nitrocellulose membrane standard	western blot	LA-ICP-MS	[166]
Konz et al.	2013	CuSO4 pentahydrate	hepcidin-25 (human serum)	HPLC	IDA-ICP-MS; ESI-MS; ELISA	[167]
Liu et al.	2013	Eu NHS-DOTA	bradykinin	LC	IDA-ICP-MS; IDA-GC/MS	[168]
Schwarz et al.	2013	Ln-MeCAT	a-Lactalbumin	LC; HPLC	ICP-MS; ESI-MS	[169]
Waentig et al.	2013	Element tagged ABs	rat liver cytochromes	RP-microarray	LA-ICP-MS	[170]

III Methods

3.1 Material

Detailed information regarding chemicals, consumables and employed equipment can be found in Appendix II, Table 20 to Table 23, starting on page 151.

3.2 Workflow

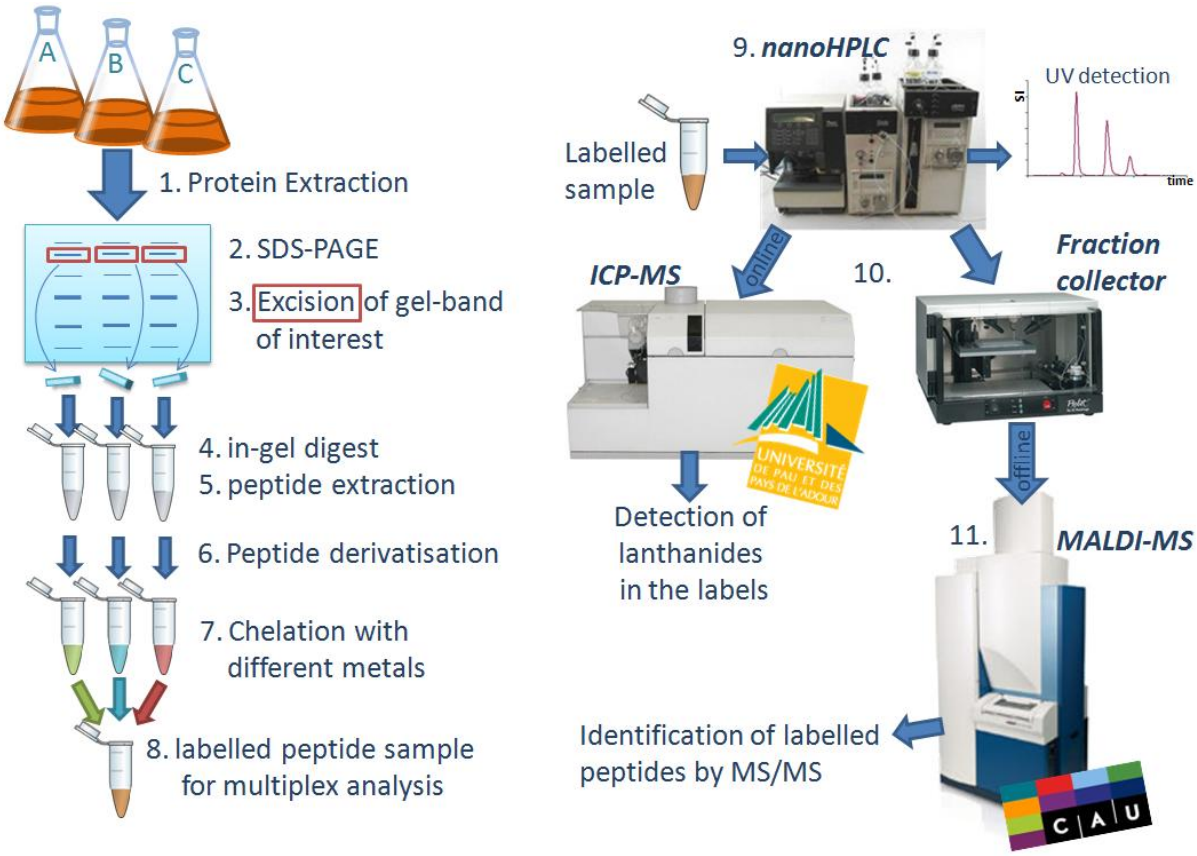

Figure 22: Generic workflow for analysis of biological samples with MALDI-MS and ICP-MS. Instrument photos from manufacturer websites.

Figure 22 shows the generic workflow for experiments conducted during this thesis. Starting point are biological samples, including experimental steps, such as protein extraction, separation via SDS-PAGE and in-gel digestion. When working with single model proteins, no separation is needed and in-solution digestion is performed instead of step 4 and 5. Standard peptides are directly derivatised, starting with step 6.

In general, digest samples were combined with differentially labelled model peptides prior to analysis. The labelled peptide samples were separated via nanoHPLC (step 9).

The nanoHPLC was coupled either directly to an Agilent 7500ce ICP-MS, to obtain information on lanthanide amounts (online analysis) or it was coupled to a Probot fraction collector (step 10). Fractions of the nanoHPLC run were collected as spots on MALDI-target plates. The fractions were mixed directly with the matrix CHCA, dried and the plates shipped to the university in Kiel (CAU). In Kiel they were measured on an ABSCIEX TOF/TOF 5800 MALDI-MS, to obtain information about the identities of the peptides (step 11).

3.3 Methods

3.3.1 Protein and Peptide Handling

In general, peptides and proteins were either stored in lyophilized form or as aliquots in buffered solution (HEPES, 50mM, pH7) at -20°C. Refreezing was avoided and working solutions were kept at 0-4°C up to maximum one fortnight.

It was also found, that the plastic ware used for experiments can hamper with quantitative analysis approaches. Different types of peptides and proteins show different behaviour regarding their unspecific interaction with the surface of the tubes. It was also seen that they might bind irreversibly and be lost during sample preparation. The binding behaviour does not follow strict rules and is not predictable. This is why plastic ware should be evaluated prior to the use with the respective protein and peptide species.[171]

One series of peptide solutions which was stored as aliquots in 200 µL PCR tubes posed problems and was not detectable anymore. Therefore for aliquotation and derivatisation experiments, only high quality Eppendorf low-bind tubes were used for peptide and protein samples. This prevented changes between experiments and ruled out errors which might be caused by the use of different tubes.

Exceptions to this were the use of the special tubes provided with the spin filter cartridges for protein extraction.

3.4 In-Solution Digestion

Solutions: 50 mM ABC; 200 mM DTT in 100 mM ABC; 1 M IAA in 100 mM ABC; 25 ng/µL protease.

For digestion of model proteins, no SDS-PAGE was necessary. Proteins were directly weighed, solved in buffer and digested in solution.

Digestion of 5 µg of the model proteins respectively: proteins were taken up in 50 mM ABC and volumes were adjusted to 100 µL. Reduction was conducted with 5µL of 200 mM DTT at 95°C for 10 min, followed by alkylation using 4 µL of 1 M IAA for 30 min at room temperature in the dark. To deactivate the remaining IAA, the sample was posed in daylight for 10 min. Digest was conducted for 18h at 37°C, using either 4 µL of trypsin or chymotrypsin (25 ng/µL).[172]

3.5 Derivatisation of Peptides and Protein Digests

3.5.1 Derivatisation using NHS-DOTA

Precautions:

The DOTA-NHS-ester is a highly reactive compound. At best, it is to be kept at -80 °C for long time storage and at least at -20 °C if it is used in a regular manner. Since it reacts readily with water, it is also recommended to keep it under a protective atmosphere (e.g. argon or nitrogen) to keep it from degradation. The stability of NHS-esters in general depends on the water content and the pH of the solution: at pH 7 the half-life is about 4 to 5 hours, 1h at pH 8 and only 10 min at pH 8.6. [173] This shows how vital the correct pH is for the derivatisation reaction. There is a need for a compromise between the best derivatisation conditions for the ε-NH_2 groups in the lysyl residues ($pK_a \sim 10.5$) and N-termini ($pK_a \sim 9.5$) and the least destructive conditions for the NHS-ester.

Optimisations:

The NHS-DOTA solution is to be prepared freshly immediately prior to its use. In the former protocol by Gregorius et al. the NHS-DOTA was solved in water-free DMSO.[137] For direct measurement via MALDI-MS, the total reaction volume must not contain more than 4 % v/v DMSO. This did not pose a problem for immediate nanoLC analysis. For lyophilisation and drying by speedvac though, it was found to be more beneficial to solve NHS-DOTA in ACN. This also resulted in the necessity of lowering the total ACN amount during derivatisation. It was supposedly necessary to conduct the derivatisation step in as less water as possible (approx. 15-25 % water). Without DMSO as a solubilising

agent though, salts were precipitating at ACN amounts higher than 80 %, especially after pH adjustment. It was found that it was already sufficient to lower the ACN amount to 70-75 % in order to obtain a homogeneous solution. The derivatisation efficiency between the two protocols did not differ.

Protocol A:

This protocol is the basic protocol used in the beginning and is based on Gregorius et al.[137] Earlier studies, including the ones presented in sections 4.1 to 4.3 employ labellings after protocol A.

Stock solutions: 1 mM TCEP; 1 mM MMTS; 10 mM NHS-DOTA in water-free DMSO; 100 mM HEPES pH 8; ACN; 6 N NaOH; 100 mM TEAA pH 5; 10 mM lanthanide(III) salt in 100 mM TEAA pH 5;

1. **Peptide reduction with TCEP** using a 2-fold molar excess of TCEP per cysteine residue, for 1 h at 60 °C with mild shaking.
2. **Alkylation of free thiol-groups** using a 6-fold molar excess of MMTS regarding free SH-groups, for 10 min in the dark.
3. **Derivatisation of amino groups with NHS-DOTA** using a 100-fold molar excess of NHS-DOTA in regard to free N-termini and ε-amino-groups in Lys residues. Reaction medium: 75 % ACN, 25 % HEPES (100mM, pH 7.5). Reaction for 1 h at room temperature and mild shaking.
   pH control and pH adjustment required: pH 7 for peptides without Lys; pH 7.5-8.5 for peptides with Lys
4. **Stabilisation and chelation** using a 10-fold molar excess of lanthanide-salt solution regarding NHS-DOTA. Reaction for 2 h at 37 °C, mild shaking and pH 5 to 5.5

Protocol B:

This protocol is the optimised version, which was modified from Protocol A. It was used for the later experiments which are presented starting in section 4.4.

Stock solutions: 500 µM TCEP; 1 mM MMTS; 75 mM NHS-DOTA in ACN; 100 mM HEPES pH 8; ACN; 6 N NaOH; 100 mM TEAA pH 5; 1M lanthanide(III) salt in 100 mM TEAA pH 5;

Molarities can be adjusted depending on sample amounts/free reactive groups. Sample volume for each step must not be lower than 30 µL, to avoid complete evaporation/condensation of the solvents in the cap of the tube.

1. **Peptide reduction with TCEP** using a 2-fold molar excess of TCEP (in HEPES) per cysteine residue, for 1h at 60 °C with mild shaking.
2. **Alkylation of free thiol-groups** using a 6-fold molar excess of MMTS (in HEPES) regarding free SH-groups, for 10 min in the dark.
3. **Derivatisation of amino groups with NHS-DOTA** using a 100-fold molar excess of NHS-DOTA regarding free N-termini and ε-amino-groups in Lys residues. Reaction medium: < 75 % ACN including the DOTA-solution, filled up to 100 % with HEPES (100mM, pH 8), including the buffer amounts from the previous steps. Reaction for 1h at 20 °C and mild shaking.

   pH control and pH adjustment required: pH 7 for peptides without Lys; pH 7.5-8.5 for peptides with Lys.
4. **Chelation** using a 10-fold molar excess of lanthanide-salt solution regarding NHS-DOTA. Reaction for 1 h at room temperature, mild shaking and pH 5 to 5.5.

   It was found that the chelation was already near 100 % after vortexing only.

3.5.2 Derivatisation using Maleimido-DOTA

Precautions:

Also the maleinimido-group in Mal-DOTA is prone to hydrolysis and reacts to a half-amide of the modified maleic acid. Therefore a reaction time of more than two hours must be avoided. The Mal-group can also react with primary and secondary amines if they are present in high concentrations. Buffers containing amines, such as TEAB and TEAA must not be used prior or during the derivatisation reaction.

Mal-DOTA, as purchased from Macrocyclics (Dallas, TX), contains non-negligible amounts of acid in form of TFA and hexafluorophosphoric acid as a result of the manufacturing process. pH adjustment with higher amounts of base might be required.

Protocol C:

This protocol was derived from the Gregorius et al.[137] Peptides must not be treated with alkylating agents (IAA or MMTS) prior to derivatisation, which is a standard step in

protein digestion. During digestion, only the reduction step should be performed. The sulfhydryl groups are the Mal-DOTA reagent's target groups and must not be blocked by other modifications.

Stock solutions: 100 µM TCEP; 1 mM Mal-DOTA in HEPES; 50 mM HEPES pH 7; 6 N NaOH; 100 mM TEAA pH 5; 1M lanthanide(III) salt in 100 mM TEAA pH 5;

Molarities can be adjusted depending on sample amounts/free reactive groups. Sample volume for each step must not be lower than 30 µL, to avoid complete evaporation/condensation of the solvents in the cap of the tube, especially during heating.

1. **Peptide reduction with TCEP** using a 2-fold molar excess of TCEP (in HEPES) per cysteine residue, for 1 h at 60 °C with mild shaking.
2. **Derivatisation of sulphhydryl groups with Mal-DOTA** using a 20-fold molar excess of Mal-DOTA regarding free thiol groups. pH adjustment using NaOH (pH must be < 7.5). Reaction in 50mM HEPES, for 2 hours at 37 °C, mild shaking.
3. **Chelation** using a 10-fold molar excess of lanthanide-salt solution regarding NHS-DOTA. Reaction for 1 h at room temperature, mild shaking and pH 5 to 5.5.

Sample is to be used immediately for analysis. Respectively it can be stored as described in Section 3.3.1 lyophilised at -20 °C or for short time at 4 °C.

3.6 nanoHPLC Parameters

Two nanoHPLC systems were employed during the thesis: Instrument 1 was situated in Pau, which was used with a fraction collector or directly coupled to an ICP-MS, while instrument 2 was situated in Kiel, used with a fraction collector for MALDI-MS experiments.

Table 7: Employed nanoHPLC systems and parameters

nanoHPLC systems	
Instrument 1	LC Packings (Dionex) FAMOS, SWITCHOS, ULTIMATE
Chromatographic column	Acclaim® Pepmap100 C18 75 µm I.D., 15 cm in length; particle size 3 µm, pore size 100 Å
Pre-column	Acclaim® Pepmap C18, 0.3 mm I.D. x 10 mm
Flow rate	Loading: 30 µL/min Nano: 300 nL/min
Sample loop	5µL (0.5 – 2.5µL Injection volume)
Instrument 2	Dionex UltiMate 3000 nanoHPLC
Chromatographic columns	Acclaim® Pepmap100, C18, 3 µm, 100 Å, 75 µm I.D. Lengths: 15 cm or 25 cm
Pre-column	Acclaim® Pepmap C18, 0.3 mm I.D. x 10 mm
Flow rate	Loading: 30 µL/min Nano: 300 nL/min
Sample loop	20 µL (2.5 – 10 µL injection volume)

3.6.1 Eluents

Eluent A: Ultrapure water, 0.05 % TFA

Eluent B: 80 % ACN in ultrapure water, 0.04 % TFA

Loading pump: 3 % ACN in ultrapure water, 0.1 % TFA

Eluents for the LC Packings nanoHPLC system were degassed using a constant helium flow. The system was purged on a daily basis.

3.6.2 Employed nanoLC Gradients and Programs

Samples were loaded onto a C18 pre-column after injection. A wash step of 6 min was employed before elution to the analytical column was performed. Optimisation of this wash step is discussed in section 4.1.

After switching of the valve to the analytical column, different gradients were employed, depending on the complexity of the sample (Figure 23). Low complexity samples of labelled model peptides were analysed with a gradient of 5 to 70 % Eluent B in 20 min (red gradient). Low complexity digests of small model proteins were analysed using a

gradient of 5 to 70 % Eluent B in 4 min (green gradient). Digests of SDS-PAGE bands were analysed with a less steep gradient of 5 to 70 % Eluent B in 60 min (blue gradient). Maximum percentage of Eluent B was 95 %, which equals 76 % ACN.

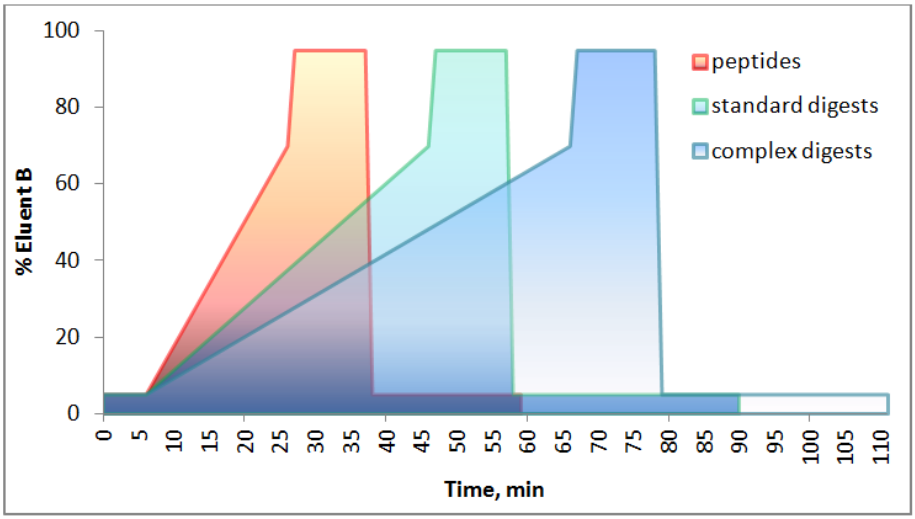

Figure 23: Gradients employed for different sample complexities

3.7 Probot Fraction Collection

For measurement using MALDI-MS, the nanoHPLC system was coupled to a LC Packings Probot fraction collector. Therefore the exit capillary from the Ultimate UV detector was connected directly to the inlet capillary of the Probot using a Teflon connector. Eluting peptides were mixed automatically with matrix solution in a T-junction and spotted in intervals of 15 s on an Opti-TOF 384-well plate. nanoHPLC flow rate was constant at 0.300 µL/min, Probot syringe speed was 0.899 µL/min.

Basic matrix solution:

3 mg/mL CHCA in 70 % ACN (v/v), 0.1 % TFA (v/v), 5 nM Glu^1-fibrinopeptide B (internal standard MALDI-MS).

Erbium matrix solution:

40 µg/L Erbium (internal standard fsLA-ICP-MS), 3 mg/mL CHCA in 70 % ACN (v/v), 0.1 % TFA (v/v), 5 nM Glu^1-fibrinopeptide B.

3.8 MALDI-MS and MS/MS Parameters

MALDI-MS mass spectra were acquired in positive ion reflectron mode by averaging the spectra of 1000 to 2000 laser shots with a laser pulse rate of 400 Hz. 10 subspectra with

200 shots per subspectrum were accumulated. Internal calibration of the MS spectra in LC-MALDI-MS experiments was performed on Glu1-fibrinopeptide B and the matrix cluster signal at m/z of 877.034.

For MALDI-MS/MS, precursor ions were separated using a 300 resolution window in timed ion selection. 2500 laser shots were averaged with a pulse rate of 1000 Hz. For peptide fragmentation, CID with deceleration of the ions to 1 kV was used. The collision gas for CID experiments was ambient air (10^{-6} Torr medium pressure). The fragmentation spectra were manually inspected and analysed with the 'Ion fragmentation calculator' tool embedded in the Data explorer software 4.10. For LC-MALDI-MS/MS analysis, a job-wide interpretation method was employed, selecting the 15 most intense precursors per spot with a minimum signal-to-noise (S/N) of 30.

3.8.1 Protein Identification by Database Search

The MALDI MS/MS data of the respective digests was analysed using Mascot 2.4 in combination with the SwissProt database, which was downloaded in the version from the 15.02.2011. The entries for the search were limited in an appropriate manner:

- to vertebrates, for the digested proteins lysozyme, cytochrome C, α-lactalbumin, β-lactoglobulin

The employed proteolytic enzyme was specified to be trypsin or chymotrypsin, respectively, with a maximum of two missed cleavages. Precursor tolerance was set to 25 ppm and the MS/MS fragment tolerance to 0.4 Da. Variable modifications were chosen depending on the experimental setup:

Table 8: Variable modifications for mascot search.

Variable modifications	Residue, target group	Remarks
Oxidation	Methionine	-
Alkylation (methylthio)	Cysteine, -SH	NHS-DOTA labelling only
Mal-DOTA	Cysteine, -SH	If complexation incomplete
Ln-Mal-DOTA	Cysteine, -SH	Ln : ^{175}Lu ; ^{169}Tm ; ^{159}Tb ; ^{165}Ho ; ^{141}Pr
NHS-DOTA	N-terminus or lysine, -NH_2	If complexation incomplete
Ln-NHS-DOTA	N-terminus or lysine, -NH_2	Ln : ^{175}Lu ; ^{169}Tm ; ^{159}Tb ; ^{165}Ho ; ^{141}Pr

3.9 ICP-MS Parameters

The nanoHPLC was coupled to the ICP-MS using a fused silica tubing (20 µm I.D., 280 µm O.D.), connecting the UV detector's outlet capillary with the nano nebuliser (nDS-200e: nebuliser type T1, spray chamber S2, see Figure 21).[146, 147] ICP-MS operating conditions are listed in Table 9.

Table 9: ICP-MS system operating conditions when coupled to nanoHPLC

ICP-MS System	
Instrument	Agilent 7500ce
Plasma Power	1500 W
Reaction mode	Off
Cones	Nickel skimmer cone (G3270-65024) Nickel sampling cone (G1820-65238)
Nebuliser	nDS-200e, type T1[146]
Spray chamber	nDS-200e, type S2[146]
Nebuliser/carrier gas flow	1.17 – 1.24 L/min
Makeup gas flow	0 L/min
Tuning isotopes	^{166}Er, ^{167}Er, ^{168}Er
Monitored isotopes	^{166}Er, ^{141}Pr, ^{159}Tb, ^{165}Ho, ^{169}Tm, ^{175}Lu

An erbium standard solution was added to the nanoHPLC eluents A and B to a final concentration of 40 µg/L. It was used for monitoring of the signal stability during nanoHPLC gradients and daily tuning of the instrumental settings. Signal behaviour during gradients is shown in Figure 24. The sudden drop in the erbium signal after 520 s is caused due to the valve switching from the trap column to the analytical column and corresponds to the arrival of erbium free loading pump eluent at the ICP-MS detector. Delay between programmed gradient and arrival of the eluents at the UV detector was 2 min, delay between UV detection and ICP-MS detection was 40 sec.

It can be seen that a less steep gradient leads to a slightly more stable erbium signal. Quick changes in the eluents compositions lead to reproducible disturbances, especially in the later part of the chromatography. All peptides are already eluted prior to 4000 s (80 min gradient), respectively 2500 s (60 min gradient), so that the grave disturbance of the signal did not interfere with the peptide signals. The erbium signal was used for normalisation of the peptide signals, during quantification.

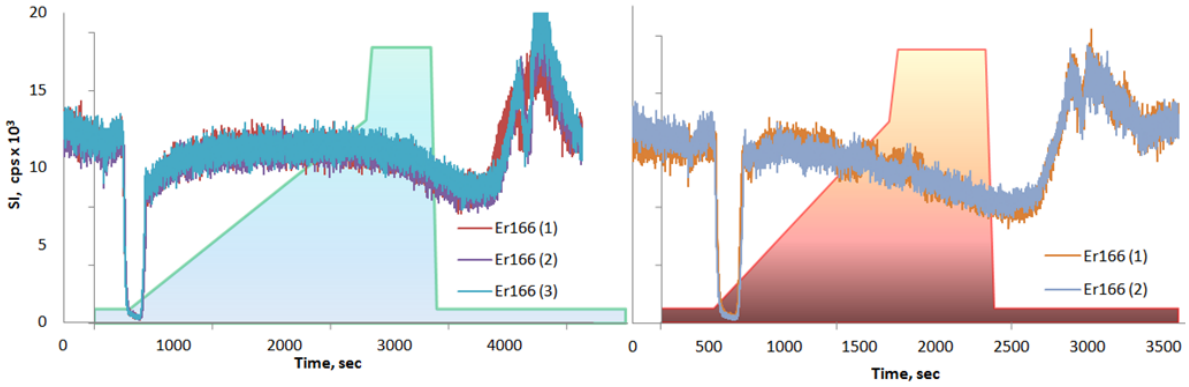

Figure 24: Erbium signals monitored by ICP-MS in the course of chromatography gradients with 4800 sec (left) and 3600 sec (right) length.

3.10 fsLA-ICP-MS Parameters

3.10.1 Instrumental Setup and fsLA-ICP-MS Parameters

Table 10: fsLA-ICP-MS system and parameters

Laser Parameters	**Novalase ALFAMAT**
crystal	Yb:KGW [Yb doped $KGd(WO_4)_2$]
Wavelength	1030 nm
Pulse width	360 fs
Vitesse platine	5 µm/s
Scanner speed	20 mm/s
Repetition rate	1000 Hz
Energy	3 µJ/pulse
Fluence	1.3 J/cm^3
Crater diameter	1350 µm (77 concentric circles)
He gas flow	300 mL/min
ICP-MS parameters	**PERKIN Elan DRC II**
Configuration	Wet
Nebuliser type	PFA µflow (100 µL/min)
Nebuliser gas flow rate	0.7 L/min
Dwell time	5 ms
Sweeps	5
Monitored isotopes	^{166}Er ; ^{175}Lu ; ^{169}Tm ; ^{159}Tb ; ^{165}Ho ; ^{141}Pr ; ^{60}Ni
Power	1050 W

Experiments were conducted using the following instruments: a Dionex U3000 nanoHPLC coupled to a Probot fraction collector and an ABSCIEX TOF/TOF 5800. The matrix was modified by addition of an erbium standard solution, to a final concentration of 40 µg/L Er (see section 3.7). ^{166}Er was monitored as an internal standard during fsLA-ICP-MS. fsLA-ICP-MS was performed on a Novalase ALFAMET high repetition rate IR fsLA-system[174] coupled to a Perkin Elmer Elan DRC II ICP-MS system.

Ablation was conducted by arranging the laser shots in concentric circles (cc). Surfaces between 900 µm and 1350 µm were covered using up to 77 cc. Microscopic images of the different diameters with the cc can be seen in section 4.5.9. 1350 µm was the approximate diameter needed to cover the surface of the faction spots made with the spotter; therefore it was employed for sample measurement after the optimisation step.

3.11 MALDI-Target Plate Design for fsLA-ICP-MS

The LA-chambers diameter was 45 mm, restricting the maximum diagonal of the rectangular target pieces to 44 mm. The targets were cut using a guillotine. A rotary cutter or a saw as means for cutting were ruled out, since they result in a significant distortion of the target surface and might cause unwanted frazzling of the cutting sites. The guillotine shows an equal force distribution during the cutting process, resulting in a better control of possible surface distortions. For TOF analysis, it is imperative to have a perfectly even target surface, to not induce variations in ion flight times. Small differences can be corrected by MALDI-MS calibration.

Two designs were tested for the cutting pattern of the Opti-TOF 384-well plates (Figure 25). Design 1 was found to be less convenient for LA of real samples. The gas flow transporting the ablated particles to the ICP-MS might have different efficiencies, depending on the position of the spot on the long metal pieces. In order to rule out such an effect, a second cut design was developed, with the fractions being spotted in a more centred manner. This is why design 1 was used mainly for preliminary testing and the spotting of standards, whereas design 2 was used for the actual nano-HPLC runs measured with MALDI-MS.

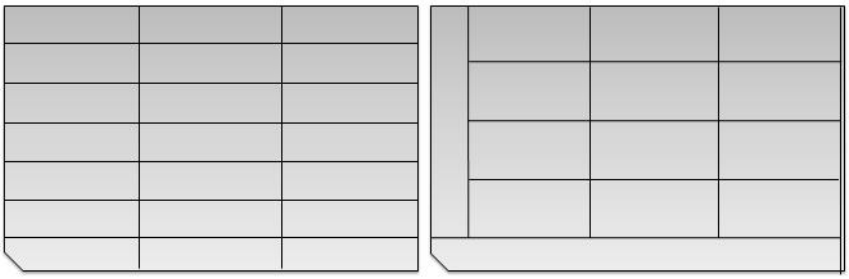

Figure 25: Scheme of the two designs for cutting of the MALDI-targets. Left hand design (1) was used for preliminary tests and spotting of standards, right hand design (2) was used for the model sample.

The plate pieces were fixated on the plate holder prior to sample spotting. The spotter had to be reprogrammed in regard to the z-axis to avoid breaking the spotter's needle due to the 1 cm height difference. Spotting alignment was done with the help of an uncut target: Spot A1 was aligned on the uncut target, the spotter table was then moved down in z-direction. The cut target on the holder was put on the table and aligned with the x and y coordinates of A1 found for the uncut target. The plate holder was then fixated on the spotter table. The spotting scheme is shown in Figure 26. An alternative approach of spotting the cut target prior to its assembly on the target holder results in severe alignment difficulties. It also increases the risk of touching and thereby rubbing off the sample spots. Consequently it was ruled out in favour of the approach using the plate holder.

Design 2 was supposed to be used for measurement of the model sample with both MALDI-MS and fsLA-ICP-MS. For MALDI-MS measurements, the three magnets in the target plate holder had to be removed. They usually serve the purpose of holding the MALDI-target in place during transport and measurement inside the MALD-MS instrument. Unfortunately they were interfering with the fixation of the cut-up plate. The cut pieces were immobilised on the target holder using twin-sided adhesive tape and the magnets on the bottom of the plate holder were causing some pieces to get partly detached from the holder. This can be particularly dangerous during the introduction of the cut plate into the instrument: magnetic arms lift the plate up very abruptly and could cause pieces to detach from the plate holder entirely. If they were to fall off from the holder into the instrument during the loading process, there would be the need to shut down the whole system and get the instrument opened up by the

technical support. Without the magnets, no detaching was observed and the cut up pieces could be analysed without harm to the instrument.

There was also the necessity to block all openings in the plate holder during experiments, when not employing all target pieces. The open holes in the plate holder (e.g. from removed magnets or the bar code area) caused a failure in settling of the source chamber pressure. Application of standard sticky tape was already sufficient to deal with this problem.

3.12 Spotting Pattern and MALDI-MS and MS^2 Calibration Parameters

For MALDI-MS calibration, it was found that it was merely impossible to use the standard calibration spots (marked as 'Cal spots standard' in Figure 26) of the original plate design, since the height differences between the different cut pieces were too big for the TOF analysis. For calibrations using the standard Cal spots, mass tolerance was off by at least 3 m/z, which is intolerable for accurate peptide identification. Plate alignment for automated measurement also posed a problem for spot groups that were spread too far across the target plate. In order to deal with these two problems, new alignment and calibration spots were set for each plate piece, so that calibration and alignment could be conducted independently on each piece. The new calibration spots were spotted in the approximate area by hand, prior to MALDI-MS measurements. For alignment the four outmost spots of each plate piece were chosen. This meant recalibration and realignment in MALDI-MS was to be done three times for a normal LC run, since the fractions were spotted on three plate pieces (four times for LC run 3 respectively).

A set of four to six Cal spots ('Cal spots new' in Figure 26) was provided for each segment of the cut target. Calibration was done on at least four different Cal spots per target piece. Repeated calibration on the same spot can also be used and is accepted by the software. MS-Calibration was conducted on the Cal spots with a min. signal to noise ratio (S/N) of 12, max. mass tolerance of ± 0.5 m/z, min. 5 to 6 calibrant peaks to match and a max. outlier of 5 ppm. MS^2 calibration was conducted with the following parameters: min. S/N of 12, max. mass tolerance ±0.5 – 1, min. peaks to match 4 to 5, max. outlier 30 ppm.

Internal calibration of each sample spot was done using the masses of GluFib and the CHCA matrix clusters, as already described in section 3.8.

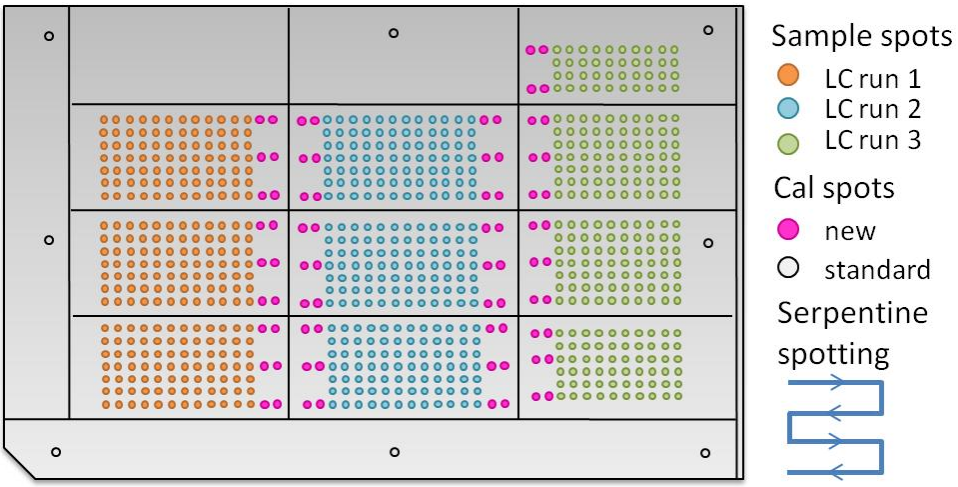

Figure 26: Spotting scheme for LC runs on cut target design 2.

3.13 Microscopy

The target plates from the LA-ICP-MS experiments were examined using a Leica dfc 280 microscope.

The employed objectives were: X5 0.12 bd, X10 0.25 bd; X20 0.40 bd; X50 0.75 bd

Photos were taken using the software “Leica im50 IAccess”, which provided the respective scale for each magnification.

IV Results

4.1 Pre-Cleaning Experiments

Due to the derivatisation procedure which employs high amounts of salt (200- to 1000-fold molar excess of lanthanide ions regarding target groups in the molecule), sample pre-cleaning is a substantial need. Not only does the excess in salt impact ionisation efficiencies in ESI- and MALDI-MS, it also hampers co-crystallisation of the matrix with the analyte. Furthermore and most importantly it leads to a significant background during ICP-MS analysis, potentially impairing quantitative approaches. The excess metal causes a tremendous peak in the beginning of the chromatography, which tails throughout the whole chromatogram. This leads to an elevated, indefinite background, which can impair detection of less abundant peptide species. It was also reported that the unbound metal-complexes can cause an additional peak later in the chromatogram, which coelutes with the analytes. [129, 132, 133, 175]

Examples from publications on different labelling approaches which do not include pre-cleaning steps are shown in Figure 27.

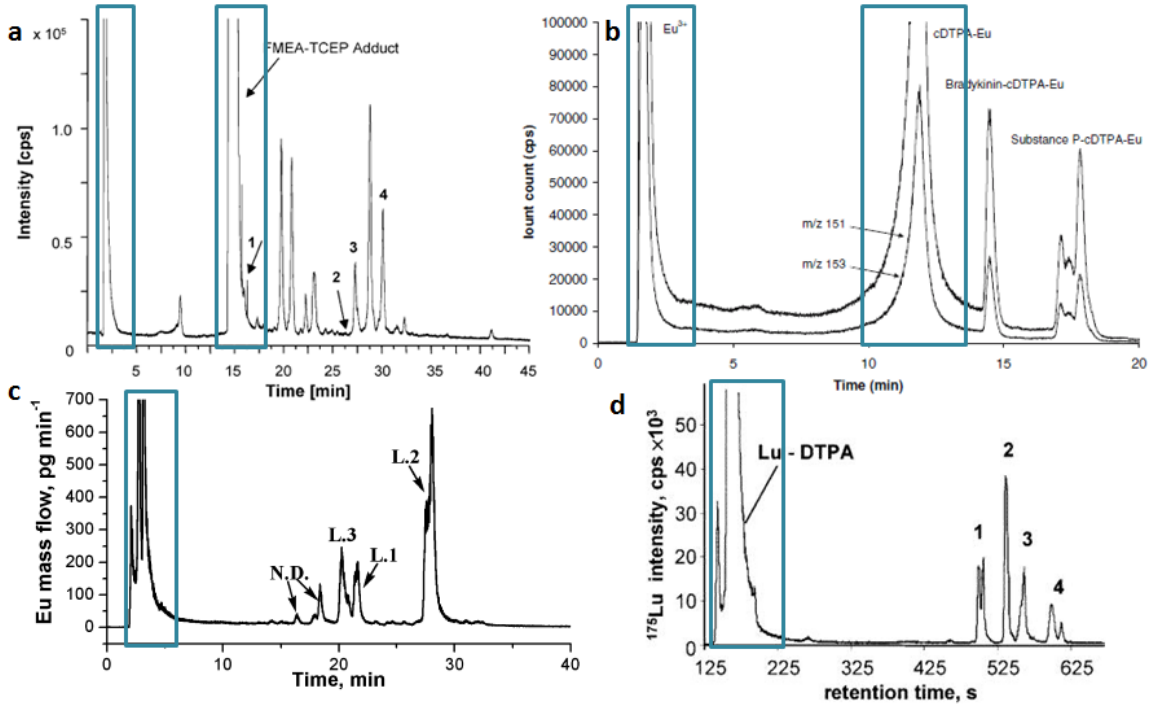

Figure 27: Selected figures from publications on labelling approaches, without pre-cleaning step prior to LC-ICP-MS analysis. (a) Ferrocene based approach by Bräutigam et al.[129] (b) DTPA based approach by Patel et al.[132] (c) Mal-DOTA-based labelling by Yan et al.[175] (d) DTPA-based labelling by Rappel and Schaumlöffel.[133]

In each of the examples, the high peak of excess metal / reagent can be seen (marked with the blue boxes). Especially in Figure 27 a and b, the coelution of analytes with the excess reagent can be observed. The height of the excess peaks in the figures cannot be determined, since the scale is commonly cut off in favour of the analyte peaks.

A multitude of purification methods is described in Section 2.3.1. Methods, such as ultrafiltration (UF) or solid phase extraction (SPE) are employed in addition to the sample analysis itself in an offline manner. This additional sample treatment contributes to the risk of sample alteration, by e.g. introduction of impurities. Also, the absolute amounts of the analytes can be lowered, leading to changes in the overall sample composition by discrimination of certain analyte species according to their properties.
As an offline purification approach, SPE is commonly implemented in most proteomics laboratories (e.g. in the form 'ZipTips'). In the following section an approach employing ZipTips as a representative of offline purification will be discussed. SPE was employed together with nanoHPLC for analysis with ICP-MS, in order to elucidate the merits of SPE for a lowered metal background.
Part of the results in this section are published in Holste et al. 2013[4]

4.1.1 Offline Purification with Solid Phase Extraction

ZipTip® pipette tips are available with different stationary phases and different capacities. For a SPE recovery test, C18 ZipTips were chosen and applied using the Merck Millipore standard protocol with 0.1 % HFBA (heptafluorobutyric acid) instead of TFA. The protocol states that other ion pairing reagents can be used as an alternative to TFA. [176]

nanoHPLC-ICP-MS measurement of the peptide mixture with and without ZipTip C18 treatment showed that more than 95 % of the sample was lost during treatment (Figure 28 a). The treated sample was eluted from the ZipTip and taken up in the same volume as the initial sample. Both samples were analysed in a multiplex approach. The loading buffer contained 0.1 % HFBA, Eluents A and B contained TFA.
Significant losses were not only found when employing HFBA. Same observations were made in SPE experiments employing ZipTips with 0.1 % TFA. The panels (b) to (f) show samples that were treated accordingly, followed by nanoHPLC-ICP-MS analysis of both the ZipTip eluate as well as the 'remnant' solution. The remnant comprises all liquids

other than the eluate which had contact with the ZipTip during treatment – namely wash solutions after peptide binding and the solution that was carrying the peptides prior to binding. By only applying 2.5 µg of labelled peptide, it was taken care, that the maximum capacity of 5 µg was far from being reached. To further ensure binding, ACN from the derivatisation reaction was removed completely from the samples and they were solved in 0.1 % TFA. Binding and elution was performed with 20 cycles minimum. The remnant solutions and the elutates were lyophilized and both taken up in the same amount of loading buffer, immediately before injection. None of the interfering substances listed in the userguide were present during SPE.

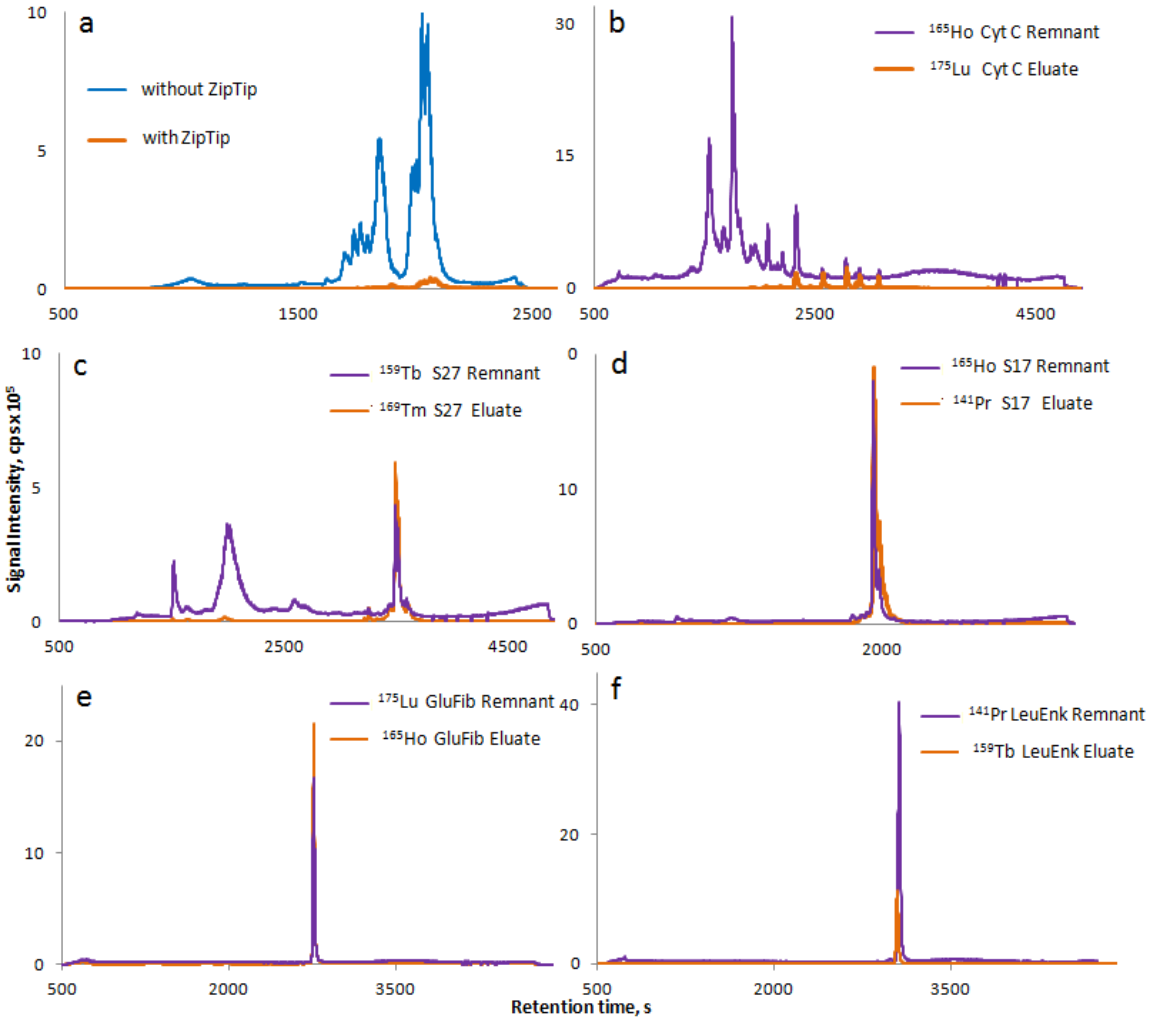

Figure 28: Monitored peptide recoveries after SPE with ZipTip C18, multiplex analysis of labelled peptide mixtures via nanoHPLC-ICP-MS. (a) Mal-DOTA labelled peptides A, B, C, with and without ZipTip treatment. (b) through (f): NHS-DOTA labelled peptides treated with ZipTip: eluate (orange) versus remnants/supernatants from the ZipTip treatment (violet). (b) Cytochrome C digest, (c) S27 (d) S17 (e) GluFib (f) LeuEnkephalin. Partly published in Holste et al. 2013 [4]

Figure 28 b shows a NHS-DOTA labelled Cytochrome C digest that was treated with SPE as decribed. It can be seen that only a fraction of the digest's peptides were bound by the C18 material of the ZipTip. The binding of the earlier eluting (more hydrophilic) peptides is obviously discriminated. This trend can also be seen for the labelled model peptides (sequences in Table 24). When run altogether in a multiplex, their elution sequence is S17 – S27 – GluFib – LeuEnk, following the GRAVY index from most hydrophilic to most hydrophobic. The GRAVY values can be seen in Table 24 on page 154, the value for S27 is not comprising phosphoserine, therefore being too high.
Peptide recovery is worst for LeuEnk (Figure 28 f), the most hydrophobic peptide, which is most likely due to its relatively low molecular weight (5 AA). The other peptides have an average length of 14 AA, equalling almost three times less single peptides to be bound by SPE for the same sample amount. For S17 (d) the losses in the remnant and the recovery in the eluent are almost equal, whereas for S27 (c) and GluFib (e) the recoveries are slightly above the losses. This is consistent with the observations in the Cyt C digest. (Quantification data for the digest can be found in Appendix III, section 9.3)

Table 11: Recoveries for the respective peptide samples in Figure 28 (c) to (f)

Sample	Label	Total counts	% recovery
S17 Eluate	Pr141	59 931 765	61.4
S17 Remnant	Ho165	37 677 021	38.6
S27 Eluate	Tm169	18 129 159	20.9
S27 Remnant	Tb159	68 755 268	79.1
LeuEnk Eluate	Tb159	28 318 326	23.7
LeuEnk Remnant	Pr141	91 342 627	76.3
GluFib Eluate	Ho165	40 104 458	56.2
GluFib Remnant	Lu175	31 241 809	43.8

This leads to the conclusion that SPE, at least in form of C18 ZipTips is not an option for sample cleanup, if quantitative analysis is to be conducted afterwards. Metal backgrounds are significantly lowered, but come along with tremendous peptide losses. Especially hydrophilic peptides do not seem to bind properly to the C18 resin, even when using HFBA as an ion pairing reagent.

4.1.2 Online Pre-Cleaning using a Trap Column

Apart from the observed peptide losses in the case of C18 ZipTips, offline purification steps are often time consuming and can have a bad influence on an experiment's reproducibility – if the purification is not by any chance automated. The alternative is an online purification, which can for example be implemented in the chromatographic routine.

The nanoHPLC systems employed in this thesis already comprised a precolumn which is mainly used for sample pre-concentration and protection of the fragile chromatographic column. The analytical column, a C18-resin filled capillary (I.D. 75 µm), is preceded by a short C18-precolumn with a higher diameter (I.D. 0.3 mm), which will not be clogged easily by impurities and can be cleaned by a back flush, if it should be necessary. The injected samples will be trapped on the precolumn and then be eluted with the same flow direction onto the analytical column. The time period before switching onto the analytical column can be programmed freely. This allowed for a series of experiments determining the optimal parameters for an online purification approach, employing the precolumn for the removal of low MW compounds, such as metal ions and metal-complexes.

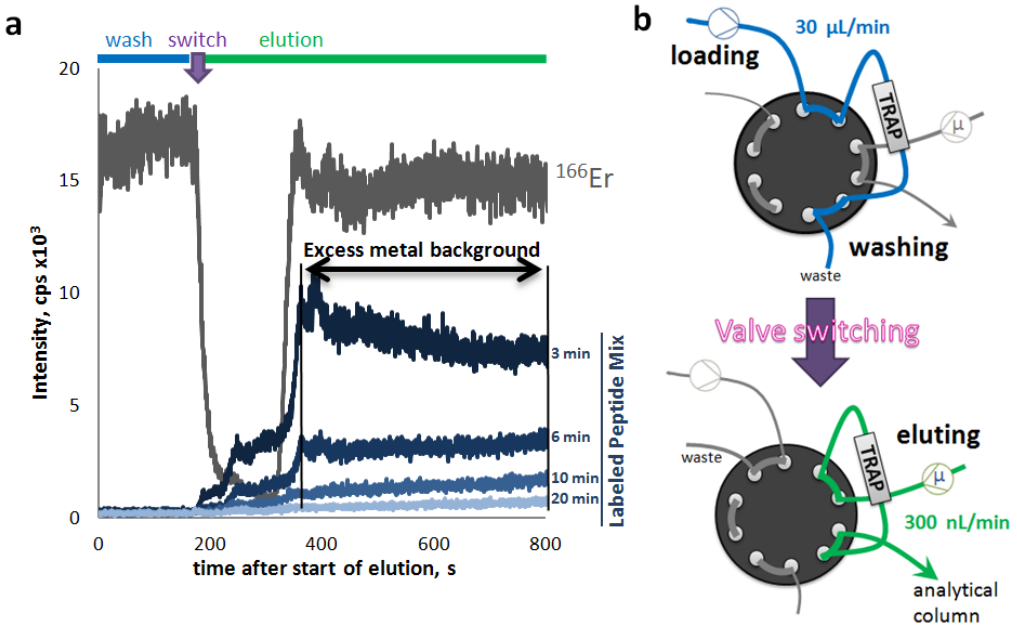

Figure 29: (a) Raw signals of metal backgrounds for a ^{165}Ho Mal-DOTA labelled peptide mixture, treated with different precolumn wash lengths. Lowest background found for 20 min. (b) Principle of valve switching between precolumn/'trap' washing (blue) and elution from the trap column to the analytical column (green).
Original data from Holste et al. 2013 [4]

Figure 29 a shows the background signals in ICP-MS for a series of experiments with wash steps of different lengths, (b) shows the connectivity of the 10-port valve and the principle of the valve switch (violet) between the precolumn wash (blue) and the elution to the analytical column (green). These phases of the analysis are also marked in (a) at the top of the diagram: During the washing of the precolumn, the signal for the internal standard erbium (grey) – found in both eluents A and B, stays steady, since the precolumn is bypassed. After the switch of the valve from position 10_1 to position 1_2, the ^{166}Er free loading buffer gets washed off the precolumn, causing the sudden drop in the erbium signal for the length of the trap column's eluent volume. The ^{166}Er signal rises and goes back to a steady level upon arrival of the gradient at the detector. At the same time the signals for the metal background of the samples rise accordingly, depending on the length of the wash step.

With reference to Figure 27 (page 69), no large excess reagent/metal peak in the beginning of the elution can be observed. Only the background of the 3 min flush shows a slight elevation in the beginning. The others show a steady background right from the start. It can also be observed, that the metal background is significantly lowered for the wash steps longer than 3 min. Percentages for the background (Figure 30, left) were calculated with the 3 min wash equalling 100 % background. With 6 min pre-cleaning, the background level is already reduced by 63 %. After 10 min it is diminished by 86 % and with a wash length of 20 min it can be further decreased to up to 93 %. At the same time significant peptide losses for more hydrophilic peptides were found, starting with a 10 min wash time (Figure 30, right). After 20 min, peptide C stayed mostly unaffected with a loss of approximately 6 %, whereas more than 75 % of peptide A and more than 25 % of peptide B were lost.

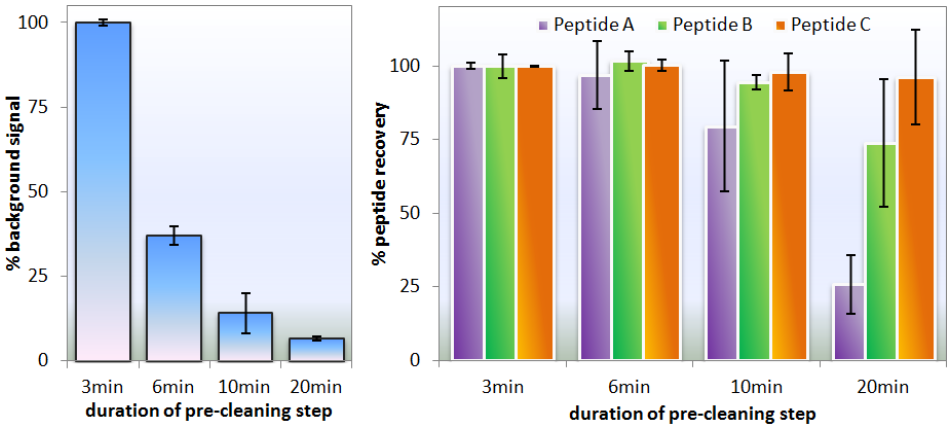

Figure 30: Decrease in background signal in percent with elongation of the wash step (left) and peptide recoveries in percent for the three Mal-DOTA labelled model peptides A, B and C for the different wash lengths (right), both diagrams with 3 min being 100 %. Average of 4 independent experiments. Original data from Holste et al. 2013, supporting information.[4]

Figure 31 shows five nanoHPLC-ICP-MS chromatograms for ^{165}Ho labelled peptides, treated with different wash lengths. The first four chromatograms correspond to the backgrounds shown in Figure 29 a. The three Mal-DOTA labelled peptides A, B and C can be clearly distinguished in those four chromatograms, with peptide A being marked by an 'A'. Taking a direct look at the peak area of peptide A after the 20 min pre-cleaning step, the decrease in peptide recovery is evident.

Another observation to be made is that metal backgrounds are generally very low, compared to the actual peptide signals. Already the 3 min wash step shows a background signal of only 1.24 % of peptide C's peak height. This is further lowered to 0.44 % for 6 min, 0.13 % for 10 min and lastly 0.08 % for the 20 min wash. The reference to peptide C was chosen, because it did not show a significant loss in recovery.

In contrast to the Mal-DOTA labelled peptide mixture, the NHS-DOTA labelled variant shows a significantly higher background. This is due to the 5-times higher excess in NHS-DOTA reagent utilised during derivatisation and the overall higher number of free amino-groups in peptide mixtures and digests, consecutively leading to the application of higher amounts of lanthanide salts. The elevated number of reactive groups is also responsible for the different peak profile of the NHS-DOTA labelled peptide mixture, due to possible double derivatisations. Even with the higher background for the NHS-DOTA mixture, no large excess peak in the beginning of the chromatography as seen in Figure 27 (page 69), can be found.

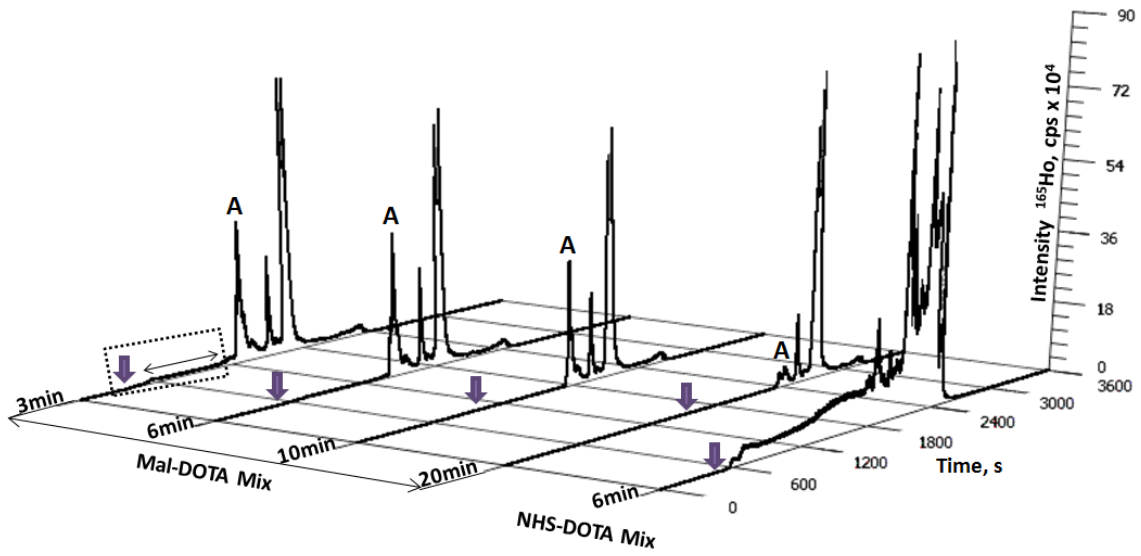

Figure 31: nanoHPLC-ICP-MS chromatograms for the ^{165}Ho labelled peptides A, B, C: Four chromatograms showing Mal-DOTA labelled peptides treated with different wash lengths and additionally, the same mixture labelled with NHS-DOTA and after 6 min washing. Peptide A is marked 'A', the arrow shows the moment of the valve switch. The double-sided arrow corresponds to the part of the chromatogram considered as the background signal (as shown in Figure 29 a). Original data from Holste et al. 2013 [4]

4.1.3 Conclusions

It was shown that the background can be significantly reduced by this simple online pre-cleaning step, which is easy to implement in common HPLC systems. Already 6 min washing decreases the background signal by more than 60 % (compared to the 3 min flush), while guarding quantitative recovery of the peptides. This was deemed to be the optimised parameter, since a 10 min flush already shows significant peptide losses for the more hydrophilic peptide species.

4.2 Eluent Additives

In the course of nanoHPLC optimisation, several additives were tested in the eluent of the loading pump. The standard ion pairing reagent TFA was compared with the more hydrophobic HFBA for analysis of hydrophilic peptide species (structures, see Figure 32). EDTA was employed in order to test whether it would aid the lanthanide metal removal during the washing step.

Part of the results in this section are published in Holste et al. 2013[4]

4.2.1 Ion Pairing Reagents

Ion pairing (IP) reagents are used in RP-HPLC setups to enhance the separation of ionisable and highly polar substances, which show low or no interaction with the RP-material of the stationary phase. Most RP-HPLC setups use a pH below 3. This usually leads to very good separation results and is due to several different effects, depending on the acid employed. In general, interactions between acidic compounds and the silica support of the packing material are suppressed through the complete protonation of both by the acid. Fluorinated acids, such as TFA are often used with RP-HPLC, mainly for acidification during peptide and protein analysis.

Fluorinated acids show several advantages, such as pH stabilisation during analysis and volatility, so they can be removed from the sample if necessary. Most importantly they supposedly ameliorate peak shapes and allow control of selectivity and retention. Several studies lead to the conclusion that this is due to interactions between basic residues in the peptides and the carboxylic group in TFA. However another study concluded that ionic and hydrophobic interactions with the RP-material are involved.[177]

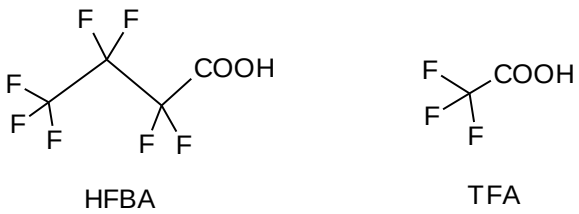

Figure 32: Ion pairing reagents for RP-HPLC. Heptafluorobutyric acid (HFBA) and tetrafluoroacetic acid (TFA)

Very hydrophilic peptides are known to have a very poor retention on RP-columns.[178] Since this is also the case when TFA is used as an IP reagent, great losses for hydrophilic

peptides were expected during the online precleaning. This is why a very hydrophilic model peptide Hy (ESLSSSEE) was chosen and the application of a more apolar fluorinated acid, HFBA (Figure 32) for the trapping on the precolumn was tested. HFBA was employed with a percentage of 0.1 % (v/v) in 3 % ACN/water to replace the standard loading buffer. Eluents A and B stayed the same and contained TFA.

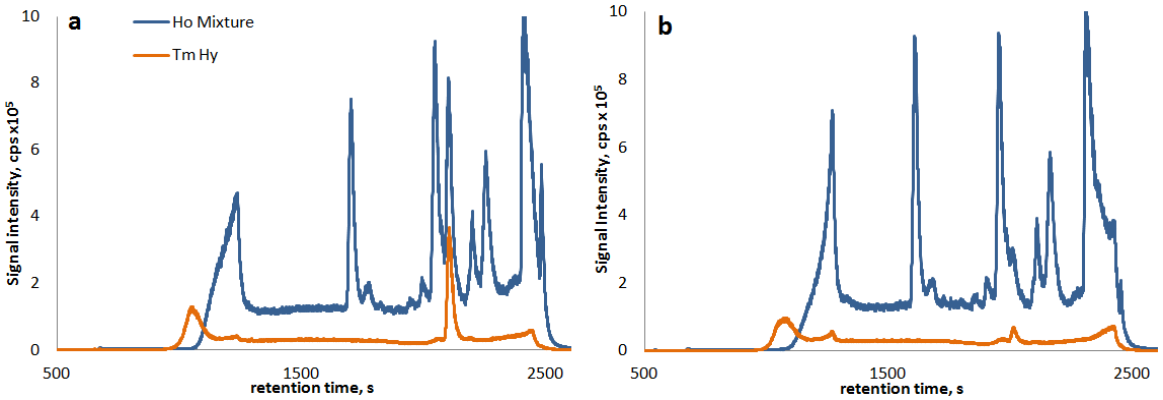

Figure 33: nanoHPLC-ICP-MS analysis of DOTA-labelled peptide mixtures, using 0.1 % HFBA in the loading buffer. Loss of the peptide signal for peptide Hy after reinjection. Original data from Holste et al. 2013, [4]

Chromatograms for these experiments were acquired using nanoHPLC-ICP-MS. Figure 33 shows the chromatograms for a ^{165}Ho NHS-DOTA labelled peptide mixture (blue) including Hy, which was analysed alongside the ^{169}Tm labelled single peptide Hy (orange). In (a) the sample was injected immediately, while (b) represents the same sample reinjected after two hours. Hy can be easily identified within the peptide sample because of the labelled single peptide which was measured in parallel. In both runs, the peak pattern for the normal model peptides stays virtually the same. Surprisingly a loss in recovery for the labelled peptide Hy was observed upon reinjection of the same sample. Already after five hours the labelled peptide could not be detected anymore (not shown). The other synthetic peptides seem completely unaffected by this effect.

In order to understand these findings, a closer look was taken at the applied parameters: The freshly labelled samples for these experiments were stored as aliquots at -20 °C in 100 mM TEAA at pH 5. Immediately before injection the labelled peptide samples were acidified by addition of TFA to a final concentration of 0.1 % (v/v) TFA for optimal binding on the trap column. After the first injection, the sample was kept at ambient temperature in the autosampler and was reinjected after two and five hours. The result

was confirmed in a second experiment series with a freshly prepared sample that showed the exactly same effect.

One possible explanation for the effect might be a hydrolysis of the bond between the peptide and its label over time. The addition of 0.1 % TFA creates a highly acidic environment (pH 2-3) which might induce acidic hydrolysis of labile bonds. In this case, the structure of the peptide must have a special influence on the stability, given the fact that the other peptides were not affected. For verification, it was tried to track the loss of the label with MALDI-MS, but neither of both Hy peptides, labelled or unlabelled, could be detected.

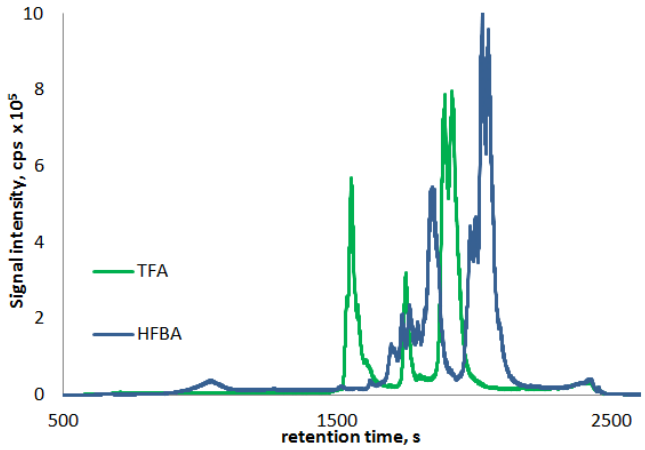

Figure 34: Difference in retention behaviour after nanoHPLC-ICP-MS analysis of Mal-DOTA-labelled peptide mixture (peptides A, B, C) with different loading buffers: 0.1% TFA (green), 0.1% HFBA (blue). Original data from Holste et al. 2013, [4]

In addition to the findings for the recovery of the hydrophilic peptide, it was found that the use of HFBA has a significant influence on the retention behaviour of the model peptide mixture (Figure 34). With the same gradient, peptides that were easily separated using TFA could not be separated anymore when employing the same amount of HFBA in the loading buffer. The carryover of HFBA from the trap column to the analytical column was deemed to be the cause of this change in retention. It was also shown, that the metal background with HFBA was significantly higher than with TFA, including a broad peak in the beginning of the elution, as seen in both Figure 33 and Figure 34. Metal background when employing HFBA instead of TFA is elevated by 145%, whereas peptide recovery stays the same as with TFA (Figure 35, last column pair).

The altered retention behaviour alongside with the elevated background lead to the decision not to follow the approach employing HFBA any further. All in all, it was found

that very hydrophilic peptides can be retained and detected using HFBA. For future applications, HFBA, applied in lower concentrations than 0.1 %, can be taken into consideration for the targeted analysis of hydrophilic peptide species. For routine analysis though, it seems to be more disadvantageous than beneficial.

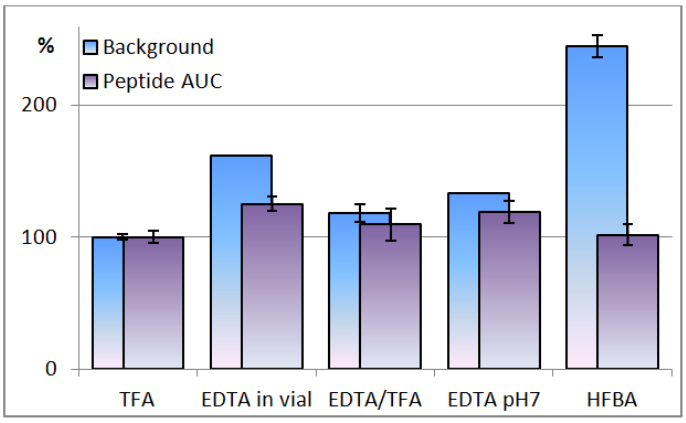

Figure 35: Background and peptide peak areas in % for different loading buffers, with TFA set as 100 %. TFA (0.1 % TFA, 3 % ACN), EDTA in vial (EDTA added to sample vial, normal loading buffer), EDTA/TFA (1 mM EDTA, 0.1 % TFA, 3 % ACN), EDTA pH7 (1 mM EDTA, 3 % ACN), HFBA (0.1 % HFBA, 3 % ACN). n=2

4.2.2 EDTA

In this study, the loading buffer was modified by addition of the chelator EDTA. As shown in Table 5, EDTA forms far less stable complexes with the lanthanide ions than DOTA (log K difference ~ 6 orders of magnitude). EDTA was applied to aid the removal of unbound metal ions during the wash step, consecutively enabling a shorter wash step. EDTA was chosen over e.g. DTPA, since the applied chelator must not compete with the already present DOTA complexes. For further avoiding competition, EDTA amounts added to the loading buffer were calculated in a way, that the amount of EDTA applied during the wash step equalled the amount of unbound metal from the injected sample. Calculations were based on the injected excess metal amount, the flow rate of the loading pump and the length of the EDTA wash step.

General experimental setup: The labelled peptide sample was loaded onto the precolumn with standard loading buffer for 1 min. Then the precolumn was flushed for 2 min with the modified EDTA buffer, followed by another 3 min wash step with standard loading buffer. The last step was applied to avoid a carryover of EDTA onto the analytical column.

In a first experiment 1 mM EDTA was added directly to the standard loading buffer (3 % ACN, 0.1 % TFA, pH 2-3). After application and analysis, the background was not lowered

in the slightest. On the contrary, the background seemed to be elevated in comparison with the standard 6 min wash step (see Figure 35, 'EDTA/TFA'). A possible explanation can be the low pH of the loading buffer, which might impair the proper complexation by EDTA. Optimal complexation with EDTA is achieved in mildly basic medium. The second attempt was therefore conducted with a TFA-free EDTA loading buffer (3 % ACN, 1 mM EDTA, pH 7), which was applied in exactly the same way as above. After analysis, the samples still showed an elevated background (Figure 35, 'EDTA pH7'). Same result was found with an alternative procedure, where EDTA was added directly to the sample vial prior to analysis. The equivalent amount of EDTA to the unbound lanthanide ions in the sample vial was added and the sample analysed using the 6 min standard wash step. The background was also elevated (Figure 35, 'EDTA in vial'). At the same time it was found that the peptide peak heights in all of the experiments were elevated.

In conclusion, EDTA did not benefit the metal removal, neither during the wash step nor as an additive in the sample vial. It rather seems to impair the removal of the unbound lanthanide ions. In addition, peptide recoveries when employing EDTA are also elevated in an unpredictable manner:
When employing EDTA with TFA, the background is elevated by 20 %, while peptide recovery is elevated by 10 %. When applying EDTA at pH 7, the background is elevated by 30 %, while peptide recovery is elevated by 20 %. When adding EDTA directly to the vial, background is elevated by 60 %, with a 25 % higher peptide recovery.
The EDTA approach was not deemed beneficial for the analysis, so it was not followed any further.

4.3 Superposition of MALDI-MS and ICP-MS Data via UV-Detection

For identification of the labelled peptides in ICP-MS chromatograms, ICP- and MALDI-MS data have to be aligned. Some difficulties were encountered regarding this task, since varying retention times of up to 2 to 3 min were observed between chromatograms recorded with the nanoHPLC coupled to the nano-nebuliser in the ICP-MS setup and the ones recorded when the nanoHPLC was coupled to the Probot fraction collector for later use with MALDI-MS. Those differences cannot be caused by only the lengths of the fused silica tubings employed in both setups. It rather seems to be a result of the

different backpressures caused by the gas flow in the nebulizer and the matrix dosage by the syringe in the Probot. While the Ar gas in the ICP-MS setup is flowing alongside the capillary in the nebulizer in order to carry the droplets into the torch in form of a fine mist, the Probot is giving a constant active backpressure through the syringe which doses the matrix. For the latter, the outlet capillary of the nanoHPLC is connected to a T-junction, which joins the matrix-dosing syringe and the nanoHPLC outlet capillary with the spotting needle. This is necessary for the mixture of the sample with the matrix before fraction collection on the target. nanoHPLC flow is set to 300 nL/min, while the flow of the matrix is set to 900 nL/min. The backpressure caused by the three times higher flow rate seems to have quite an impact on the retention times.

To overcome these difficulties, the analysis of low complexity samples, such as standard peptide mixtures and digests from single proteins (lysozyme, cytochrome C, α-lactalbumin and β-lactoglobulin) were taken as a starting point. In those cases, the peak patterns can usually be recognised easily in both UV-chromatograms acquired from the separate nanoHPLC runs. After alignment of the UV-trails, the ICP-MS and MALDI-MS data can be aligned accordingly. An example for the alignment of a simple peptide mixture is shown in Figure 36.

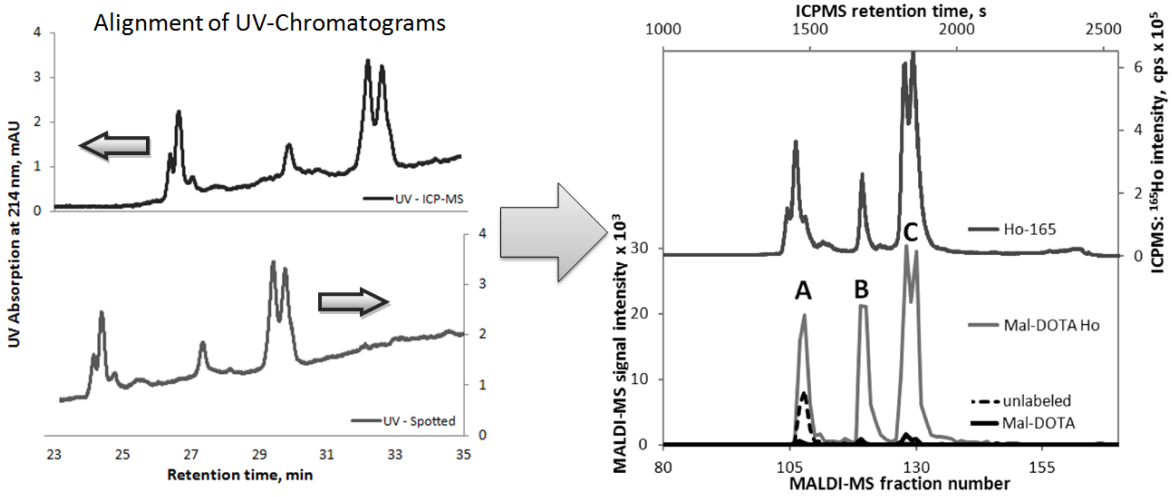

Figure 36: Example for the superposition of MALDI-MS and ICP-MS data of a simple three peptide mixture. Alignment was achieved using the respective UV-chromatograms (left). Identified peaks from MALDI-MS are assigned to the detected signals in ICP-MS (right). Original data from Holste et al. 2013, [4]

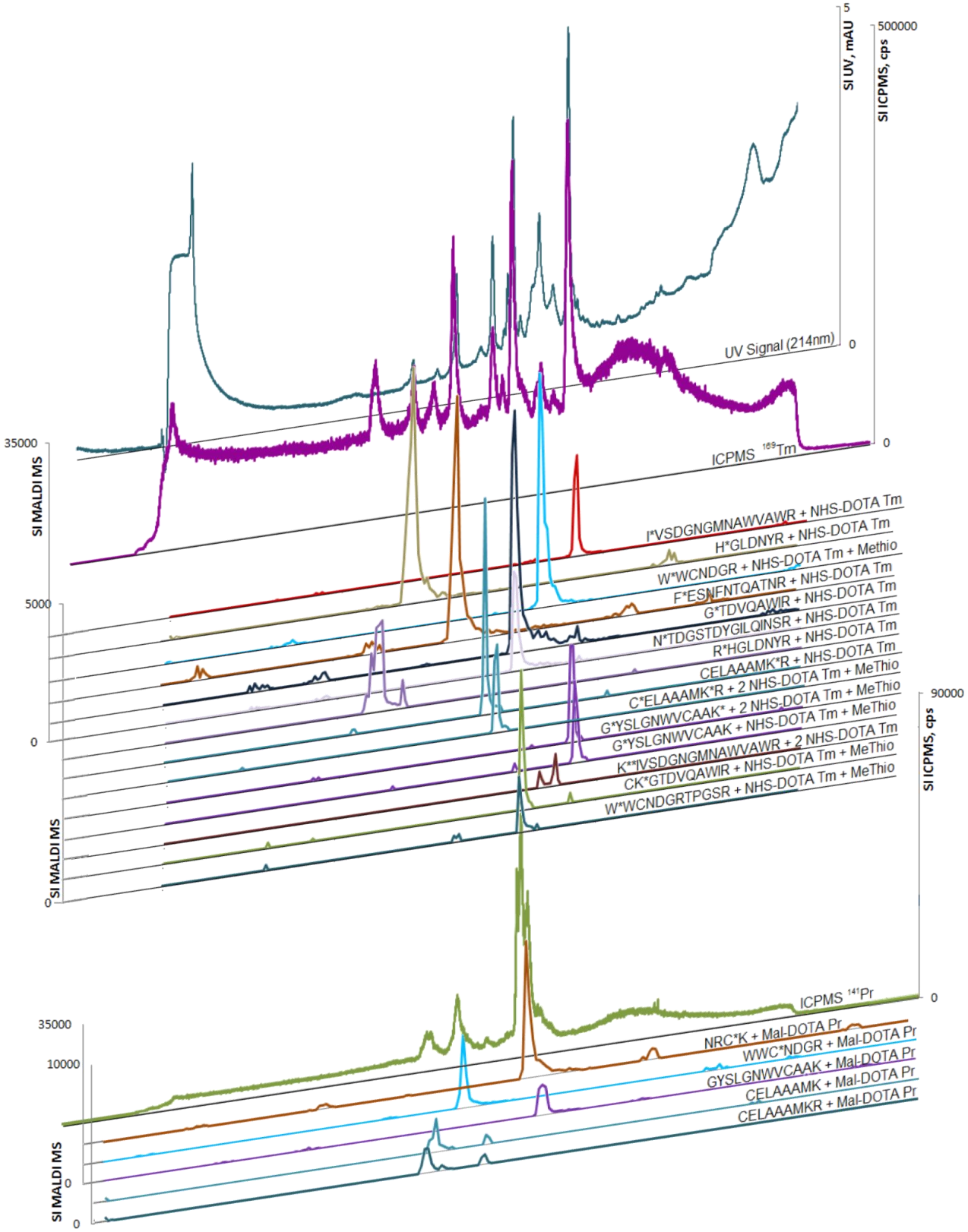

Figure 37: Overlays of nanoHPLC (UV 214 nm), ICP-MS and MALDI-MS data for a ^{169}Tm NHS-DOTA and ^{141}Pr Mal-DOTA labelled tryptic digest of chicken lysozyme.

The peptide mixture consisted of the three ^{165}Ho Mal-DOTA labelled synthetic peptides A, B and C (sequences in Table 24). Since Mal-DOTA can form stereoisomers (see reaction scheme in section 9.5.1), this leads to characteristic split-peaks in the chromatograms, which in the case of peptide C can be seen with all three detection methods. The formation of stereoisomers was reported before by several groups.[39, 160, 179] After alignment of the UV-chromatograms the retention time shift between the two methods was applied to both MALDI- and ICP-MS data, resulting in the unambiguously assignment of the identified peptide peaks – in form of extracted ion chromatograms (XICs), to the respective signals acquired in ICP-MS.

The same alignment principle was employed for a labelled lysozyme digest and is shown in Figure 37. The digest was labelled with both DOTA-reagents separately, employing different lanthanides for each reagent. Thereafter, the samples were pooled for multiplex analysis in ICP-MS. They were spotted separately for analysis in MALDI-MS. The labelled peptides were identified and XICs were generated. Even though the online precleaning was employed, the ^{169}Tm background in the ICP-MS chromatogram is elevated. This is due to the application of NHS-DOTA, which needs to be employed with a very high excess of the reagent, leading to an accordingly high excess in lanthanide ions. Nonetheless the elevated background did not interfere with data interpretation. There is only a small excess peak in the beginning, and the background stays on a steady level.

Being more complex than a simple peptide mixture, it was far less evident to recognise the peak patterns in both UV chromatograms. In this case, the alignment was still a success and the XICs could be assigned. Already for the peptide mixture in Figure 36, the signal intensities of the labelled peptides differ between MALDI- and ICP-MS and UV-detection. When taking a closer look at the signal intensities of several peptides in the lysozyme digest in MALDI- and ICP-MS, it can also be seen that intensities are not always comparable: for example the second, third and last peptide peak in the ICP-MS chromatogram of ^{169}Tm have different intensities. In MALDI-MS the second peptide of the thulium series is among the most intense peaks, while in ICP-MS it only shows a medium intensity. The third peptide was not detectable using MALDI-MS and the last peptide seems to be less intense in MALDI- than it is in ICP-MS detection. This shows yet

again, that MALDI-MS is very limited as a stand-alone technique for absolute quantification, if not used with specially developed approaches.

A simple correction factor for the alignment cannot be determined, since the retention times of the chromatograms were not only shifted, the chromatograms were also stretched horizontally.

Since the digest shown above was not completely labelled, a coelution of labelled and unlabelled peptides could be observed in the latter MALDI-MS fractions (Figure 38).

Data regarding the identified peptides in MALDI-MS can be found in Appendix 9.1.

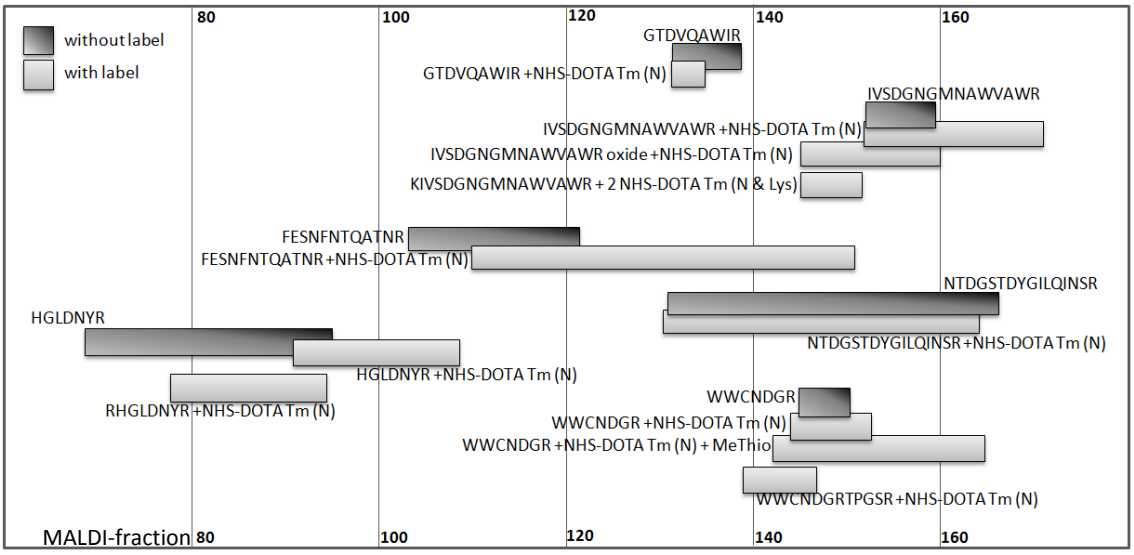

Figure 38: Overlapping elution of labelled and unlabelled peptides of a tryptic lysozyme digest, detected with MALDI-MS^2

For more complex samples, a differentially labelled model peptide mixture was developed. These peptides with known quantities should be applicable for absolute quantification and as retention time markers in more complex samples. With the marker-peptides distributed throughout the chromatography, the alignment should be simplified, since they are specifically detectable with both techniques, independent from the labelled sample itself: in ICP-MS, the label containing a differently chosen metal will be detected, while in MALDI-MS, the m/z ratio and the following MS^2 can be applied for identification, by e.g. the use of an inclusion list. (Approach shown in section 4.6)

4.3.1 Sequence Coverage for Labelled Digests

Three model proteins were chosen and digested with trypsin: lysozyme (LYSC_CHICK), α-lactalbumin (LALBA_BOVIN) and β-lactoglobulin (LACB_BOVIN). Additionally, a cytochrome C (CYC_BOVIN) digest from Dionex was employed. After labelling of the

tryptic digests with both Mal- and NHS-DOTA (protocol C and A), the samples were analysed both with ICP-MS and MALDI-MS. In the following step the sequence coverage was studied. The nanoHPLC-ICP-MS chromatograms and sequence details can be found in Appendix 9.2.

Data in Table 12 is based on MALDI-MS measurements and consecutive Mascot search. For labelling with NHS-DOTA all peptides contain target groups for the reagent, whereas Mal-DOTA only targets peptides containing cysteine residues. This is why peptides for the NHS-DOTA series are categorised in 'labelled' and 'not detected', while for Mal-DOTA also sequences and peptides are listed that are no target for the reagent.

Table 12: Sequence coverage in percent for differentially labelled model protein digests and detected peptides using Mascot search

Protein	NHS-DOTA		Mal-DOTA	
	Sequence coverage	N° of detected peptides (mascot)	Sequence coverage	N° of detected peptides (mascot)
Lysozyme	67.35 % labelled 32.65 % not detected	19 labelled 6 unlabelled	28.89 % labelled 28.57 % not detected 42.18 % no target	5 labelled target 3 unlabelled target 16 peptides in total
α-Lactalbumin	49.30 % labelled 50.70 % not detected	13 labelled 5 unlabelled	33.80 % labelled 29.58 % not detected 36.62 % no target	4 labelled target 1 unlabelled target 6 peptides in total
β-Lactoglobulin	68.54 % labelled 31.46 % not detected	11 labelled 3 unlabelled	13.48 % labelled 25.28 % not detected 61.24 % no target	3 labelled target 0 unlabelled target 13 peptides in total
Cytochrome C	50.48 % labelled 49.52 % not detected	16 labelled 2 unlabelled	N/A	N/A

It was found that for each protein, between 32 % and 51 % of the sequence could neither be detected in form of labelled nor unlabelled peptides. The overlap of the undetected sequences in both the Mal- and NHS-DOTA experiments hinted that it is not a problem of the derivatisation itself: taking a closer look at the undetected sequences and their hydrophobicities, it was found that all of the resulting peptides are most likely very poorly soluble in water (positive GRAVY values). Therefore it cannot be ruled out that they are lost prior to or during their analysis. No precipitate was visible during sample treatment, which is not a surprise regarding the very limited concentration range

of the experiments (pmol to nmol per µL). For nanoHPLC analysis, peptide mixtures were diluted to a 5 pmol/µL solution in 3% ACN, 0.1 % TFA. The low amount of ACN might not be sufficient for solubilisation of highly hydrophobic peptides. On the other hand, it is also possible that the interaction between these hydrophobic species and the C18 material of the columns is too strong. Very hydrophobic peptides might not be eluted with the employed gradients (max. 76 % ACN). Another possibility is that these peptides are not ionisable in the MALDI process. Thus they are not visible in the MALDI-MS chromatograms and spectra, while they might still be detected with ICP-MS. This could also explain the peaks observed in ICP-MS, which show no match when compared with peptides identified by MALDI-MS. The example in Figure 39 confirms this assumption: signal intensities (SI) for peak 1 and 2 are in the same range in ICP-MS, with peak 1 being more intense. In contrast to this the SI for peak 1 in MALDI-MS is far lower than the SI of peak 2. This hints towards a lower ionisation efficiency of peptide 1. It can be assumed that peak 3 has an even lower ionisation efficiency than 1, so that it was not detectable with MALDI-MS and MS^2 anymore, but on the contrary still shows a prominent peak in ICP-MS.

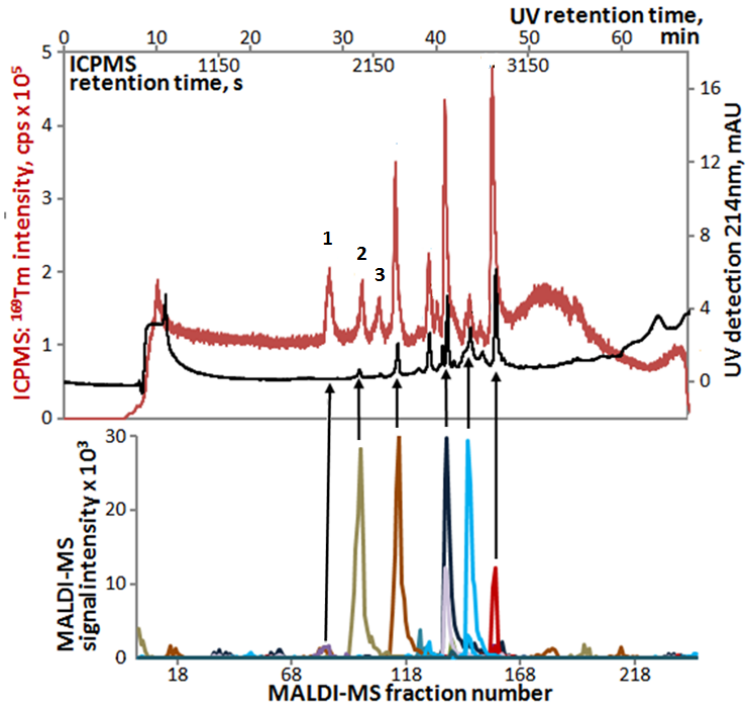

Figure 39: Extracted ion chromatograms (MALDI-MS, below) attributed to the corresponding peaks in the ICP-MS chromatogram. SI for peak 1 is very low in MALDI-MS, peak 2 has a very good SI, whereas peak 3 did not show a match in MALDI-MS.

To conclude, for quantification approaches with this nanoHPLC setup, a set of target peptides has to be chosen carefully. It should be made sure that they are detectable

with MALDI-MS. Incomplete derivatisation at this time point still posed a problem. Mascot search identified several peptides that were only partly labelled. In addition, double derivatisations occurred which further contribute to sample complexity. When a doubly and singly labelled peptide coelute, quantification is merely impossible, since the ratio between the two peptides is unknown. In contrast to this, application of Mal-DOTA leads to far less complex ICP-MS chromatograms and can be considered as an alternative for NHS-DOTA in order to obtain more conclusive data.

In theory, only a few completely labelled peptides should be sufficient for a reliable quantification, due to the theoretically equal proportion of the peptides in the digest. Therefore the aim is to identify these peptides in order to conduct an absolute quantification.

4.4 Labelled Model Peptides for Quantification in nanoHPLC ICP-MS

Aim was the development of the mentioned set of labelled standard peptides (sequences in Table 24) which could be used as a standard for quantification purposes. The chosen peptides should cover the major part of the chromatogram and they should be well characterised in terms of their quantities. They could also be used for simplifying the alignment of data acquired with ICP-MS and MALDI-MS, which will be discussed in section 4.6.

4.4.1 Labelling of Model Peptides and their Quantification

The set of model peptides was labelled separately using NHS-DOTA according to protocol B. The NHS-DOTA labelled single peptide solutions were split into three equal parts and complexation was performed with different lanthanide salt solutions. The lanthanides for each peptide were chosen in a way which would allow the generation of three peptide mixtures, each containing five differentially labelled model peptides.

In order to be able to use these peptides as standards, quantification needed to be performed. For quantification via ICP-MS total metal analysis, the excess metal employed during derivatisation had to be removed in order to determine the concentration of the peptide bound metal only.

Peptide samples after derivatisation and complexation were dried using a speedvac – mainly for ACN removal. The samples were then resolubilised in 0.1 % TFA and treated

with C18 ZipTips according to protocol, for excess reagent removal. After elution the samples were lyophilised as aliquots and kept at -20 °C for later use.

For quantification using ICP-MS total analysis, the instrument was tuned using a rare earth tuning solution with a concentration of 500 ng/L for each metal in 2 % HNO_3. Monitored elements: ^{141}Pr, ^{159}Tb, ^{165}Ho, ^{169}Tm, ^{175}Lu. Sensitivity for the respective elements: approximately 25 000 cps with a RSD between 2.5 and 3.4 %.
A dilution series of the respective metals in 2 % HNO_3 was prepared, ranging from 0.5 ng/L to 1000 ng/L. This concentration range was chosen, since the amounts of the labelled peptides were limited. A minimum of 2 mL sample solution was needed for the total metal analysis. The lyophilised peptide samples were each solved in a matching amount of 100 mM TEAA (pH 5) to reach a concentration of 100 µg lanthanide per litre: around 500 µL were used, depending on the employed lanthanide. These solutions were further diluted using 2 % HNO_3, to be in the range of the dilution series. The first dilutions analysed (approximately 10 ng/kg) were too low in concentration for reliable quantification. A second, five times more concentrated series was prepared and analysed.
Quantities of the labelled peptides in the respective aliquots were determined to be 0.78 nmol GluFib (Lu, Ho or Tb), 0.25 nmol LeuEnk (Lu, Tb or Pr), 0.45 nmol S17 (Ho, Tm or Pr), 0.44 nmol S19 (Lu, Ho or Tm) and 0.16 nmol S27 (Tb, Tm or Pr).

The lowered recoveries for the peptides LeuEnk and S27 are in coherence with the findings in Figure 28 (page 71), where the analysed remnant solutions after ZipTip treatment of the samples contained more lanthanide than the eluate.

4.4.2 Semi-Quantitative Analysis of a Labelled Cytochrome C Digest

For the development of a semi-quantitative approach for the analysis of a digest sample, several assumptions were made. Firstly, in order to simplify the calculations, the monoisotopic lanthanide metals and lutetium were expected to behave the same way during ICP-MS analysis, since their first ionisation energies are similar (see Table 13). This would mean that same amounts of the lanthanides in mol results in a similar number of counts. Lutetium alone was expected to show a slightly lower number of counts, due to its second isotope. This assumption should allow for a first approximation

of the quantity of one lanthanide through calibration with another. With a relative standard deviation (RSD) for the ionisation efficiencies of 0.058, it is expected that the resulting systematic error is lower as the statistical error of the approach.

Table 13: Isotopes and first ionisation energies for the employed lanthanides.[180]

Lanthanide	Isotopes	1st ionisation energy
Praseodymium	100.0% ^{141}Pr	527.0 kJ/mol
Terbium	100.0% ^{159}Tb	565.8 kJ/mol
Holmium	100.0% ^{165}Ho	581.0 kJ/mol
Thulium	100.0% ^{169}Tm	596.7 kJ/mol
Lutetium	97.4% ^{175}Lu 2.6% ^{176}Lu	523.5 kJ/mol

Secondly it was presumed that it is sufficient to quantify only a few representative peaks of a digest chromatogram to determine its absolute amount, given that the peaks are well separated.

Based on these presumptions, an absolute quantification experiment employing standard peptides of known quantities was conducted.

In connection with the experiments in 4.1.1 on the reduced recoveries after SPE, a special interest lay in the determination of the absolute losses with a quantitative approach. This is why the peptide recoveries after SPE treatment with ZipTips, as well as the quantification of the total peptide quantity in a treated and labelled cytochrome C digest, were the focus in this approach.

The semi-quantitative approach utilised in this section was based on the approximate quantification of the most prominent peaks in the Cyt C chromatogram by calibration with the standard peptide signals, which were acquired in a multiplex analysis.

Experimental:

Alongside the quantified standard peptides from the section before, a Dionex cytochrome C model digest was labelled with NHS-DOTA. The labelled digest sample was split in half and complexation was performed with the lanthanides ^{175}Lu or ^{165}Ho respectively.

In order to quantify the recovery for the digest peptides after ZipTip treatment, the digest was treated with ZipTip C18. During SPE all leftover solutions (remnant), such as the solution from which the peptides were extracted, as well as all wash solutions, were collected and pooled. Bound peptides were eluted from the C18-material applying two

times 4 µL elution solution. After elution from the ZipTip, the eluate as well as the remnant solution were dried separately and reconstituted in each the same amount of 100 mM TEAA (pH 5).
The ZipTip eluate contained all the labelled peptides that were bound to the C18-material during the purification procedure, whereas the remnant contained all the unbound components, such as excess reagent and the unbound labelled peptide fraction (see also: section 4.1.1, p. 70).

Two sample series were analysed, one based on a Lu-NHS-DOTA labelled eluate and one on a Ho-DOTA-labelled eluate (exact series compositions in Table 14). The employed amount of the digest in the samples was based on the following calculation: The recovery of peptides in the remnant (X) plus the recovery of the peptides in the eluate (Y) equals 100%. Since the actual recovery was unknown in the beginning, employed amounts were based on an implied recovery of 100 % in the eluate.
Example: 1 pmol digest should be employed, at 100 % recovery this equalled 1 µL, thus employing 1 µL of the eluate and 1 µL of the remnant solution. The actual employed amounts were therefore X % of 1 pmol in the eluate and Y % of 1 pmol in the remnant sample. This nomenclature will be used in Table 14, together with the determined recoveries.
The labelled digest variants were, together with a set of the labelled standard peptides of known quantity, analysed using nanoHPLC ICP-MS. Analysis was done in a multiplex, monitoring six elements at the same time, including the internal standard erbium (an exemplary chromatogram is shown in Figure 40). Each digest was accompanied by up to four labelled standard peptides. In one measurement a comparison of the eluate with the respective ZipTip remnant was conducted (sample 1). For series one, all sample components were employed in equimolar amounts. Series two employed the standard peptides and the digest eluate in a ratio of 1:2.

The results of the measurements in greater detail are shown in appendix 9.3, Table 27 and Table 28. The peak areas were integrated directly from the raw data in a reproducible manner, employing the in-house developed software *T.S.T* (Logiciel de traitement de signaux transitoires, v1.1) from the LCABIE in Pau.

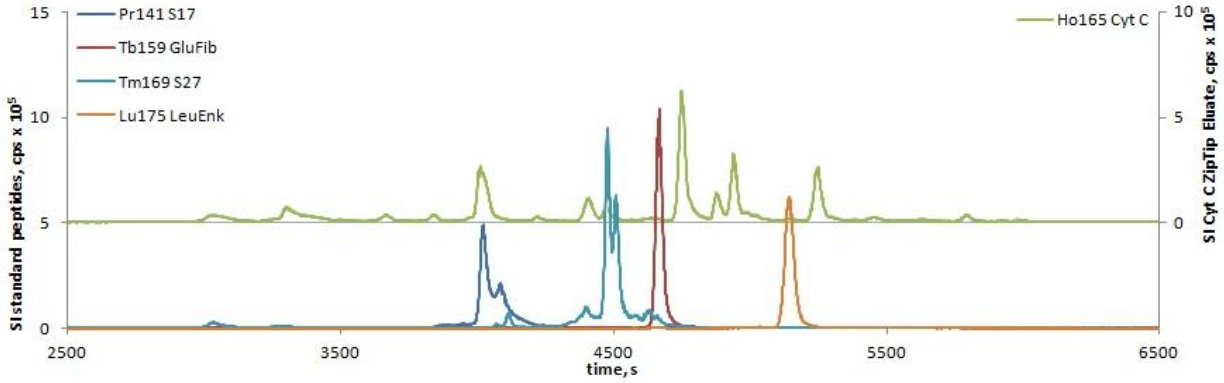

Figure 40: nanoHPLC ICP-MS chromatograms of a set of standard peptides (1 pmol each) and the ZipTip eluate of a Ho-NHS-DOTA labelled cytochrome C digest (2 pmol –X pmol)

Results

Figure 40 illustrates one of the sample sets of the Ho-labelled Cyt C eluate together with the four standard peptides. The peak areas of the respective standard peptides are greater than the peak areas in the digest sample. Peak areas for all four equimolar standard peptides were in the same order of magnitude throughout the whole experiment series, with an average of 21 x 10^6 counts and a RSD of 0.674. As a basis for the semi-quantitative approach, the peak area average (in counts) of the employed standard peptides was set as a representative peak area in total counts, equalling 1 pmol absolute injected amount of whichever of the employed lanthanide.

For determination of the overall peptide recoveries of both the eluate and the remnant, the entire area underneath the two corresponding Cyt C chromatograms was integrated (chromatograms in Figure 28 b, page 71). For the Lu-labelled eluate this resulted in a value of 29 x 10^6 total counts, for the Ho-labelled remnant solution this gave a number of total counts of 232 x 10^6. Taking these two amounts together shows that 88.7 % of the digest peptides were left behind in the remnant solution during ZipTip treatment and only 11.3 % were recovered in the eluate.

For sample series 1 and 2 this consecutively lead to an expected value for the eluate quantity of 11.3 % of 1 pmol injected amount, so that the determined values should be close to 0.113 pmol ('expected' value in Table 14).

In order to determine the recovered amounts for the Cyt C digest eluates, the four highest representative peaks were chosen from the chromatogram of the Cyt C eluate and integrated. An average was calculated from the peak areas and compared to the peak area average of the standard peptides.

This resulted in the determined values ranging from 0.144 to 0.196 pmol in the samples 1 and 2, which is very close to the expected value mentioned above. Analysis of a 10-times less concentrated sample (sample 3) affirms this result and shows at the same time, that the findings are seemingly concentration independent in the observed range. The second series is also in good accordance with the results of series 1. Employing two-times more of the eluate, the expected value should be around 0.226 pmol. Applying the calculation method to the representative digest peaks from sample 4 and 5, both show calculated average quantities between 0.293 and 0.299 pmol.

The results and sample compositions are summarised in Table 14. Employed amounts for the digest samples are based on the determined recoveries as explained in the 'experimental' section.

Table 14: ZipTip eluate sample series of the NHS-DOTA labelled Cytochrome C digest. Sample compositions and component amounts (injected total amounts in nanoHPLC ICP-MS). Expected and acquired values were calculated based on ICP-MS total counts after peak integration, with the standard peptides as 1 pmol and 0.1 pmol respectively.

Sample series 1	Sample component	Component quantities		
		Employed	Expected	Determined
Sample 1	Eluate Lu-NHS-DOTA Cyt C	11.3 % of 1 pmol	0.113 pmol	0.144 pmol
	Remnant Ho-NHS-DOTA Cyt C	88.7% of 1 pmol		
	3 Standard peptides (Tb, Tm, Pr)	1 pmol each		
Sample 2	Eluate Lu-NHS-DOTA Cyt C	11.3 % of 1 pmol	0.113 pmol	0.196 pmol
	4 Standard peptides (Ho, Tm, Tb, Pr)	1 pmol each		
Sample 3	Eluate Lu-NHS-DOTA Cyt C	11.3 % of 0.1 pmol	0.013 pmol	0.020 pmol
	4 Standard peptides (Ho, Tm, Tb, Pr)	0.1 pmol each		
Sample Series 2	**Sample component**	**Employed**	**Expected**	**Determined**
Sample 4	Eluate Ho-NHS-DOTA Cyt C	11.3 % of 2 pmol	0.226 pmol	0.299 pmol
	4 Standard peptides (Lu, Tm, Tb, Pr)	1 pmol each		
Sample 5	Eluate Ho-NHS-DOTA Cyt C	11. 3 % of 2 pmol	0.226 pmol	0.293 pmol
	4 Standard peptides (Lu, Tm, Tb, Pr)	1 pmol each		

Conclusion and outlook

The results from this experiment provided a quantitative approximation of the recoveries for labelled Cyt C digest samples after ZipTip treatment. The acquired data of this experiment was in the expected range, taking into account the lowered recoveries. Calculated average peak quantities were in the expected order of magnitude and

showed a reproducible deviation from the expected value (35 % for series 1 and 32 % for series 2). Variability of the results between the different corresponding samples was low. Taking a look at the standard error in % for the standard peptide peaks, it shows that it is more than ten times higher than the standard error of the 1st ionisation energies mentioned in the beginning (30 % for the peptides, 2.6 % for the ionisation energies). This leads to the conclusion that the deviation due to the different ionisation efficiencies would not have a great impact on the determined values.
At this time point it is not yet finally elucidated, whether the method is suitable for absolute quantification purposes. For validation, the method should be further tested with characterised standard material, e.g. on a Ln-NHS-DOTA labelled standard digest that was quantified with a validated method (MeCAT for example). After this, its application on other protein samples needs to be verified. Additional validation is also needed for the utilisation of the representative digest peaks on which the quantification is supposed to be performed.

It should also be noted that in this case, no identifications were taken into account, so that possible multiple labels on the same peptides and coelutions were not considered for calculations, for reasons of simplification. This might also explain why the calculated values are generally higher than the expected values.

Keeping Figure 28 b (page 71) in mind, showed that the peptide recoveries cannot be generalised throughout the whole chromatogram. This is why the average values were given. It should be noted that the peptides in the eluate should show increasing recoveries/quantities with rising hydrophobicity/retention time.

4.5 Offline Coupling of nanoHPLC with MALDI-MS and fsLA-ICP-MS

Experiments for a novel approach, combining analysis via fsLA-ICP-MS and MALDI-MS on MALDI-targets were conducted. The approach is based on the idea of measuring the exactly same spotted sample twice, firstly with MALDI-MS for identification and a second time via LA-ICP-MS for quantification. The main principle is shown in Figure 41. First the labelled peptide sample is separated via IP-RP-nanoHPLC and then spotted on a special MALDI-target. Secondly, peptide identification of the fractions is conducted via MALDI-MS and MS^2. In the last step, the remains of the MALDI-spots are ablated using LA-ICP-MS, to obtain quantitative data for the fractions.

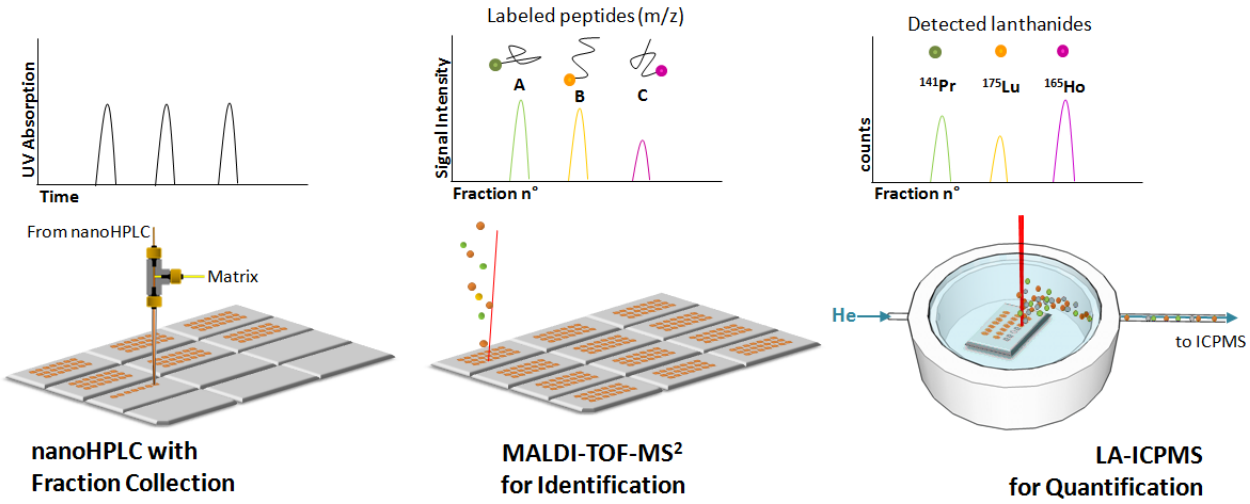

Figure 41: Generic scheme for the hyphenation of MALDI-MS with fsLA-ICP-MS: consecutive measurement of a Ln-labelled sample, including nanoHPLC separation and spotting on a MALDI-target (left), analysis via MALDI-TOF-MS and MS^2 for peptide identification (middle) and lanthanide detection via fsLA-ICP-MS for quantification (right). Ablation cell design by C. Pécheyran

Figure 42 shows a comparison of different hyphenations, which can be employed together in order to obtain complementary data sets. In (a) the coupling used in the earlier sections is shown (online nanoHPLC ICP-MS and offline nanoHPLC MALDI-MS), plus the third commonly used option, the online hyphenation of nanoHPLC with ESI-MS. Approaches based on (a) require an individual separation for each of the different hyphenations and detections. In contrast to this, the hyphenations in (b) require only one separation. The sample is separated and spotted on a MALDI-target, which is then measured firstly via MALDI-MS (1). The same target is measured a second time using LA-ICP-MS (2), resulting in two detections for only one separation.

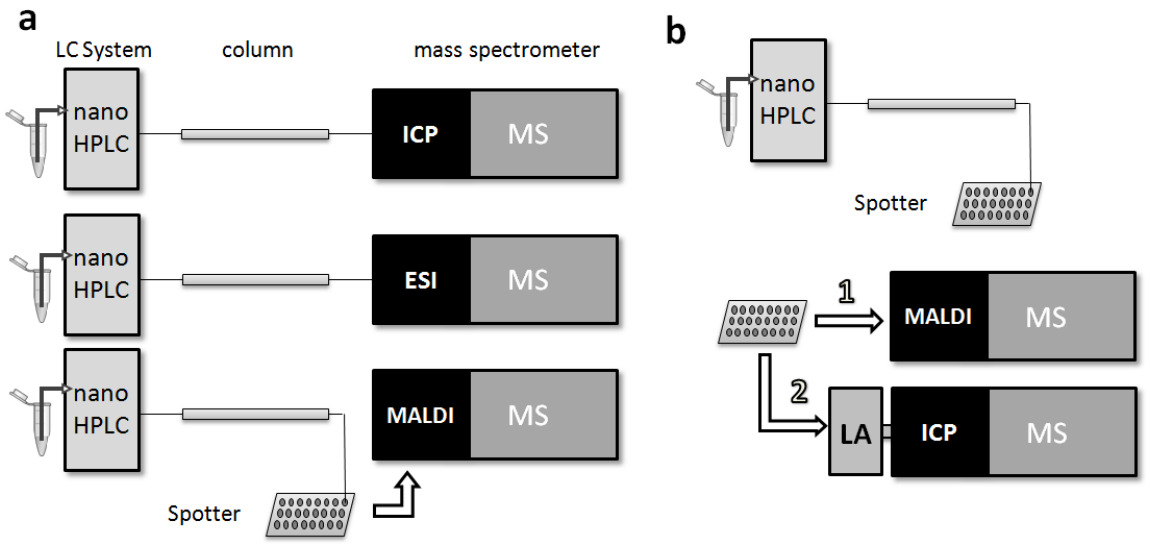

Figure 42: Schematic comparison of hyphenations of chromatographic separation with (a) online coupling with ICP-MS or ESI-MS, offline coupling with MALDI-MS using a spotter, and (b) offline coupling using a spotter for the consecutive measurement of the same sample via (1) MALDI-MS and (2) LA-ICP-MS. Based on Tholey and Schaumlöffel.[3]

In the earlier sections, issues regarding the comparability of independently acquired data sets were addressed. Especially the comparability regarding retention times and thus the attribution of identities to the respective peaks in ICP-MS chromatograms were challenging. The possibility of a consecutive measurement of the same sample with both elemental and molecular MS would rule out such an issue.

LA-ICP-MS, being mostly employed on solid samples, therefore would be the perfect option for a second measurement of the already solid sample on the MALDI-target. The laser of the MALDI-instrument does not ablate everything, thus leaving entire parts of the sample spots untouched. This can already be seen with the bare eye when looking at the measured sample spots after MALDI-MS. The remaining sample spot therefore would be available for analysis with LA-ICP-MS. Given the high sensitivity of the ICP-MS detection regarding the lanthanides, it is very likely, that there will be enough material left for the LA-approach.

The following sections describe a proof of concept study. The experiments showed very promising results demonstrating the general potential of this novel approach.

The model sample consisted of a labelled peptide mixture, comprising Ln-NHS-DOTA labelled peptides from a cytochrome c digest and a set of differentially labelled standard peptides with known quantities.

4.5.1 MALDI-Target Preparation and Plate Design for fsLA-ICP-MS

Dimensions of the LA-chamber were the limiting factor for the size of the MALDI-plate pieces. Therefore the MALDI-targets were cut using a guillotine. Because of the equal force distribution of this type of cutting, surface distortions were avoided, which is an imperative prerequisite for MALDI-TOF-MS. Grave differences in the height of the target surface could result in variations of the ion flight times. Slight differences can be cleared out by MALDI-MS calibration. Details on the plate design and occurring difficulties can be found in methods section 3.11. MALDI-MS calibration parameters can be found in section 3.12.

4.5.2 Preliminary Tests using MALDI-MS

The first question to be answered was how much sample material will be removed from the MALDI-plate by MALDI-MS and MS^2 and if there would still be enough material left for fsLA-ICP-MS. A quantitative determination would be possible by comparison of the same sample, once measured with MALDI-MS prior to fsLA-ICP-MS and once measured directly using fsLA-ICP-MS.

To ensure proper detection of the labelled peptides and high peptide signal intensities even without such a quantitative determination, a sample with higher concentrations was spotted and analysed via MALDI-MS on a normal plate: the injected amounts of each sample component were 10 pmol. The sample was separated using nanoHPLC and the fractions were spotted using a Probot and a normal CHCA matrix, containing the internal standard GluFib (5nM end concentration).

Internal calibration in MALDI-MS failed for most spots and it was found that there was no GluFib signal for internal calibration to be detected. For some of the spots, internal calibration was only successful because of calibration on the masses of the matrix clusters.

In a following experiment, 2x, 4x and 8x GluFib was added to the matrix and spotted alongside a normal sample. GluFib signals in the 2x matrix had still low intensities, whereas in the 8x matrix, signal intensities of 2000 counts were detected. The same matrix without sample was remeasured and the signal was in the same range.

The massive excess metal evidently lead to a quenching of low abundance peptide signals which needs to be taken into account for the future analysis of peptide species

with a low abundance. For the preliminary tests this effect did not pose a problem, since the model digests and peptides were present in sufficient concentrations for proper identification.

After optimisation of the MALDI-MS calibration parameters (listed in section 3.12), it was possible to identify as many peptides using the cut-target as on a normal target plate.

4.5.3 Compilation of MALDI-MS Chromatograms

Sample composition: Cyt C digest labelled with ^{175}Lu-NHS-DOTA; ^{159}Tb-NHS-DOTA GluFib; ^{141}Pr-NHS-DOTA LeuEnk; ^{169}Tm-NHS-DOTA S17 (standard peptides of known quantities, from section 4.4.1, for sequences see Table 24)

After nanoHPLC separation and spotting of the sample on a cut target it was consecutively analysed via MALDI-MS and MS^2 using the optimised parameters: the chromatographic run – distributed on three different target pieces, was measured using three independent spot sets. As already mentioned, this was necessary because of MALDI-MS alignment and calibration problems when using a vendor defined plate spot set. Between measurements, the plate had to be ejected and re-loaded again, in order to apply the matching spot set template for each part. The plate was then aligned and calibration was performed (parameters in section 3.12). The MALDI-MS and MS^2 measurements were fully automated.

A Mascot search was performed (parameters, see section 3.8.1), identifying all of the labelled standard peptides, except S27, which could not be found by manual inspection of the spectra either. For the labelled Cyt C digest, 35 labelled peptide species could be identified, including some with missed cleavages; only 4 unlabelled species were found, of which only one showed a considerable signal intensity (a list of the identified peptides can be found in Table 29).

For visualisation, the peak explorer software from ABSCIEX was employed. Extracted ion chromatograms (XICs) for each precursor m/z ratio were generated, plotting the respective signal intensities of the precursor against the different fractions. Precursor masses were verified by Mascot search, manual inspection and/or generation of ion current chromatograms for characteristic fragment ions (XFC). Matching fragments and precursors from the XIC and XFC would show peaks in the same Probot fraction.

An example for the XICs of three labelled standard peptides is shown in Figure 44, including the manually inspected MS^2 spectra and the identified fragment ions. The 'cut' between the target pieces is marked with an arrow. The cuts are also visible in the XICs from the labelled Cyt C digest in Figure 43 after the fractions 86 and 170. In this figure only the most intense peaks are shown, which had matching MS^2 data. Due to the fact that this data was acquired completely independent from the fsLA-ICP-MS data, it was not possible to align both chromatograms perfectly. Being only a preliminary test, the fsLA-ICP-MS measurements in the following sections did not cover the whole length of the chromatography (80 spots instead of 245), thus making it difficult to conduct a proper alignment. Nevertheless, an alignment of the data will be shown in section 4.6.

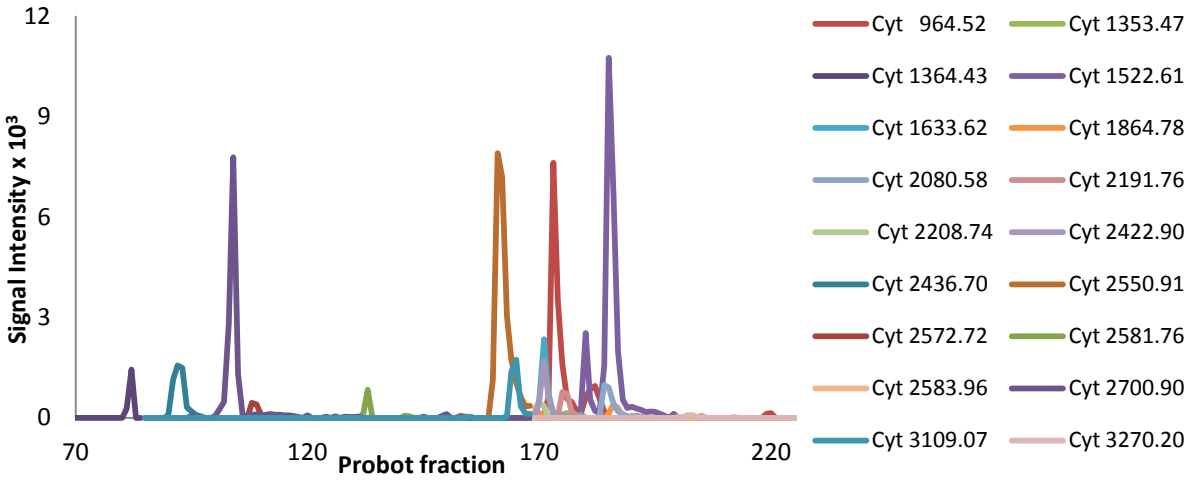

Figure 43: MALDI-MS extracted ion currents for peptides from a ^{175}Lu-NHS-DOTA labelled cytochrome C digest (most intense signals), analysed on a cut target plate.

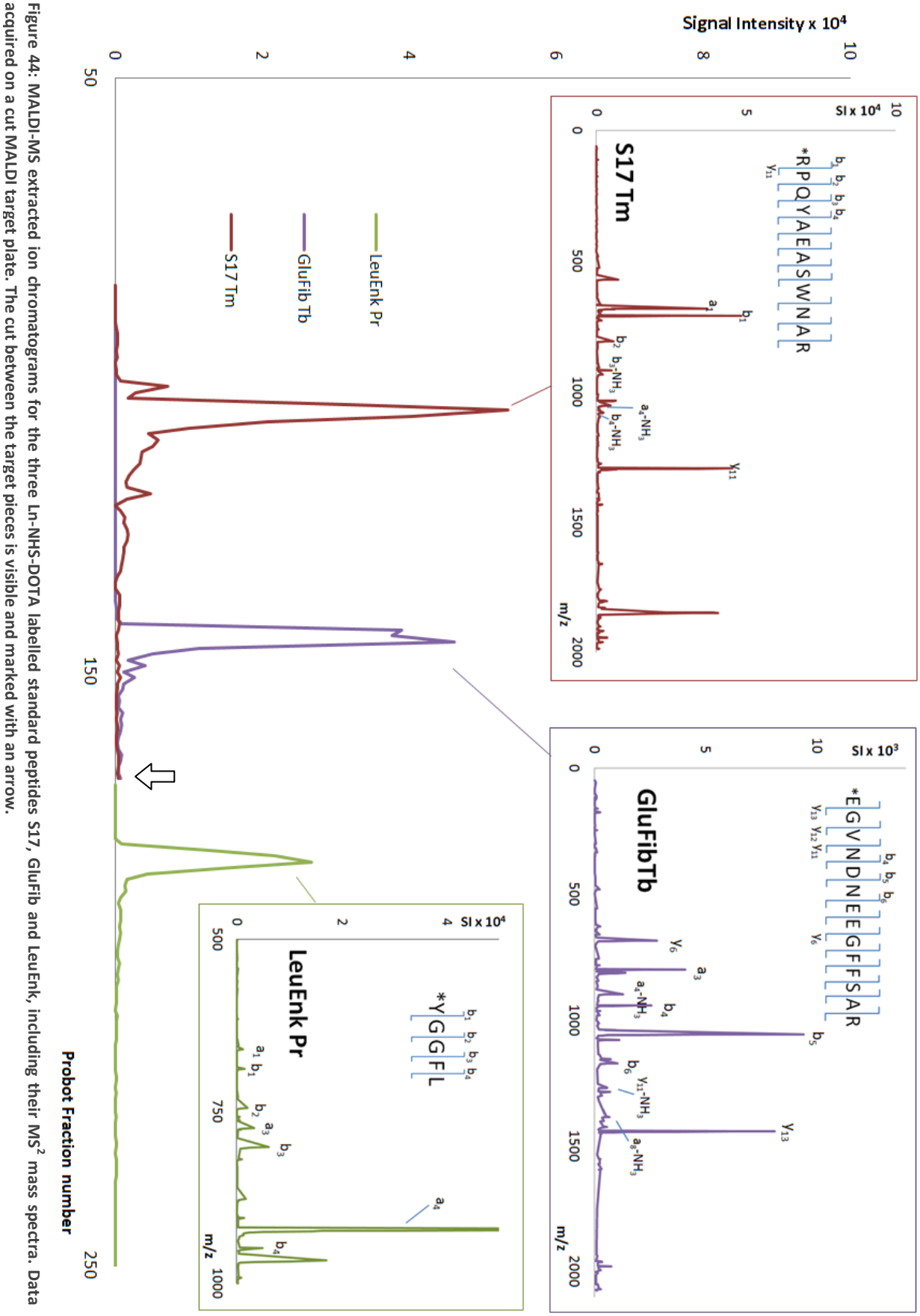

Figure 44: MALDI-MS extracted ion chromatograms for the three Ln-NHS-DOTA labelled standard peptides S17, GluFib and LeuEnk, including their MS^2 mass spectra. Data acquired on a cut MALDI target plate. The cut between the target pieces is visible and marked with an arrow.

4.5.4 fsLA-ICP-MS on MALDI-Targets

The measurements using fsLA-ICP-MS were conducted according to the parameters shown in section 3.10.

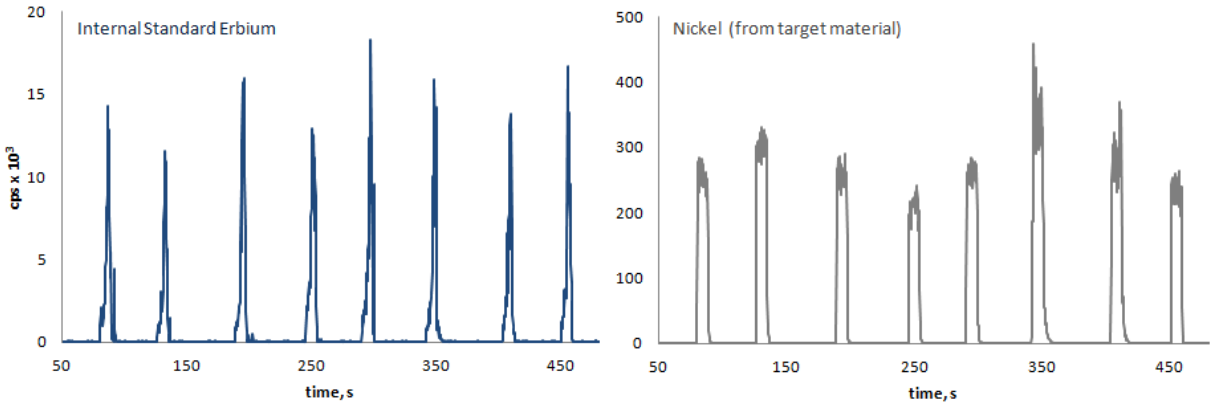

Figure 45: fsLA-ICP-MS signals for the internal standard erbium in the matrix and nickel as a representative for the ablated material of the steel target itself.

Figure 45 shows typical raw signals from the ablation of eight MALDI-spots, with the internal standard ^{166}Er on the left and ^{60}Ni as the representative for the ablated target material on the right. ICP-MS data acquisition was running constantly, the peaks being the signals acquired during the ablations of the matrix spots. The time in between the peaks was used to move to the next spot on the target and refocus the laser for the next ablation. Since the signal always goes back down to the baseline level after each peak, there is evidently no contamination of the tubing system. The ablated sample is carried to the ICP-MS in a quantitative manner. To further exclude spot-to-spot sample carryover (e.g. no sample deposit on the neighbouring spot) samples were placed in the ablation cell with the first sample spot to measure closest to the exit of the ablation cell and the last sample spot closest to the cell entrance.

4.5.5 Detection Limit and Calibration Curves

A determined limit of detection (LOD) for the method was calculated based on the blank measurement. The blank sample consisted of the MALDI-matrix CHCA containing the internal standard erbium in a fixed concentration without addition of any other lanthanide salts, which was spotted on a ground steel MALDI-target. Lanthanide signals were normalised on the respective ^{166}Er signal.

The ablation of the steel target without matrix already hinted that some lanthanide metals were present in the target material: while ^{166}Er showed virtually no signal, ^{175}Lu and ^{159}Tb showed low signal intensities. Important quantities were detected for ^{169}Tm, ^{165}Ho and ^{141}Pr. This observation is also reflected in the determined LODs for the respective elements (Table 15).

The instrument noise level was calculated based on the counts acquired between the ablations of the blank where no material was ablated. The method noise was based on the acquired blank signal in form of its standard deviation when ablating the erbium matrix. Detection limits were calculated using the equation taken from the IUPAC compendium of chemical terminology[181]:

$$x_L = \bar{x}_{bi} + k\, s_{bi}$$

with x_L being the smallest measure, $\bar{x}_{bi}$ being the average of the blank measures, k representing the confidence level (k = 3) and s_{bi} being the standard deviation of the blank measures.

Table 15: Noise levels and limits of detection for the utilised lanthanide metals.

Element	Instrument noise in cps	Method noise in cps	Limit of detection[181]		
			in counts	in µg/kg	in amol/µg Matrix
^{175}Lu	30.7	30.4	103.3	5.38	30.72
^{169}Tm	38.0	264.6	1228.7	27.04	160.00
^{159}Tb	33.4	54.5	189.4	4.58	28.80
^{165}Ho	31.2	150.8	601.5	10.55	63.92
^{141}Pr	58.6	307.0	1423.3	20.99	148.90

The LODs for the respective elements is in the expected range for a fsLA-ICP-MS approach (see also Figure 5 on page 26, LOD < 100 µg/kg)[41]. LODs for the elements present in the steel target material were elevated.

For acquisition of the calibration curves, the respective lanthanide salts were diluted in erbium matrix and spotted on the steel target with a pipette. The first trial with a dilution series was too low in concentration with several dilutions being below the later determined LOD. In addition the LA-parameters were chosen poorly, since it was still during the optimisation process. Therefore a second, more concentrated series was prepared ranging from 1 pg/µL to 1000 pg/µL Ln^{3+} in liquid matrix, equalling a range from 333 µg/kg to 333 mg/kg Ln^{3+} in the dried matrix spots. The measurements from the

first (low concentration) dilution series cannot be compared directly with the ones acquired for the LOD, due to the great difference in the acquisition parameters.

Taking a look at the calibration curves in Figure 46, most of the observed lanthanides have a similar behaviour. Only Lu-175 varies significantly from the other four metals. This is also represented by the slopes listed in Table 16. Tm-169, Tb-159, Ho-165 and Pr-141 seem to be comparable, having a very similar steepness of the slope. As for 175-Lu, the difference in the slope might be influenced by the fact that it is not monoisotopic (2.6 % Lu-176). It cannot be ruled out that also statistical reasons are involved. With a higher number of measurements, the slopes might show a lower deviation.

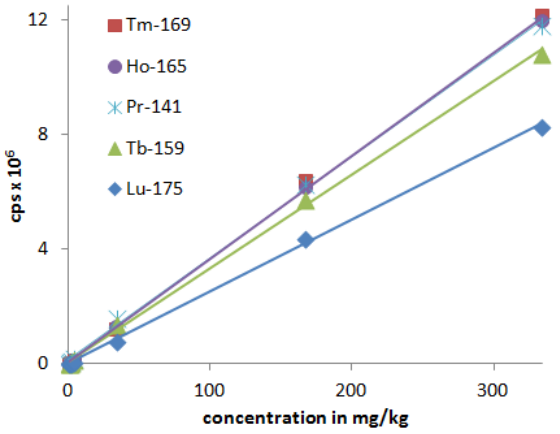

Figure 46 (left): fsLA-ICP-MS calibration curves

Table 16 (below): fsLA-ICP-MS calibration curves and equation data from trend lines

Element	slope	y-intercept	R^2
^{169}Tm	36889	28733	0.9995
^{165}Ho	36114	47891	0.9998
^{141}Pr	35502	115435	0.9985
^{159}Tb	32743	84992	0.9988
^{175}Lu	25212	-1102	0.9993

4.5.6 Quantification of the Labelled Standard Peptides

The labelled standard peptides were analysed together with a labelled Cyt C digest using nanoHPLC. Fractions were collected and mixed with Er matrix using a Probot. The resulting spots were ablated completely using the same parameters as for the calibration curves in Figure 46.

The standard peptides were used in different quantities, in order to elucidate whether the peptide ratios can be recovered as expected. The measurements were normalised using the respective erbium signal. Integration of the peaks and calculation of the quantities for the peptides lead to the following results:

Table 17: Results for the quantification of the Ln-NHS-DOTA labelled standard peptides via fsLA-ICP-MS

Peptide	Employed quantity	Normalised signal	Recovered quantities		
	in pmol	in total counts	pg Ln / µg matrix	in pg Ln	in pmol
^{165}Ho GluFib	**1.0**	841 684	22.0	148.2	**0.90**
^{169}Tm S17	**2.0**	not available	-	-	**-**
^{159}Tb LeuEnk	**4.0**	3 141 459	93.3	629.4	**3.96**
^{141}Pr S27	**5.0**	3 300 638	89.7	604.9	**4.29**

Unfortunately no integration data is available for peptide S17, which did not show a proper peak after fsLA-ICP-MS. Only the respective ^{169}Tm background was elevated (see Figure 47). In contrast to this, the same peptide gave a proper peak in both MALDI-MS (Figure 44, page 100) and nanoHPLC ICP-MS analysis (see Figure 28 d, page 71). Up to now it was not clear why this was not the case for fsLA-ICP-MS.

The determined quantities for the three other peptides are all in the expected order of magnitude: deviation from the expected value was 10.18 % for ^{165}Ho GluFib, 1.04 % for ^{159}Tb LeuEnk and 14.19 % for ^{141}Pr S27. In general, values for recovered quantities were smaller than the expected values. The deviations are consistent with the measurements from the experiment in section 4.4.2: Calculation of an average from all standard peptide measurements gave a value of roughly 27 x 10^6 total counts. The average counts for ^{165}Ho GluFib with 24 x 10^6 counts (-13 %) were lower than this reference value. ^{159}Tb LeuEnk with 28 x 10^6 counts (+2.8 %) was very close to the reference value, whereas ^{141}Pr S27 showed the biggest deviation with only 17 x 10^6 total counts (-39 %).

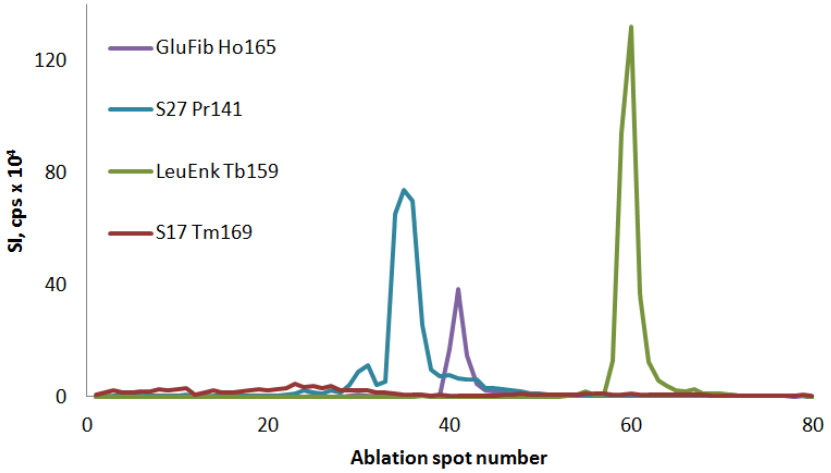

Figure 47: Normalised fsLA-ICP-MS chromatogram for the four Ln-NHS-DOTA labelled standard peptides GluFib, S27, LeuEnk and S17, applied in different quantities.

4.5.7 Quantification of a Labelled Cytochrome C Digest

The same ^{175}Lu NHS-DOTA labelled Cyt C digest as previously analysed in section 4.4.2, was also analysed in this experiment, employing it with doubled concentration for nanoHPLC fsLA-ICP-MS. In section 4.4.2 supposedly 1 pmol of ^{175}Lu Cyt C was injected, which due to the application of ZipTips lead to a lowered average recovery and an expected value of 0.113 pmol. For 2 pmol this leads to an expected average quantity of 0.226 pmol.

After nanoHPLC analysis and fraction collection of the new sample, the spots were ablated completely and the counts were normalised on the erbium signal; the resulting chromatogram is shown in Figure 48. The peaks are not baseline resolved very well. This is due to the limited number of spotted fractions, resulting in a low number of data points for the measurements. Each fraction represents 15 s of the chromatographic separation, thus one fraction contains everything eluting from the chromatographic column during this time period. Therefore peaks that were resolved on the nanoHPLC, might not be resolved properly anymore after laser ablation. Less abundant peptides might disappear as a fronting or tailing of a more dominant peak. The loss in resolution can also be seen in MALDI-MS analysis of the 15 s fractions. Still, in this case it did not pose a problem, since peptides with overlapping elution can still be identified independently. However this problem needs to be resolved for future applications encompassing more complex sample mixtures.

Being aware of this resolution problem, a quantification approach was still conducted on the more dominant peaks of the chromatogram. Through identification via MALDI-MS, it was known that the peaks 1 a and b contain the same peptide with one (b) or two labels (a). Peak 2 also contained a singly and doubly labelled peptide, whereas peak 3 could not be identified unambiguously. Peak 4 contained a mixture of 4 mainly singly labelled peptides. Peaks 5 and 6 were mainly consisting of variations of similar peptides with and without missed cleavages, which most likely coelute with some other peptides, of which the ratios are unknown.

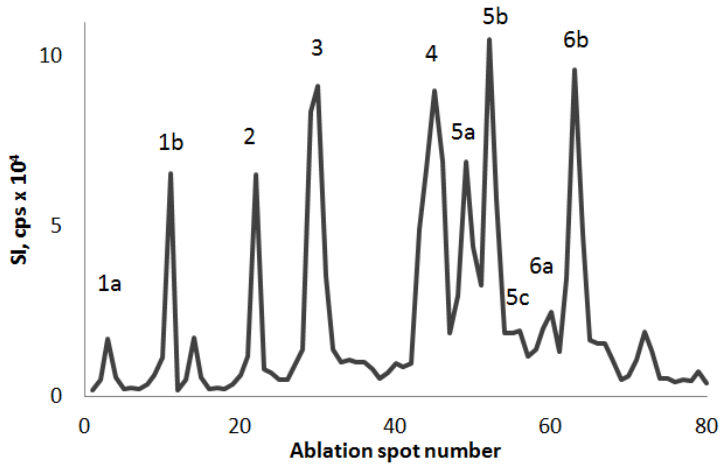

Figure 48: Normalised fsLA-ICP-MS chromatogram for the ^{175}Lu NHS-DOTA-labelled cytochrome C digest. Numbers and letters indicate peaks used for the quantification approach in Table 18. (The same chromatogram is shown in an overlay with MALDI-MS in Figure 50)

In a simplified quantification approach, the normalised data was integrated and the acquired signal was then multiplied with a correction factor, taking into account the multiple labels and the expected number of peptides comprised in the peak. Applying the ^{175}Lu calibration curve from Table 16 to the counts, an approximation of the peptide quantities was given. Values for the quantities were expected to rise from earlier to later fractions, due to the ZipTip treatment.

Table 18: Set of integrated peaks from the chromatogram in Figure 48 and calculated quantities.

Peak		Start spot	End spot	Counts	Factor	Sum counts x factor	pg absolute	pmol absolute
1	**a**	1	5	31 368	0.5	108 439	29.3	0.167
	b	6	12	92 755	1.0			
2		19	25	106 544	0.75	79908	21.6	0.123
3		28	33	248 140	?		66.7	0.381
4		42	47	303 317	0.25	75 829	20.6	0.118
5	**a**	48	50	142 313	0.5	163 935	44.1	0.252
	b	51	53	195 482	0.33			
	c	54	60	56 540	0.5			
6	**a**	57	60	70 380	1.0	238 302	64.0	0.366
	b	61	66	223 896	0.75			

The employed factors are based on the number of labels and the number of peptides identified in the respective peak:

- For Peak 1 a, the factor was 0.5 since the corresponding peptide had two labels and did not show coelution. The peptide in peak 1 b carried one label and showed no coelution (factor 1).
- For Peak 2, a peptide with both one and two labels was identified. Since the ratio between the doubly and singly labelled peptide was unknown, they were estimated to be found in the same proportion, thus a factor of 0.75 was employed (0.5 x 1.0 + 0.5 x 0.5).
- Peptide composition of peak 3 was unknown, this is why there was no correction factor employed, resulting in a calculated quantity for peak 3 which is most likely too high (possible coelution with other peptides and/or double derivatisations).
- Peak 4 showed coelution of 4 mainly singly labelled peptides. Those peptides were estimated to contribute to the peak in equal proportion (factor 0.25).
- For peak sets 5 and 6, the factors depended on the number of labels in the respective peak (a, b or c), mainly including double derivatisations (factor 0.5) but also showing single (factor 1.0) and triple (0.33) labelled peptides. Most likely there are more peptides coeluting in the fractions whose contribution to the peak areas cannot be predicted with certainty. This is why the quantities for the peptides in these peaks were probably also overestimated.

These factors can only be applied, because the sample composition is known. For a completely unknown sample or a protein mixture this approach would not be applicable this way.

The lower peptide complexity in the fractions at lower retention times identified by MALDI-MS, is in good accordance with the lowered recovery for the earlier fractions due to the ZipTip treatment as seen in section 4.1.1. This is why the calculated quantities in the earlier fractions (peaks 1, 2 and 4) are around 0.136 pmol, whereas the quantities for the later fractions (3, 5 and 6) are more than doubled. Averaging all calculated amounts enables a comparison to the results from section 4.4.2. Having applied twice the amount, the expected value should be around 0.226 pmol. The average acquired in this experiment is 0.234 pmol and thereby deviates from the expectation by only 3.5 %.

This shows that both methods give comparable results, even if one uses the averaged quantities of the standard peptides as reference system and the other one separately acquired calibration curves.

4.5.8 Manual Construction of a fsLA-ICP-MS Chromatogram

During one acquisition period of 10 min on the Perkin Elmer ICP-MS, approximately 11 spots were ablated without automation. For the ablation of 80 spots – equalling a chromatogram of 20 min length, this meant an analysis time of 73 min, not counting the time needed for changing the target pieces and restarting the ICP-MS for the next series. With automation, this time can most likely be reduced significantly.

As shown in Figure 45 on page 101, the acquired signals for the fsLA-ICP-MS measurements did not result in a chromatogram directly, so that the chromatograms had to be generated manually after data acquisition: the peaks for each ablated spot were integrated separately using the software T.S.T. and the signals were then attributed to the respective spot numbers in an excel sheet.

Examples for chromatograms acquired in this way were shown in Figure 47 and Figure 48 on the pages before. The ablated spots correspond to a retention time window from 35 min to 55 min.

4.5.9 Microscopic Examinations of Ablation Craters

Several examples for images of laser ablations on the MALDI target are shown in Figure 49. (A) shows a 5x magnification of four ablated nanoHPLC spots, with an ablated diameter of 1350 µm (77 concentric circles), (B) is the lower left spot with 10x magnification. (C) to (F) show an ablated standard spot from the preliminary test in magnifications from 5x to 50x. Matrix crystals can still be seen around the ablated areas. The smaller circles represent diameters of 900 µm which were shot with 20 % laser intensity, the bigger circle (1350 µm) was ablated with 7 % laser intensity. This difference in laser intensity is represented by the difference in depth of the single craters in (E) and (F). In Figure 49 (F) marked by a blue arrow, the lower crater depth for 7 % laser intensity can be observed, the craters left behind by 20 % laser intensity are hinted by an orange arrow.

Figures (G) and (H) show matrix spots after MALDI-MS analysis: Spot parts where the MALDI-laser had hit during MS and MS^2 were already visible by naked eye. MS^2 is not

conducted on the entire spot, but only on a randomised area. Under the microscope it became visible, that even in areas where MS^2 seemingly left a hole in the spot, matrix crystals were still as abundant as in untouched areas. The surface which was hit by the laser showed iridescent discolouration on a microscopic scale, which was the only visible trace of the MALDI-laser. A rough estimation of the covered surface showed that not even one third of the matrix spot was used for the MALDI-MS measurements. This leads to the conclusion that there should be enough material left for LA after MALDI-MS and MS^2. The visible scratches on the target surface were a result of the target cutting process in the workshop.

The dilution series for the calibration curves obtained in fsLA-ICP-MS were also examined under a microscope in order to find out whether the rising concentration of the lanthanide salts had an influence on the crystallisation behaviour of the matrix. As can be seen in the series of pictures in appendix 9.6, there was no great influence observable between the lowest lanthanide concentration and the dilution with the highest concentration of the series (33 µg/kg to 500 mg/kg in dry matrix). The size of the matrix crystals varied with the amounts of salts: only few, but big crystals were present on the spot area starting with the lowest concentration of 30 µg/kg. With rising amount of salt a slight tendency for formation of bigger crystals was observable. When comparing the dilution series spots to the erbium blank and a lanthanide free matrix, it can be seen that there is a huge difference between the crystal sizes and their distribution.

In the Er blank, as well as in the metal ion free matrix the crystals were much smaller and distributed more evenly on the whole spot area. This might also explain why at high salt contents, the peptide signals were seemingly quenched: less unevenly distributed crystals obviously lower the ionisation efficiency of the MALDI process. This was also observed earlier for ionic liquid matrices based on 2,5-DHB.[182]

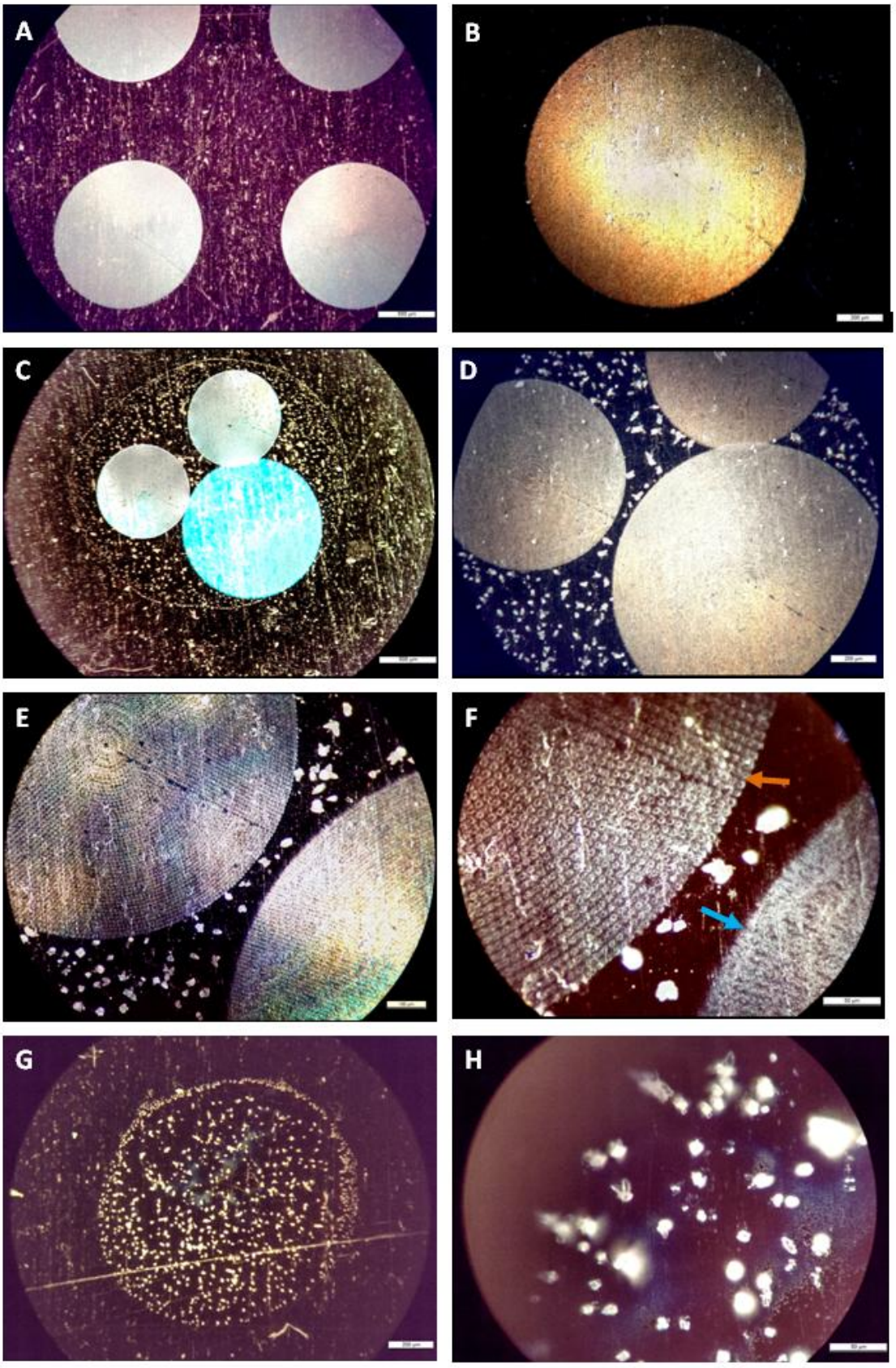

Figure 49: Laser Ablation craters under the microscope with different magnifications (5x to 50x). A and B: ablated nanoHPLC fractions (A: 5x, B: 10x), C to F: ablated standard spots, preliminary test with 900 an 1350 µm ablation diameter (C: 5x, D: 10x, E: 20x, F: 50x), G and H: discolourations after MALDI-MS and MS^2 (G: 10x, H: 50x)

4.5.10 Conclusion and Outlook

The results shown here demonstrate the high potential of this novel approach. The consecutive measurement with MALDI-MS and fsLA-ICP-MS enables the acquisition of complementary data sets for the same chromatographic separation. The first approaches showed very promising results. Parameters could be optimised for both fsLA-ICP-MS and MALDI-MS, including an ameliorated cut target design. Optimised calibration and the use of target piece specific spot sets resulted in very good identification results using Mascot search after MALDI-MS^2.

Data normalisation taking the erbium signals as reference in fsLA-ICP-MS reduces spot to spot variations and makes the acquired data more reliable concerning the quantities of ablated sample. Monitoring of ^{80}Ni signal intensities during laser ablation allows for evaluation of the ablation crater depth and thus the amount of ablated target material from the steel target. Therefore the ^{80}Ni signal might be used for correction of signals from samples with low lanthanide content. The ^{80}Ni signal should be in direct relation to the signals from lanthanides which were present in the target material in traces.

Lanthanide traces in the target material also caused a slight elevation of the LODs for several elements. Still the LODs stayed in the expected range for LA-ICP-MS approaches (< 100 µg/kg, see Figure 5 on page 26). The exact lanthanide content of the target material needs to be verified in additional measurements.

It is also necessary to acquire more statistical data, in order to elucidate questions about sensitivity and accuracy of the method. The LOD needs to be verified and it would also be interesting to determine the limit of quantification.

The determined quantities for the model peptides in the sample were generally close to the expected values. Especially the quantity for the ^{159}Tb-labelled standard peptide showed a low deviance with a determined value of 3.96 pmol (expected 4.0 pmol) and also the quantities for the ^{175}Lu-labelled digest peptides were in the range of the expectation, taking their hydrophobicities into account.

Surprisingly two of the standard peptides were not detectable with either one of the analytical methods: S27 was not identifiable using MALDI-MS, whereas S17 did not show a peak in fsLA-ICP-MS (sequences in Table 24). In contrast to this, both peptides showed

signals in UV detection and normal ICP-MS analysis. It needs to be determined whether this finding is reproducible.

Furthermore it needs to be elucidated whether ionisation in MALDI-MS is the same for free lanthanide ions and peptide bound lanthanides: when conducting MALDI-MS and MS^2 on the matrix spot, Ln-labelled peptides and the internal standard erbium need to be removed from the spot to the same degree. This is necessary for the normalisation of the peptide signals with the internal standard erbium in LA-ICP-MS. The erbium signal stands in direct relation to the amount of ablated matrix/overall sample material and can be employed to rule out spot to spot variation. It should therefore be made sure that the sample composition is not altered after MALDI-MS and that erbium can be employed for normalisation. If the comparability would not be given an alternative peptide-bound internal standard could be developed.

It was found that the chromatographic resolution of the method with both MALDI-MS and LA-ICP-MS detection was low compared to the chromatographic resolution of the nanoHPLC. This is due to the fractionation and the relatively big fraction volumes. At the same time the analysis time is very long because of the number of spots to be analysed by hand. This shows the need for automation of the method, should it be implemented in a laboratory workflow. A reduction in analysis time could already be achieved by the use of standardised material, such as specially developed target plates or adapted LA-equipment. Already an automated measurement of the spots, including auto focussing of the laser would reduce the measurement time tremendously.

Microscopic observations indicate that spots after measurement with MALDI-MS^2 do not suffer a visible reduction of the matrix amount. The surface covered by the MALDI laser is roughly one third of the matrix spot, leading to the conclusion that there will still be a sufficient amount of sample left for the following fsLA-ICP-MS measurement. It was also found that the size and distribution of the matrix crystals are influenced by the lanthanide content of the sample. Already the lowest dilution of the series with 33 µg/kg of lanthanide, together with the erbium standard resulted in a deviant crystallisation behaviour. With rising metal content, the crystal size rose, while at the same time less crystals were observable on the spot surface. A high metal content therefore attributed to less efficient ionisation in MALDI-MS. This effect was also observable in the quenching of GluFib peptide signals during analysis of a sample with higher salt content.

4.6 Superposition of Chromatograms using Retention Time Markers

Not only were the labelled standard peptides thought to serve as a standard for quantification purposes, they were also thought to aid the alignment of data acquired with different methods, serving as retention time markers (RTM).

The problem of shifted retention times was already addressed in section 4.3. Probot fraction collection caused an active backpressure to the nanoHPLC outlet due to the addition of the matrix by a syringe. This backpressure differed from the conditions in the online coupling of the nanoHPLC with ICP-MS, thus resulting in a retention time shift for chromatograms of the same sample measured with the different techniques. For low complexity samples, alignment could be achieved by comparison of the UV-chromatograms. For samples of higher complexity, this alignment technique will not be applicable.

The addition of a set labelled standard peptides to the sample of interest prior to analysis can add reference points to the chromatograms, which thereafter can be employed for alignment purposes. As shown in the sections before, the peptide standards are detectable independently from the sample itself: through their specific m/z in molecular MS and through their differential labels in ICP-MS. Therefore, by aligning these retention time marker signals in the respective chromatograms, an alignment of the sample chromatograms should be achieved, thus ensuring sample comparability for data sets acquired with different methods.

An example for such an alignment is shown in Figure 50 on the following page. The analysed samples were each composed of a ^{175}Lu-NHS-DOTA labelled Cyt C digest (grey scale) and different sets of Ln-NHS-DOTA labelled standard peptides (colour coded).

Standard peptides for fsLA-ICP-MS and ICP-MS: ^{169}Tm S17, ^{141}Pr S27, ^{165}Ho GluFib and ^{159}Tb LeuEnk.

Standard peptides for MALDI-MS: PPA PPL and PPQ with ^{165}Ho, ^{169}Tm S17, ^{159}Tb GluFib and ^{141}Pr LeuEnk.

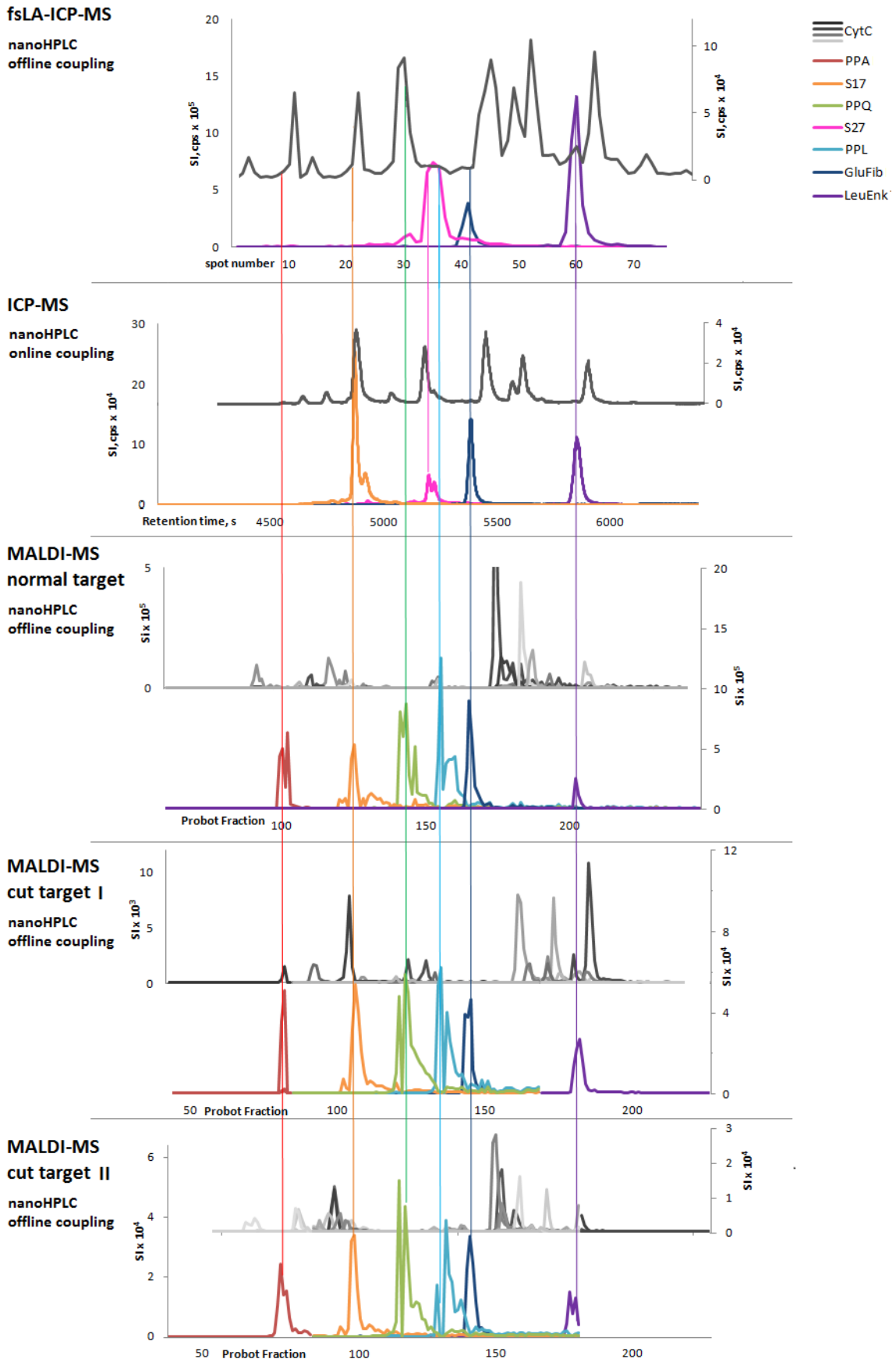

Figure 50: Superposition of five independent chromatogram sets using retention time markers. (Explanation in text)

The data sets in Figure 50 are acquired by application of four different experimental setups:

- For fsLA-ICP-MS, the sample was separated on a nanoHPLC with a 15 cm C18-column, coupled to a Probot for fraction collection on a cut target. The dry matrix/sample spots were then ablated using fsLA-ICP-MS (details in section 4.5).
- For ICP-MS, the same nanoHPLC as above was coupled directly to an Agilent 7500 ICP-MS for online data acquisition.
- For MALDI-MS (normal target), a nanoHPLC with a 25 cm C18-column was coupled to a Probot fraction collector. Fractions were spotted on a normal target and measured using MALDI-TOF-MS and MS^2.
- For MALDI-MS (cut targets I and II), the same nanoHPLC and spotter as above for MALDI-MS was employed, only difference was the faction collection on a cut target.

To resume, the data sets encompass techniques employing two different ionisation types (MALDI and ICP) and two sample introduction techniques for ICP-MS (LA and nanonebuliser). The data was acquired on three different instruments (Agilent 7500, Perkin Elmer Elan II and ABSCIEX TOF/TOF 5800). One method was based on an online coupling (nanoHPLC-ICP-MS), while the others were offline setups and two different nanoHPLC systems with varying column lengths and varying gradients were employed.
All of these different parameters lead to a very limited comparability of fraction numbers and retention times.

By alignment of the RTM peptides in each data set, the chromatograms for the Cyt C digest should be aligned automatically. Even after alignment, a difference can be seen in the peak patterns of the two Cyt C ICP-MS chromatograms. This is mainly due to the low chromatographic resolution of the LA-approach. Unfortunately S17 (orange) did not give a signal in the fsLA-ICP-MS, so that one of the RTMs is missing for this data set, leaving the fsLA-ICP-MS alignment unconfirmed.
Cyt C peptides identified via MALDI-MS and Mascot search were assigned to the peaks in the ICP-MS chromatograms. The labels (a) to (k) in Figure 50 are explained in Table 19, with an asterisk marking the labelling site.

Table 19: Assigned peptide identities for the most prominent peaks in Figure 50, with labelling sites (*) and m/z

	Labelled Cyt C peptide	m/z		Labelled Cyt C peptide	m/z
a	*KYIPGTK*	2580.71	**g**	*KGEREDLIAYLK*	2550.91
b	KYIPGTK*	1922.64	**h**	**KGEREDLIAYLK*	3109.12
c	*KIFVQK*	2436.70	**i**	*GEREDLIAYLK*	2422.92
d	YIPGTK*	1236.42	**j**	EDLIAYLK*	1522.61
	YIPGTK	1794.52			
e	*KTGQAPGFSYTDANK*	2700.90	**k**	EDLIAYLK*	1522.61
	*KTGQAPGFSYTDANK	2142.85		*EDLIAYLK*	2080.73
f	*TGPNLHGLFGR	1337.52		*MIFAGIK*	1895.63
	*MIFAGIK	1726.72		*KGEREDLIAYLK	1992.64

Table 19 shows that there are several groups of similar peptides assigned to the peaks in Figure 50. The groups consist of peptides with and without missed cleavages, which can carry up to 3 labels (see peak h) and have a similar retention behaviour. Unfortunately the peaks are overlapping, as seen for the peaks g to k, making a quantitative analysis difficult. The ratios between the singly and multiply labelled peptides are unknown and cannot be easily determined using ICP- or MALDI-MS.

It can also be observed that not all peptides are identified likewise in the three MALDI-MS data sets, or that at least the signal intensities are not alike. The overlapping and multiple labels emphasise yet again the difficulties when working with DOTA-labellings.

Still data interpretation was facilitated by the application of the RTM peptides. It was shown that even chromatograms acquired with different instrument setups and varying chromatographic parameters, which would not be comparable otherwise, could be aligned. The superposition using RTM peptides enabled proper peptide identification and unambiguous assignment to previously unidentified peaks in ICP-MS.

It was also observed that the different lanthanides used in the two sets of RTM peptides do not have an influence on the retention behaviour. The Ln-labels can be chosen freely according to their application in the multiplex analysis. For future applications the number of different metals employed in the RTM peptides can be further reduced. The standard peptides are well characterised, they show low overlapping and their retention behaviour is known. In theory the number of Ln could be reduced to only one or maximum two. This would leave the other multiplex channels open for the labelling of other sample components.

The peptide mixture was still in the course of development at the stage where the fsLA-ICP-MS experiment was performed. The peptides PPA, PPL and PPQ (see Table 24 in Appendix III) were purchased only after this and will be implemented in the future fsLA-ICP-MS experiments. As can be seen in Figure 50, the whole RTM set covers most of the chromatographic separation. S27 and S17, not detectable in either one of the techniques, were deemed unreliable for analysis. Still, a proper alignment of the five chromatogram sets was achieved. At least 4 RTMs seem to be necessary for a definite adjustment. The RTMs should also have an adequate retention time distance to each other.

V Discussion and Outlook

5.1 DOTA Derivatisation Efficiencies and Reagent Excess

Both DOTA-reagents used in this work have their advantages and disadvantages. Kinetically, the lanthanide DOTA-label on the peptide is very stable, making it a potentially very interesting and useful tag. The biggest issue is with the derivatisation procedure itself: as with every chemical label, the reaction is not quantitative in the majority of cases, and a huge excess of reagent is required in order to get close to 100 % labelling efficiency. This is due to many factors, such as steric effects, e.g. due to the AA side chains and experimental conditions. Another issue is that under basic conditions both reagents hydrolyse very quickly, which is most unfortunate as a slightly basic pH is needed for the derivatisation. Keeping the pH in the necessary range was found to be the biggest challenge during the entire labelling procedure. With the adequate pH though, efficient derivatisation can be ensured.

The labelling procedure using NHS-DOTA was further simplified in the course of the research and now provides a nearly 100 % derivatisation efficiency for protein digest samples. The underivatised peptides were mainly present in traces and showed negligible peak intensities in MALDI-MS.

NHS-DOTA is very universal in its application, and can be used on virtually any peptide sample which contains free amino-groups. Unfortunately, this typically results in a high complexity of the respective sample as almost every peptide can be labelled, and when peptides contain one or more lysine residues, multiple labelling occurs frequently – even more so when missed cleavages following enzymatic digestion are involved. This complexity, and the requirement of digestion of the samples for quantification using ICP-MS, makes the baseline separation of even low complexity samples very difficult.

Mal-DOTA on the other hand, seems to be an elegant alternative to NHS-DOTA, since in theory it should only target the much rarer sulfhydryl groups in Cys residues. Therefore, it should have less target peptides in digested samples and analysis should show a far lower complexity. Unfortunately, due to its rarity, it can occur that there are no proper target peptides in the protein of interest. It must also be taken care, that the sample is

not treated with alkylation reagents prior to derivatisation with Mal-DOTA, which can cause unwanted scrambling of disulfides or lead to inefficient digestion.

The protocol for the derivatisation of model peptides by Mal-DOTA was optimised and employed a 20-fold molar excess regarding free sulfhydryl groups. In the course of this study it was found that by employing a 20-fold molar excess of reagent on protein digest samples, the resulting labelling efficiency was far below the efficiency of respective NHS-DOTA labellings. This is most likely due to the fact that the Mal-DOTA can also react with primary and secondary amines if present in high amounts, groups which are more frequently present in protein digests compared to the sulfhydryl-groups. The consequence of this is the need for an elevated molar excess of the reagent (more than 20-fold) for application on protein digests. The problems encountered with this lead to the decision that the later experiments with protein digests were only performed using NHS-DOTA. If the application of Mal-DOTA to a digest sample is deemed essential, possibilities for targeted blocking of amino-groups could be taken into consideration, in order to reduce the above mentioned side reactions. However, this comes with the cost of additional –error prone – derivatisation steps.

Even when using the optimised derivatisation protocol together with nanoHPLC online precleaning, the lanthanide background can still be far too high for real world applications. In general, the lanthanide background increases with increasing complexity of the sample, caused by the need of higher excess of DOTA-reagent.

For further reduction of the lanthanide salt excess, a pre-complexation of the reagent with clean-up could be considered. The DOTA reagent could be incubated with the respective lanthanide salt and cleaned up afterwards in preparative HPLC. The derivatisation would then be conducted with the Ln-DOTA reagents, without further addition of lanthanide salts. A similar preparation procedure is employed for the commercially available MeCAT reagents.[179]

However, the preparative pre-complexation approach was ruled out because of economical and practical reasons in this study. The approach requires larger amounts of highly expensive NHS-DOTA reagent as starting material. However, the practical reasons held more importance for the decision: being prone to hydrolysis, the reagents hold the prospect of degradation during the pre-complexation and clean-up procedure. It is also

highly doubted that the degraded (hydrolysed) DOTA can be separated from its active form with ease. This probably leads to the necessity to employ an even larger excess of complexed DOTA reagent, thus negating the benefits from the prior removed excess metal to a degree.

Another point against the pre-complexation is due to the possibility of splitting the derivatisation preparations prior to complexation with different metals in the normal approach, thus ensuring that resulting samples are labelled with DOTA to the same degree, before adding the lanthanides. With pre-complexed DOTA-reagents, two samples would need to be derivatised, not ensuring their direct comparability. It may also be viable to guard the uncomplexed DOTA-peptides in buffered solution at -20 °C (pH 5) for later complexation with lanthanides, according to the needs of the experimental setup.

An alternative labelling protocol using NHS-DOTA, which might be interesting regarding higher derivatisation efficiencies, was presented in a preliminary study by Christopher et al. [165] The approach employed microwave assisted derivatisation and chelation using NHS-DOTA on peptides for the use with ICP-MS. Microwave heating was theorised to increase reaction kinetics, thus enabling reduction of the incubation time under basic conditions. Derivatisation with the microwave system was conducted for up to 10 min and for another 5 min to aid complexation. The authors showed that the labelling was up to 40% more efficient compared with a 2 h derivatisation / 2 h complexation at RT.

Comparing these results to the optimised protocol B presented in section 3.5.1, it might be considered in future applications to employ microwave assisted derivatisation. As the method seems capable of increasing labelling efficiency, and may help to reduce the currently employed 100-fold molar excess of NHS-DOTA in the optimised protocol.

It was also found that the quality of the DOTA reagents can vary largely between the fabrication batches. Generally, it is advisable to test the labelling efficiency for each new batch using standard peptides.

5.2 NHS-DOTA Peptide Retention Behaviour

By monitoring the retention times of labelled peptides and their unlabelled counterparts, it was found that both could be separated at lower solvent polarities, thus

earlier fractions, in reversed-phase LC (Figure 38, page 85). The labelled peptides in most cases eluted later than their unlabelled counterparts. This peptide elution time difference grew smaller with rising retention time and the labelled and unlabelled peptides showed complete coelution in the very late fractions. This lead to the conclusion that the DOTA-label adds to the interaction of the peptides with the stationary phase. The influence on the retention time of hydrophobic peptide species is less pronounced, resulting in the coelution of unlabelled, singly and multiply labelled peptides. The increasing coelution in the later fractions though, posed a serious problem for quantification approaches. This can already be seen for samples with low complexity, such as digests of single model proteins. Data interpretation gets more complicated with rising sample complexity making it necessary to use bioinformatics tools for calculation of peptide ratios in overlapping/coeluting peaks and assignment of the signals to the respective peptides.

5.3 Separation Efficiency versus Quantitative Analysis

Separation efficiency still remains one of the biggest challenges in protein and peptide analysis. This is in accordance with the findings of recent publications on similar LC-based approaches: they mostly concern themselves with the separation of peptide mixtures or digests of purified proteins (see Table 23). For molecular MS, the coelution of peptides can, in many cases, be balanced by the additional separation in the m/z domain, unless the analytes are (close to) isobaric.

Baseline separation is an important prerequisite for a reliable quantification in nanoHPLC ICP-MS. Since structural information is lost in the ICP process, the signals for coeluting analytes form a single peak and are therefore indistinguishable. In this case the acquired quantitative data cannot be confidently attributed to the complementary identification data e.g. from MALDI-MS. A complete baseline separation of peptides could only be achieved for the synthetic peptide mixtures used in this study, whereas for protein digests baseline separation could only be partially achieved. In the latter case, groups of coeluting peptides usually consisted of variations of the same peptide with and without missed cleavages and different numbers of attached tags. It can be considered to quantify them as groups.

In this prospect, and regarding applicability of the DOTA label, a whole proteome analysis by these means does not seem possible under quantitative conditions. As shown with the application of ZipTips, quantitative recovery is not always ensured for routine standard protocols in proteomics. Each additional purification and separation step holds the potential risk of analyte losses. In quantitative analysis, protein and peptide recovery must not be sacrificed for efficient separation or purification. Therefore it would be very interesting to analyse the sample losses in routine proteomics approaches, e.g. a bottom-up approach, starting with a cell culture or lysate sample and monitoring each step until it is broken down to its peptides. The results could thereafter be compared to the results from the recovery (sample loss) monitoring in a top-down approach. The presented approach holds the potential to perform such a study. For the monitoring of the recoveries of the different procedures used in a proteomics workflow, a set of labelled model proteins with different sizes and properties could be spiked into a lysate sample. During each step of the proteomics workflow, including SDS-PAGE (1D or 2D) and chromatographic separations, a sample could be drawn and analysed in regard to the present lanthanide signals. On the peptide level, labelled model peptides could be employed and monitored.

5.4 fsLA-ICP-MS on MALDI-Targets

A novel approach employing the combination of MALDI-MS together with fsLA-ICP-MS was presented. The consecutive application of both techniques together has been shown to provide a great potential in this first proof-of-concept study. The combination of a molecular and an ablation based elemental mass spectrometric method allows complementary information from a single LC-run to be gathered by permitting unambiguous attribution of peptide identifications from MALDI-MS to the corresponding quantitative information from LA-ICP-MS. Beside applications in bioanalytics, e.g. proteomics, this basic principle will certainly also find widespread applications in other fields such as environmental analysis etc.. However, some virtues may still need to be uncovered prior to this approach becoming a standard method.

The chromatographic resolutions of both MALDI- and fsLA-ICP-MS chromatograms were very low, which is due to the limitations of the spot sizes during Probot fractionation.

Smaller spotter fractionation time is plausible but most likely very impractical in its application. Reducing the fractionation time equals a reduction in the spot size which may pose problems for automated MALDI-MS measurements, especially in regard to the alignment. Spots may also be missed more easily by the randomised laser shots.

For better chromatographic resolution, it might also be considered to modify the spotting in a way that decreases only the nanoHPLC fraction size, but still guards the size of the matrix spots. This would simply result in a higher number of measurement spots for the same chromatogram. For this purpose, spot intervals could be shortened while the dosage flow of the matrix would need to be increased accordingly. A potential solution is the choice of alternative matrices which allow proper measurement at altered matrix-to-analyte ratios. However this still needs to be evaluated, especially in regard to the sensitivity of the MALDI-MS measurements. Lower fraction volumes equal less analyte in each spot, which may result in analyte levels encroaching on the limits of detection of the MALDI-MS.

Another option might lie in longer gradients for a greater separation of the peaks and thus a decrease in coelution. This would also allow for the proper matching of LA-ICP-MS signals to their identified peaks in MALDI-MS. Unfortunately, both of these mentioned possibilities would result in a further elongation of the analysis time in LA-ICP-MS, which on the current stage is already a very long and tedious process. The manual LA-ICP-MS analysis is quite time consuming: the measurement of 80 spots, equalling barely 20 min of chromatography, took longer than an hour. So far no automation is possible but would be highly beneficial both in terms of reproducibility and overall measurement times.

A compromise for lowering of the required measurement times could be a pre-evaluation of the MALDI-MS and UV data: interesting parts of the chromatography could be identified prior to LA-measurements. By only measuring the spots of interest using LA-ICP-MS, the measurement time could be reduced significantly.

The manual measurement of LA-ICP-MS spectra bears the danger of performing errors. During the preliminary test, two persons were involved in the experiment: one conducting the measurements and a second to keep track of the data. A high level of

attention needed to be maintained and already small diversions could have accounted for errors.

For further reduction of analysis time, an automation of LA-ICP-MS would be an option. To achieve this, either the cut target pieces would need to be standardised, including a specific holder, or an adapted ablation cell would need to be designed. In both cases, a spot set pattern could be applied in a reproducible manner, so that the spots can be located automatically in LA-ICP-MS. This could be achieved in a similar way to MALDI-MS, in which manual alignment of MALDI target plates is performed. Like this the laser could also autofocus itself properly, avoiding too deep ablation craters.
One possibility for an adapted ablation cell that can be applied on an uncut target would be a small cell which can be put on the target and be moved around as needed. A cell which can contain a whole MALDI-plate is not a feasible option. The cell size must not be too big because of a higher risk of turbulences in the cell volume and thus ineffective transfer of the analytes to the ICP-MS.
For the adapted cell design a matching spotting pattern would be easy to be programmed on the robotic plate spotter, avoiding areas were the ablation cell comes into contact with the target. In order to get the ablation cell air-tight, a rubber seal could be employed, together with a set of clips. Like this, the cell could be positioned on different areas of the target.
It is also imaginable to employ standardised targets of small size that fit in normal-sized ablation cells. Special targets could be developed in collaboration with a manufacturer of MALDI-MS instruments. In this context the reusability of already ablated targets for further use in MALDI-MS could be inquired. However, the re-use of targets is not a very practical option due to the destructive nature of the LA. This is why it would be more practical to consider disposable target slips/plate covers which could be composed of different materials or combinations, such as metal covered glass slides; however this would require extensive validation and testing.

The current workload during application of the method, especially regarding the measurement time during LA-ICP-MS, underlines the need for automation of the method. Still, it already shows some important virtues: most of all the possibility to

reanalyse exactly the same sample twice with two complementary techniques. As with every new method, all of its merits will only become apparent once it is refined further.

Recent developments in the application of LA related to MALDI-MS typically concern themselves with a sample transfer from one medium to another. Park et al. used an infrared LA-system to resolve a solid sample which was deposited on a steel target surface into small solvent droplets. The solved samples were then either measured via ESI-MS or redeposited on a MALDI-target together with matrix and the sample measured in MALDI-MS.[183] LA-sample transfer was also used in combination with MALDI-imaging for the analysis of tissue samples.[184]

The approaches shown in this thesis did not employ a reaction cell for ICP-MS measurements. The lanthanides show only a few polyatomic interferences among each other (see Table 1 on page 25) and it is questionable that a reaction cell will be able to rule out those interferences. Currently, there are only a handful of reports on the application of collision/reaction cell technology for analysis of lanthanides, all of which show only limited improvements.[185, 186]

Given that the interfering element is not present in the sample, these interferences will not pose a problem. This was mainly the case for the samples employed in nanoHPLC ICP-MS. For fsLA-ICP-MS though, the sample matrix in form of the MALDI-plate might contain significant amounts of interfering lanthanides, as was hinted during the determination of the LODs (section 4.5.5). Lanthanides tend to form oxides, which is the main reason for the interferences. The impact of those interferences can be measured by application of single element solutions and monitoring of the signal at the element's mass + 16 mass units. The determined impact can then be applied in form of a correction factor.[187] Alternatively, the targeted oxidation of lanthanides using a dynamic reaction cell with oxygen as reactive gas has been reported.[185]

In both mentioned cases, correction factors would need to be employed. It can be questioned whether the effort of employing such a correction will have a great impact on the outcome of the presented quantitative approaches. The correction is mainly meant for trace element analysis, where the impact of these interferences can result in significant errors. The systematic error from the interferences is conceivably much

smaller than the sample to sample variation from the peptide samples, thus must not be overlooked but can be considered as of negligible effect.

5.5 Superposition of Chromatograms

Problems with data alignment are commonly encountered in many analytical applications, in form of stretching or shrinking of signals along a horizontal scale. This is especially problematic for data destined for automated computation at a later stage. There are a multitude of approaches that address these alignment problems, e.g. dynamic and parametric time warping. They are based on warping algorithms, which can compare and align large data sets ,[188] and have also been reported for the use with LC-MS based proteomics.[189] The alignment is commonly based on searching for matching peaks in two chromatograms.[190] However, the basic aim of all warping algorithms is a reliable automatic alignment of data.

The retention time marker (RTM) peptides developed in this thesis might contribute to the reliable superposition of differentially acquired chromatograms, also in automatic warping methods. The recognition of the RTM peptides would need to be implemented into the algorithms, leading to a facilitation of the computational approach. This way, the RTMs could improve the accuracy of the alignments and make them more comprehensible.

The RTMs are expected to be applicable in a broad range of experiments and with a multitude of application possibilities, which are not reduced to the marking of retention times. A set of labelled peptides e.g. with different pI values could be employed as pI-markers for isoelectric focussing strips used in LA-ICP-MS.

5.6 Final Conclusions

It could be shown that even with the geographical distance between two laboratory facilities, complementary experiments could still provide conclusive data. By following some strict rules regarding sample transportation in between the experiments, it was made sure that no sample alterations occurred. On the whole, the complementarity of both laboratories was combined to the benefit of both parties. Collaborations of this

kind can contribute largely to the forthcoming of projects and to intensive scientific interchange between laboratories in general.

Several novel approaches were developed in the course of this PhD thesis, which can contribute to the analysis of metal labelled peptide samples. The presented online precleaning step enables a reliable metal background reduction for labelling approaches, while guarding peptide recoveries. Samples can be analysed directly after labelling without prior desalting and the precleaning can be implemented into normal nanoHPLC workflows very easily. The optimal precleaning step only took 6 min, resulting in an extension of the analysis time of usually less than 10 %.

The development of a set of retention time marker peptides largely facilitated the alignment of complementary data which was acquired independently. By application of these peptides there was no need to strictly apply exactly the same analysis parameters, such as gradient or column length in nanoHPLC, to all samples while not compromising their comparability. This is especially interesting for data acquired on different instruments or by different operators, e.g. in the different laboratories of two cooperation partners. It was also shown that this set of labelled peptides might be employed as a standard for a quick and approximate absolute quantification when conducting online nanoHPLC ICP-MS analysis. There was no need for an additional setup with an additional pump for the generation of an isotope spike flow, like in isotope dilution analysis. [133, 151]

The different independent quantification approaches showed conclusive and comparable results in the range of the expected values. The developed quantification techniques are promising, however further refinement is required, and it the results need to be confirmed with an independent technique, e.g. using MeCAT or an isobaric tagging approach.

The novel approach employing MALDI-MS and fsLA-ICP-MS for acquisition of complementary data by re-measurement of the same separation, showed great potential and after refinement will certainly also be applicable for approaches outside the field of proteomics.

It could also be shown that there is still some potential left for the refinement of the DOTA-labelling protocols. The versatility of the label is unrivalled regarding the number

of possible labels for multiplex analysis. Still some limitations of the label have surfaced, especially in regard to quantitative analysis after chromatographic separation. The baseline separation remains the limiting factor when employing ICP-MS for quantification of complex samples. This is why it will be very hard to apply the DOTA labelling to proteome analysis.

New tags could be developed in the future, such as lanthanide DOTA based isobaric tags, which could be quantified via both MALDI-MS and ICP-MS, in order to elucidate the ratios of overlapping peaks and the behaviour of similar peptides. This could also allow for the development of a computational model which would consecutively enable ICP-MS based quantification of peaks that are not baseline separated.

VI References

[1] Wasinger, V. C.; Zeng, M.; Yau, Y. *Current status and advances in quantitative proteomic mass spectrometry*, Int. J. Proteomics, 2013, *2013*, 180605.

[2] Bantscheff, M.; Schirle, M.; Sweetman, G.; Rick, J.; Kuster, B. *Quantitative mass spectrometry in proteomics: a critical review*, Anal. Bioanal. Chem., 2007, *389*, 1017-1031.

[3] Tholey, A.; Schaumlöffel, D. *Metal labeling for quantitative protein and proteome analysis using inductively-coupled plasma mass spectrometry*, TrAC, Trends Anal. Chem., 2010, *29*, 399-408.

[4] Holste, A.; Tholey, A.; Hung, C. W.; Schaumlöffel, D. *Nano-high-performance liquid chromatography with online precleaning coupled to inductively coupled plasma mass spectrometry for the analysis of lanthanide-labeled peptides in tryptic protein digests*, Anal. Chem., 2013, *85*, 3064-3070.

[5] Wilkins, M. R.; Sanchez, J.-C.; Gooley, A. A.; Appel, R. D.; Humphery-Smith, I.; Hochstrasser, D. F.; Williams, K. L. *Progress with Proteome Projects: Why all Proteins Expressed by a Genome Should be Identified and How To Do It*, Biotechnology and Genetic Engineering Reviews, 1996, *13*, 19-50.

[6] Karas, M.; Bachmann, D.; Hillenkamp, F. *Influence of the wavelength in high-irradiance ultraviolet laser desorption mass spectrometry of organic molecules*, Anal. Chem., 1985, *57*, 2935-2939.

[7] Fenn, J. B.; Mann, M.; Meng, C. K.; Wong, S. F.; Whitehouse, C. M. *Electrospray ionization for mass spectrometry of large biomolecules*, Science, 1989, *246*, 64-71.

[8] Anderson, L.; Seilhamer, J. *A comparison of selected mRNA and protein abundances in human liver*, ELECTROPHORESIS, 1997, *18*, 533-537.

[9] Griffiths, W. J.; Wang, Y. *Mass spectrometry: from proteomics to metabolomics and lipidomics*, Chemical Society Reviews, 2009, *38*, 1882-1896.

[10] Velculescu, V. E.; Zhang, L.; Zhou, W.; Vogelstein, J.; Basrai, M. A.; Bassett Jr, D. E.; Hieter, P.; Vogelstein, B.; Kinzler, K. W. *Characterization of the Yeast Transcriptome*, Cell, 1997, *88*, 243-251.

[11] Szpunar, J. *Advances in analytical methodology for bioinorganic speciation analysis: metallomics, metalloproteomics and heteroatom-tagged proteomics and metabolomics*, Analyst, 2005, *130*, 442-465.

[12] Wesenberg, D.; Krauss, G.-J.; Schaumlöffel, D. *Metallo-thiolomics: Investigation of thiol peptide regulated metal homeostasis in plants and fungi by liquid chromatography-mass spectrometry*, International Journal of Mass Spectrometry, 2011, *307*, 46-54.

[13] Fulton, A. B.; Isaacs, W. B. *Titin, a huge, elastic sarcomeric protein with a probable role in morphogenesis*, BioEssays, 1991, *13*, 157-161.

[14] Donovan, J.; Copeland, P. R. *The Efficiency of Selenocysteine Incorporation Is Regulated by Translation Initiation Factors*, Journal of Molecular Biology, 2010, *400*, 659-664.

[15] Krzycki, J. A. *The direct genetic encoding of pyrrolysine*, Current Opinion in Microbiology, 2005, *8*, 706-712.

[16] Müller-Esterl, W.; Plenikowski, M. *Biochemie: Eine Einführung für Mediziner und Naturwissenschaftler*; Spektrum Akademischer Verlag: Heidelberg, Germany, 2009.

[17] Lottspeich, F. *Bioanalytik*, 2nd Edition ed.; Elsevier GmbH: München, 2006.

[18] Ahmed, H. *Principles and reactions of protein extraction, purification, and characterization*; CRC Press: Boca Raton, 2005.

[19] Zhang, Y.; Cremer, P. S. *Interactions between macromolecules and ions: the Hofmeister series*, Curr. Opin. Chem. Biol., 2006, *10*, 658-663.

[20] Baldwin, R. L. *How Hofmeister ion interactions affect protein stability*, Biophysical Journal, 1996, *71*, 2056-2063.

[21] Jiang, L.; He, L.; Fountoulakis, M. *Comparison of protein precipitation methods for sample preparation prior to proteomic analysis*, Journal of Chromatography A, 2004, *1023*, 317-320.
[22] Cheryan, M. *Ultrafiltration and microfiltration handbook*; Technomic Pub. Co: Lancaster, Pa, 1998.
[23] Rehm, H.; Letzel, T. *Proteinbiochemie/Proteomics*; Spektrum Akademischer: Heidelberg, 2010.
[24] O'Farrell, P. H. *High resolution two-dimensional electrophoresis of proteins*, Journal of Biological Chemistry, 1975, *250*, 4007-4021.
[25] Li, S. F. Y. *Capillary electrophoresis: principles, practice, and applications*; Elsevier: Amsterdam; London; New York, 1993.
[26] Stellwagen, E.; Murray, P. D. In *Methods in Enzymology*; Academic Press, 1990; Vol. Volume 182, pp 317-328.
[27] Issaq, H. J.; Conrads, T. P.; Janini, G. M.; Veenstra, T. D. *Methods for fractionation, separation and profiling of proteins and peptides*, ELECTROPHORESIS, 2002, *23*, 3048-3061.
[28] Carr, D., third ed.; GraceVYDAC, 2002.
[29] Buszewski, B.; Noga, S. *Hydrophilic interaction liquid chromatography (HILIC) - a powerful separation technique*, Anal. Bioanal. Chem., 2012, *402*, 231-247.
[30] Delmotte, N.; Lasaosa, M.; Tholey, A.; Heinzle, E.; Huber, C. G. *Two-Dimensional Reversed-Phase x Ion-Pair Reversed-Phase HPLC:â€‰ An Alternative Approach to High-Resolution Peptide Separation for Shotgun Proteome Analysis*, Journal of Proteome Research, 2007, *6*, 4363-4373.
[31] Nägele, E.; Vollmer, M.; Hörth, P.; Vad, C. *2D-LC/MS techniques for the identification of proteins in highly complex mixtures*, Expert Rev Proteomics, 2004, *1*, 37-46.
[32] Hart-Smith, G.; Blanksby, S. J. In *Mass Spectrometry in Polymer Chemistry*; Wiley-VCH Verlag GmbH & Co. KGaA, 2012, pp 5-32.
[33] Thomas, R. *Practical guide to ICP-MS: a tutorial for beginners*, Third Edition ed.; CRC Press, Taylor & Francis Group: Boca Raton, 2013.
[34] Thermo Scientific *Thermo Scientific Element XR: Extended Dynamic Range High Resolution ICP-MS*; Thermo Fisher Scientific: Bremen, Germany, 2007.
[35] Agilent Technologies *Agilent 7700 Series ICP-MS*; Agilent Technologies Inc.: USA, 2010.
[36] Thermo Scientific *Thermo Scientific iCAP Q ICP-MS*; Thermo Fisher Scientific: Bremen, Germany, 2012.
[37] Svantesson, E.; Pettersson, J.; Markides, K. E. *The use of inorganic elemental standards in the quantification of proteins and biomolecular compounds by inductively coupled plasma spectrometry*, Journal of Analytical Atomic Spectrometry, 2002, *17*, 491-496.
[38] May, T. W.; Wiedmeyer, R. H. *A Table of Polyatomic Interferences in ICP-MS*, Atomic Spectroscopy, 1998, *19*, 150-155.
[39] Pieper, S. *Metallchelatkomplexe für die element-massenspektrometrische Quantifizierung von Peptiden und Proteinen*,Metallchelatkomplexe für die element-massenspektrometrische Quantifizierung von Peptiden und Proteinen. PhD Thesis, Humboldt University Berlin, 2008.
[40] Houk, R. S. *Mass spectrometry of inductively coupled plasmas*, Anal. Chem., 1986, *58*, 97A-105A.
[41] Günther, D. In *European Winter Conference on Plasma Spectrochemistry*: Krakow, 2013.
[42] Agilent Technologies *Agilent 7500 Series ICP-MS*; Agilent Technologies Inc.: USA, 2004.
[43] Gray, A. L. *Solid sample introduction by laser ablation for inductively coupled plasma source mass spectrometry*, Analyst, 1985, *110*, 551-556.

[44] Shaheen, M. E.; Gagnon, J. E.; Fryer, B. J. *Femtosecond (fs) lasers coupled with modern ICP-MS instruments provide new and improved potential for in situ elemental and isotopic analyses in the geosciences*, Chemical Geology, 2012, *330-331*, 260-273.

[45] Le Harzic, R.; Huot, N.; Audouard, E.; Jonin, C.; Laporte, P.; Valette, S.; Fraczkiewicz, A.; Fortunier, R. *Comparison of heat-affected zones due to nanosecond and femtosecond laser pulses using transmission electronic microscopy*, Applied Physics Letters, 2002, *80*, 3886-3888.

[46] D'Abzac, F. X.; Seydoux-Guillaume, A. M.; Chmeleff, J.; Datas, L.; Poitrasson, F. *Study of near infra red femtosecond laser induced particles using transmission electron microscopy and low pressure impaction: Implications for laser ablation-inductively coupled plasma-mass spectrometry analysis of natural monazite*, Spectrochimica Acta - Part B Atomic Spectroscopy, 2011, *66*, 671-680.

[47] Seydoux-Guillaume, A. M.; Freydier, R.; Poitrasson, F.; D'Abzac, F. X.; Wirth, R.; Datas, L. *Dominance of mechanical over thermally induced damage during femtosecond laser ablation of monazite*, European Journal of Mineralogy, 2010, *22*, 235-244.

[48] Wiltsche, H.; Günther, D. *Capabilities of femtosecond laser ablation ICP-MS for the major, minor, and trace element analysis of high alloyed steels and super alloys*, Anal. Bioanal. Chem., 2011, *399*, 2167-2174.

[49] Ricard, E.; Pécheyran, C.; Sanabria Ortega, G.; Prinzhofer, A.; Donard, O. F. X. *Direct analysis of trace elements in crude oils by high-repetition-rate femtosecond laser ablation coupled to ICPMS detection*, Anal. Bioanal. Chem., 2011, *399*, 2153-2165.

[50] Fernández, B.; Claverie, F.; Pécheyran, C.; Alexis, J.; Donard, O. F. X. *Direct determination of trace elements in powdered samples by in-cell isotope dilution femtosecond laser ablation ICPMS*, Anal. Chem., 2008, *80*, 6981-6994.

[51] Margetic, V.; Niemax, K.; Hergenröder, R. *Application of femtosecond laser ablation time-of-flight mass spectrometry to in-depth multilayer analysis*, Anal. Chem., 2003, *75*, 3435-3439.

[52] Mateo, M. P.; Garcia, C. C.; Hergenröder, R. *Depth analysis of polymer-coated steel samples using near-infrared femtosecond laser ablation inductively coupled plasma mass spectrometry*, Anal. Chem., 2007, *79*, 4908-4914.

[53] Becker, J. S.; Matusch, A.; Palm, C.; Salber, D.; Morton, K. A.; Becker, J. S. *Bioimaging of metals in brain tissue by laser ablation inductively coupled plasma mass spectrometry (LA-ICP-MS) and metallomics*, Metallomics, 2010, *2*, 104-111.

[54] Pedrero, Z.; Madrid, Y.; Camara, C.; Schram, E.; Luten, J. B.; Feldmann, I.; Waentig, L.; Hayen, H.; Jakubowski, N. *Screening of selenium containing proteins in the Tris-buffer soluble fraction of African catfish (Clarias gariepinus) fillets by laser ablation-ICP-MS after SDS-PAGE and electroblotting onto membranes*, Journal of Analytical Atomic Spectrometry, 2009, *24*, 775-784.

[55] Chéry, C. C.; Günther, D.; Cornelis, R.; Vanhaecke, F.; Moens, L. *Detection of metals in proteins by means of polyacrylamide gel electrophoresis and laser ablation-inductively coupled plasma-mass spectrometry: Application to selenium*, ELECTROPHORESIS, 2003, *24*, 3305-3313.

[56] Karas, M.; Hillenkamp, F. *Laser desorption ionization of proteins with molecular masses exceeding 10,000 daltons*, Anal. Chem., 1988, *60*, 2299-2301.

[57] Tanaka, K.; Waki, H.; Ido, Y.; Akita, S.; Yoshida, Y.; Yoshida, T.; Matsuo, T. *Protein and polymer analyses up to m/z 100 000 by laser ionization time-of-flight mass spectrometry*, Rapid Communications in Mass Spectrometry, 1988, *2*, 151-153.

[58] Lewis, J. K.; Wei, J.; Siuzdak, G. *Matrix-Assisted Laser Desorption/Ionization Mass Spectrometry in Peptide and Protein Analysis*, Encyclopedia of Analytical Chemistry, 2000.

[59] Zenobi, R.; Knochenmuss, R. *Ion formation in MALDI mass spectrometry*, Mass Spectrometry Reviews, 1998, *17*, 337-366.
[60] Knochenmuss, R. *Ion formation mechanisms in UV-MALDI*, Analyst, 2006, *131*, 966-986.
[61] Knochenmuss, R.; Zenobi, R. *MALDI Ionization: The Role of In-Plume Processes*, Chemical Reviews, 2002, *103*, 441-452.
[62] Karas, M.; Krüger, R. *Ion Formation in MALDI: The Cluster Ionization Mechanism*, Chemical Reviews, 2003, *103*, 427-440.
[63] Hillenkamp, F. *MALDI MS a practical to instrumentation, methods and applications*; Wiley-VCH: Weinheim, 2007.
[64] Jaskolla, T.; Karas, M. *Compelling Evidence for Lucky Survivor and Gas Phase Protonation: The Unified MALDI Analyte Protonation Mechanism*, Journal of The American Society for Mass Spectrometry, 2011, *22*, 976-988.
[65] Gaskell, S. J. *Electrospray: Principles and Practice*, Journal of Mass Spectrometry, 1997, *32*, 677-688.
[66] Mallet, A. I. *Dictionary of mass spectrometry*; Wiley: Chichester ; Hoboken, NJ, 2009.
[67] Khalsa-Moyers, G.; McDonald, W. H. *Developments in mass spectrometry for the analysis of complex protein mixtures*, Brief Funct. Genomic. Proteomic., 2006, *5*, 98-111.
[68] Wasinger, V. C.; Cordwell, S. J.; Cerpa-Poljak, A.; Yan, J. X.; Gooley, A. A.; Wilkins, M. R.; Duncan, M. W.; Harris, R.; Williams, K. L.; Humphery-Smith, I. *Progress with gene-product mapping of the Mollicutes: Mycoplasma genitalium*, ELECTROPHORESIS, 1995, *16*, 1090-1094.
[69] Jungblut, P. R.; Holzhutter, H. G.; Apweiler, R.; Schluter, H. *The speciation of the proteome*, Chem Cent J, 2008, *2*, 16.
[70] Pandey, A.; Mann, M. *Proteomics to study genes and genomes*, Nature, 2000, *405*, 837-846.
[71] Zhou, J.; Cidlowski, J. A. *The human glucocorticoid receptor: One gene, multiple proteins and diverse responses*, Steroids, 2005, *70*, 407-417.
[72] Ideker, T.; Thorsson, V.; Ranish, J. A.; Christmas, R.; Buhler, J.; Eng, J. K.; Bumgarner, R.; Goodlett, D. R.; Aebersold, R.; Hood, L. *Integrated Genomic and Proteomic Analyses of a Systematically Perturbed Metabolic Network*, Science, 2001, *292*, 929-934.
[73] Anderson, N. L.; Anderson, N. G. *The human plasma proteome: history, character, and diagnostic prospects*, Mol. Cell Proteomics, 2002, *1*, 845-867.
[74] UniProtKB; http://www.uniprot.org/; accessed 07.10.2013
[75] Matrix Science; http://www.matrixscience.com/help/scoring_help.html; accessed 08.10.2013
[76] Linscheid, M. *Quantitative proteomics*, Anal. Bioanal. Chem., 2005, *381*, 64-66.
[77] Liu, H.; Sadygov, R. G.; Yates, J. R. *A Model for Random Sampling and Estimation of Relative Protein Abundance in Shotgun Proteomics*, Anal. Chem., 2004, *76*, 4193-4201.
[78] Findeisen, P.; Neumaier, M. *Mass spectrometry based proteomics profiling as diagnostic tool in oncology: current status and future perspective*, Clin. Chem. Lab. Med., 2009, *47*, 666-684.
[79] Rifai, N.; Gillette, M. A.; Carr, S. A. *Protein biomarker discovery and validation: the long and uncertain path to clinical utility*, Nat. Biotechnol., 2006, *24*, 971-983.
[80] Hawkridge, A. M.; Muddiman, D. C. *Mass spectrometry-based biomarker discovery: toward a global proteome index of individuality*, Annu. Rev. Anal. Chem. (Palo Alto Calif.), 2009, *2*, 265-277.
[81] Vinci, V.; Parekh, S.; Jenkins, N. In *Handbook of Industrial Cell Culture*; Humana Press, 2003, pp 3-20.
[82] Chu, L.; Robinson, D. K. *Industrial choices for protein production by large-scale cell culture*, Current Opinion in Biotechnology, 2001, *12*, 180-187.
[83] Scopus; www.scopus.com/; accessed 07.10.2013

[84] Matthiesen, R.; Friedman, D. In *Mass Spectrometry Data Analysis in Proteomics*; Humana Press, 2007; Vol. 367, pp 219-239.

[85] Gygi, S. P.; Corthals, G. L.; Zhang, Y.; Rochon, Y.; Aebersold, R. *Evaluation of two-dimensional gel electrophoresis-based proteome analysis technology*, Proc. Natl. Acad. Sci. U.S.A., 2000, *97*, 9390-9395.

[86] Jaffe, J. D.; Mani, D. R.; Leptos, K. C.; Church, G. M.; Gillette, M. A.; Carr, S. A. *PEPPeR, a Platform for Experimental Proteomic Pattern Recognition*, Mol. Cell Proteomics, 2006, *5*, 1927-1941.

[87] Mueller, L. N.; Rinner, O.; Schmidt, A.; Letarte, S.; Bodenmiller, B.; Brusniak, M.-Y.; Vitek, O.; Aebersold, R.; Müller, M. *SuperHirn – a novel tool for high resolution LC-MS-based peptide/protein profiling*, PROTEOMICS, 2007, *7*, 3470-3480.

[88] Lundgren, D. H.; Hwang, S.-I.; Wu, L.; Han, D. K. *Role of spectral counting in quantitative proteomics*, Expert Rev. Proteomics, 2010, *7*, 39-53.

[89] Lu, P.; Vogel, C.; Wang, R.; Yao, X.; Marcotte, E. M. *Absolute protein expression profiling estimates the relative contributions of transcriptional and translational regulation*, Nat. Biotech., 2007, *25*, 117-124.

[90] Ishihama, Y.; Oda, Y.; Tabata, T.; Sato, T.; Nagasu, T.; Rappsilber, J.; Mann, M. *Exponentially Modified Protein Abundance Index (emPAI) for Estimation of Absolute Protein Amount in Proteomics by the Number of Sequenced Peptides per Protein*, Mol. Cell Proteomics, 2005, *4*, 1265-1272.

[91] Conrads, T. P.; Alving, K.; Veenstra, T. D.; Belov, M. E.; Anderson, G. A.; Anderson, D. J.; Lipton, M. S.; Paša-Tolić, L.; Udseth, H. R.; Chrisler, W. B.; Thrall, B. D.; Smith, R. D. *Quantitative Analysis of Bacterial and Mammalian Proteomes Using a Combination of Cysteine Affinity Tags and 15N-Metabolic Labeling*, Anal. Chem., 2001, *73*, 2132-2139.

[92] Gouw, J. W.; Tops, B. B.; Krijgsveld, J. *Metabolic labeling of model organisms using heavy nitrogen (15N)*, Methods Mol. Biol., 2011, *753*, 29-42.

[93] Ong, S. E.; Blagoev, B.; Kratchmarova, I.; Kristensen, D. B.; Steen, H.; Pandey, A.; Mann, M. *Stable isotope labeling by amino acids in cell culture, SILAC, as a simple and accurate approach to expression proteomics*, Mol. Cell Proteomics, 2002, *1*, 376-386.

[94] Zhu, H.; Pan, S.; Gu, S.; Bradbury, E. M.; Chen, X. *Amino acid residue specific stable isotope labeling for quantitative proteomics*, Rapid Commun. Mass Spectrom., 2002, *16*, 2115-2123.

[95] Gygi, S. P.; Rist, B.; Gerber, S. A.; Turecek, F.; Gelb, M. H.; Aebersold, R. *Quantitative analysis of complex protein mixtures using isotope-coded affinity tags*, Nat. Biotechnol., 1999, *17*, 994-999.

[96] Yi, E. C.; Li, X. J.; Cooke, K.; Lee, H.; Raught, B.; Page, A.; Aneliunas, V.; Hieter, P.; Goodlett, D. R.; Aebersold, R. *Increased quantitative proteome coverage with (13)C/(12)C-based, acid-cleavable isotope-coded affinity tag reagent and modified data acquisition scheme*, Proteomics, 2005, *5*, 380-387.

[97] Ye, X.; Luke, B.; Andresson, T.; Blonder, J. *18O stable isotope labeling in MS-based proteomics*, Brief Funct. Genomic. Proteomic., 2009, *8*, 136-144.

[98] Yao, X.; Freas, A.; Ramirez, J.; Demirev, P. A.; Fenselau, C. *Proteolytic ^{18}O Labeling for Comparative Proteomics: Model Studies with Two Serotypes of Adenovirus*, Anal. Chem., 2001, *73*, 2836-2842.

[99] Kellermann, J. *ICPL--isotope-coded protein label*, Methods Mol. Biol., 2008, *424*, 113-123.

[100] Leroy, B.; Rosier, C.; Erculisse, V.; Leys, N.; Mergeay, M.; Wattiez, R. *Differential proteomic analysis using isotope-coded protein-labeling strategies: comparison, improvements and application to simulated microgravity effect on Cupriavidus metallidurans CH34*, PROTEOMICS, 2010, *10*, 2281-2291.

[101] Ross, P. L.; Huang, Y. N.; Marchese, J. N.; Williamson, B.; Parker, K.; Hattan, S.; Khainovski, N.; Pillai, S.; Dey, S.; Daniels, S.; Purkayastha, S.; Juhasz, P.; Martin, S.;

Bartlet-Jones, M.; He, F.; Jacobson, A.; Pappin, D. J. *Multiplexed protein quantitation in Saccharomyces cerevisiae using amine-reactive isobaric tagging reagents*, Mol. Cell Proteomics, 2004, *3*, 1154-1169.

[102] Zieske, L. R. *A perspective on the use of iTRAQ™ reagent technology for protein complex and profiling studies*, Journal of Experimental Botany, 2006, *57*, 1501-1508.

[103] Shadforth, I.; Dunkley, T.; Lilley, K.; Bessant, C. *i-Tracker: For quantitative proteomics using iTRAQ™*, Bmc Genomics, 2005, *6*.

[104] Thompson, A.; Schäfer, J.; Kuhn, K.; Kienle, S.; Schwarz, J.; Schmidt, G.; Neumann, T.; Hamon, C. *Tandem Mass Tags: A Novel Quantification Strategy for Comparative Analysis of Complex Protein Mixtures by MS/MS*, Anal. Chem., 2003, *75*, 1895-1904.

[105] Dayon, L.; Hainard, A.; Licker, V.; Turck, N.; Kuhn, K.; Hochstrasser, D. F.; Burkhard, P. R.; Sanchez, J.-C. *Relative Quantification of Proteins in Human Cerebrospinal Fluids by MS/MS Using 6-Plex Isobaric Tags*, Anal. Chem., 2008, *80*, 2921-2931.

[106] Rosenzweig, A. C. *Metallochaperones: Bind and deliver*, Chemistry and Biology, 2002, *9*, 673-677.

[107] Zhang, H.; Yan, W.; Aebersold, R. *Chemical probes and tandem mass spectrometry: a strategy for the quantitative analysis of proteomes and subproteomes*, Curr. Opin. Chem. Biol., 2004, *8*, 66-75.

[108] Julka, S.; Regnier, F. *Quantification in Proteomics through Stable Isotope Coding: A Review*, Journal of Proteome Research, 2004, *3*, 350-363.

[109] Peters, E. C.; Horn, D. M.; Tully, D. C.; Brock, A. *A novel multifunctional labeling reagent for enhanced protein characterization with mass spectrometry*, Rapid Communications in Mass Spectrometry, 2001, *15*, 2387-2392.

[110] Cagney, G.; Emili, A. *De novo peptide sequencing and quantitative profiling of complex protein mixtures using mass-coded abundance tagging*, Nat. Biotech., 2002, *20*, 163-170.

[111] Leitner, A.; Foettinger, A.; Lindner, W. *Improving fragmentation of poorly fragmenting peptides and phosphopeptides during collision-induced dissociation by malondialdehyde modification of arginine residues*, Journal of Mass Spectrometry, 2007, *42*, 950-959.

[112] Kutscher, D. J.; Bettmer, J. *Absolute and relative protein quantification with the use of isotopically labeled p-hydroxymercuribenzoic acid and complementary MALDI-MS and ICPMS detection*, Anal. Chem., 2009, *81*, 9172-9177.

[113] Qiu, Y.; Sousa, E. A.; Hewick, R. M.; Wang, J. H. *Acid-Labile Isotope-Coded Extractants: A Class of Reagents for Quantitative Mass Spectrometric Analysis of Complex Protein Mixtures*, Anal. Chem., 2002, *74*, 4969-4979.

[114] Sechi, S. *A method to identify and simultaneously determine the relative quantities of proteins isolated by gel electrophoresis*, Rapid Communications in Mass Spectrometry, 2002, *16*, 1416-1424.

[115] Reynolds, K. J.; Yao, X.; Fenselau, C. *Proteolytic ^{18}O Labeling for Comparative Proteomics: Evaluation of Endoprotease Glu-C as the Catalytic Agent*, Journal of Proteome Research, 2002, *1*, 27-33.

[116] Goodlett, D. R.; Keller, A.; Watts, J. D.; Newitt, R.; Yi, E. C.; Purvine, S.; Eng, J. K.; Haller, P. v.; Aebersold, R.; Kolker, E. *Differential stable isotope labeling of peptides for quantitation and de novo sequence derivation*, Rapid Communications in Mass Spectrometry, 2001, *15*, 1214-1221.

[117] Kuyama, H.; Watanabe, M.; Toda, C.; Ando, E.; Tanaka, K.; Nishimura, O. *An approach to quantitative proteome analysis by labeling tryptophan residues*, Rapid Communications in Mass Spectrometry, 2003, *17*, 1642-1650.

[118] Chen, X.; Chen, Y. H.; Anderson, V. E. *Protein Cross-Links: Universal Isolation and Characterization by Isotopic Derivatization and Electrospray Ionization Mass Spectrometry*, Analytical Biochemistry, 1999, *273*, 192-203.

[119] Zhang, R.; Regnier, F. E. *Minimizing Resolution of Isotopically Coded Peptides in Comparative Proteomics*, Journal of Proteome Research, 2002, *1*, 139-147.

[120] Mason, D. E.; Liebler, D. C. *Quantitative Analysis of Modified Proteins by LC-MS/MS of Peptides Labeled with Phenyl Isocyanate*, Journal of Proteome Research, 2003, *2*, 265-272.

[121] Zheng, L. N.; Wang, M.; Wang, H. J.; Wang, B.; Li, B.; Li, J. J.; Zhao, Y. L.; Chai, Z. F.; Feng, W. Y. *Quantification of proteins using lanthanide labeling and HPLC/ICP-MS detection*, J. Anal. At. Spectrom., 2011, *26*, 1233-1236.

[122] El-Khatib, A. H.; Esteban-Fernandez, D.; Linscheid, M. W. *Dual labeling of biomolecules using MeCAT and DOTA derivatives: application to quantitative proteomics*, Anal. Bioanal. Chem., 2012, *403*, 2255-2267.

[123] Gerber, S. A.; Rush, J.; Stemman, O.; Kirschner, M. W.; Gygi, S. P. *Absolute quantification of proteins and phosphoproteins from cell lysates by tandem MS*, Proc. Natl. Acad. Sci. U.S.A., 2003, *100*, 6940-6945.

[124] Thermo Scientific; http://www.piercenet.com/product/amine-reactive-10-plex-tandem-mass-tag-reagents; accessed 09.10.2013

[125] Sciex; http://www.sciex.com/products/standards-and-reagents/iTRAQ-Reagents.xml; accessed 09.10.2013

[126] Broussard, L. A.; Hammett-Stabler, C. A.; Winecker, R. E.; Ropero-Miller, J. D. *The toxicology of mercury*, Lab Medicine, 2002, *33*, 614-625.

[127] Lu, M.; Li, X.-F.; Le, X. C.; Weinfeld, M.; Wang, H. *Identification and characterization of cysteinyl exposure in proteins by selective mercury labeling and nano-electrospray ionization quadrupole time-of-flight mass spectrometry*, Rapid Communications in Mass Spectrometry, 2010, *24*, 1523-1532.

[128] Kutscher, D. J. *Protein labelling with mercury tags: fundamental studies on ovalbumin derivatised with p-hydroxymercuribenzoic acid (pHMB)* J. Anal. At. Spectrom., 2008, 1359–1364.

[129] Bräutigam, A.; Bomke, S.; Pfeifer, T.; Karst, U.; Krauss, G. J.; Wesenberg, D. *Quantification of Phytochelatins in Chlamydomonas reinhardtii using ferrocene-based derivatization*, Metallomics, 2010, *2*, 565-570.

[130] Seiwert, B.; Karst, U. *Analysis of cysteine-containing proteins using precolumn derivatization with N-(2-ferroceneethyl)maleimide and liquid chromatography/electrochemistry/mass spectrometry*, Anal. Bioanal. Chem., 2007, *388*, 1633-1642.

[131] Jahn, S.; Lohmann, W.; Bomke, S.; Baumann, A.; Karst, U. *A ferrocene-based reagent for the conjugation and quantification of reactive metabolites*, Anal. Bioanal. Chem., 2011, *402*, 461-471.

[132] Patel, P.; Jones, P.; Handy, R.; Harrington, C.; Marshall, P.; Evans, E. H. *Isotopic labelling of peptides and isotope ratio analysis using LC-ICP-MS: a preliminary study*, Anal. Bioanal. Chem., 2008, *390*, 61-65.

[133] Rappel, C.; Schaumlöffel, D. *Absolute Peptide Quantification by Lutetium Labeling and NanoHPLC-ICPMS with Isotope Dilution Analysis*, Anal. Chem., 2009, *81*, 385-393.

[134] Byegard, J.; Skarnemark, G.; Skalberg, M. *The stability of some metal EDTA, DTPA and DOTA complexes: Application as tracers in groundwater studies*, J. Radioanal. Nucl. Chem., 1999, *241*, 281-290.

[135] Wang, X.; Qin, W.; Lin, H.; Wang, J.; Wei, J.; Zhang, Y.; Qian, X. *Metal-tag labeling coupled with multiple reaction monitoring-mass spectrometry for absolute quantitation of proteins*, Analyst, 2013, *138*, 5309-5317.

[136] Waentig, L.; Jakubowski, N.; Hardt, S.; Scheler, C.; Roos, P. H.; Linscheid, M. W. *Comparison of different chelates for lanthanide labeling of antibodies and application in*

a Western blot immunoassay combined with detection by laser ablation (LA-)ICP-MS, J. Anal. At. Spectrom., 2012, *27*, 1311-1320.

[137] Gregorius, B.; Schaumlöffel, D.; Hildebrandt, A.; Tholey, A. *Characterization of metal-labelled peptides by matrix-assisted laser desorption/ionization mass spectrometry and tandem mass spectrometry*, Rapid Commun. Mass Spectrom., 2010, *24*, 3279-3289.

[138] Esteban-Fernandez, D.; Ahrends, R.; Linscheid, M. W. *MeCAT peptide labeling for the absolute quantification of proteins by 2D-LC-ICP-MS*, J. Mass Spectrom., 2012, *47*, 760-768.

[139] Bergmann, U.; Ahrends, R.; Neumann, B.; Scheler, C.; Linscheid, M. W. *Application of Metal-Coded Affinity Tags (MeCAT): Absolute Protein Quantification with Top-Down and Bottom-Up Workflows by Metal-Coded Tagging*, Anal. Chem., 2012, *84*, 5268-5275.

[140] Ahrends, R.; Pieper, S.; Kuhn, A.; Weisshoff, H.; Hamester, M.; Lindemann, T.; Scheler, C.; Lehmann, K.; Taubner, K.; Linscheid, M. W. *A metal-coded affinity tag approach to quantitative proteomics*, Mol. Cell Proteomics, 2007, *6*, 1907-1916.

[141] Schwarz, G.; Beck, S.; Weller, M. G.; Linscheid, M. W. *MeCAT-new iodoacetamide reagents for metal labeling of proteins and peptides*, Anal. Bioanal. Chem., 2011, *401*, 1203-1209.

[142] Haxel, G. B.; Hedrick, J. B.; Orris, G. J., *Rare Earth Elements - Critical Resources for High Technology | USGS Fact Sheet 087-02*; http://pubs.usgs.gov/fs/2002/fs087-02/; 2013/10/17/10:02:13

[143] al-Rashdan, A.; Heitkemper, D.; Caruso, J. A. *Lead speciation by HPLC-ICP-AES and HPLC-ICP-MS*, J. Chromatogr. Sci., 1991, *29*, 98-102.

[144] Sannac, S. b.; Chen, Y.-H. *Benefits of HPLC-ICP-MS coupling for mercury speciation in food*, HANDBOOK OF HYPHENATED ICP-MS APPLICATIONS, 2012.

[145] Schaumlöffel, D.; Ruiz Encinar, J.; Lobinski, R. *Development of a sheathless interface between reversed-phase capillary HPLC and ICPMS via a microflow total consumption nebulizer for selenopeptide mapping*, Anal. Chem., 2003, *75*, 6837-6842.

[146] Rappel, C.; Schaumlöffel, D. *Improved nanonebulizer design for the coupling of nanoHPLC with ICP-MS*, J. Anal. At. Spectrom., 2010, *25*, 1963-1968.

[147] Giusti, P.; Lobinski, R.; Szpunar, J.; Schaumlöffel, D. *Development of a nebulizer for a sheathless interfacing of nanoHPLC and ICPMS*, Anal. Chem., 2006, *78*, 965-971.

[148] Giusti, P.; Schaumlöffel, D.; Lobinski, R.; Szpunar, J. *Couplage parallèle de la nanoHPLC à l'ICP-MS et à l'ESI-MS. Bénéfices de cette approche pour l'analyse de biomolécules*, Spectra analyse, 2006, *35*.

[149] Pröfrock, D.; Prange, A. *Inductively coupled plasma-mass spectrometry (ICP-MS) for quantitative analysis in environmental and life sciences: a review of challenges, solutions, and trends*, Appl. Spectrosc., 2012, *66*, 843-868.

[150] Sanz-Medel, A.; Montes-Bayón, M.; Bettmer, J.; Luisa Fernández-Sanchez, M.; Ruiz Encinar, J. *ICP-MS for absolute quantification of proteins for heteroatom-tagged, targeted proteomics*, TrAC, Trends Anal. Chem., 2012, *40*, 52-63.

[151] Rodriguez-Gonzalez, P.; Marchante-Gayon, J. M.; Alonso, J. I. G.; Sanz-Medel, A. *Isotope dilution analysis for elemental speciation: A tutorial review*, Spectrochim. Acta, Part B, 2005, *60*, 151-207.

[152] Liu, J. M.; Li, Y.; Jiang, Y.; Yan, X. P. *Gold nanoparticles amplified ultrasensitive quantification of human urinary protein by capillary electrophoresis with on-line inductively coupled plasma mass spectroscopic detection*, Journal of Proteome Research, 2010, *9*, 3545-3550.

[153] Giesen, C.; Waentig, L.; Mairinger, T.; Drescher, D.; Kneipp, J.; Roos, P. H.; Panne, U.; Jakubowski, N. *Iodine as an elemental marker for imaging of single cells and tissue sections by laser ablation inductively coupled plasma mass spectrometry*, Journal of Analytical Atomic Spectrometry, 2011, *26*, 2160-2165.

[154] Giesen, C.; Mairinger, T.; Khoury, L.; Waentig, L.; Jakubowski, N.; Panne, U. *Multiplexed immunohistochemical detection of tumor markers in breast cancer tissue using laser ablation inductively coupled plasma mass spectrometry*, Anal. Chem., 2011, *83*, 8177-8183.

[155] Peng, H.; Chen, B.; He, M.; Zhang, Y.; Hu, B. *Magnetic quantitative immunoanalysis of carcinoembryonic antigen by ICP-MS with mercury labels*, Journal of Analytical Atomic Spectrometry, 2011, *26*, 1217-1223.

[156] Tang, Y.; Jiao, X.; Liu, R.; Wu, L.; Hou, X.; Lv, Y. *Inductively coupled plasma mass spectrometry for determination of total urinary protein with CdTe quantum dots label*, Journal of Analytical Atomic Spectrometry, 2011, *26*, 2493-2499.

[157] Waentig, L.; Jakubowski, N.; Roos, P. H. *Multi-parametric analysis of cytochrome P450 expression in rat liver microsomes by LA-ICP-MS*, Journal of Analytical Atomic Spectrometry, 2011, *26*, 310-319.

[158] Waentig, L.; Jakubowski, N.; Hayen, H.; Roos, P. H. *Iodination of proteins, proteomes and antibodies with potassium triodide for LA-ICP-MS based proteomic analyses*, Journal of Analytical Atomic Spectrometry, 2011, *26*, 1610-1618.

[159] Zhang, Z.; Yan, X.; Xu, M.; Yang, L.; Wang, Q. *A dual-labelling strategy for integrated ICPMS and LIF for the determination of peptides*, Journal of Analytical Atomic Spectrometry, 2011, *26*, 1175-1177.

[160] Esteban-Fernandez, D.; Scheler, C.; Linscheid, M. W. *Absolute protein quantification by LC-ICP-MS using MeCAT peptide labeling*, Anal. Bioanal. Chem., 2011, *401*, 657-666.

[161] Liu, R.; Lv, Y.; Hou, X.; Yang, L.; Mester, Z. *Protein quantitation using Ru-NHS ester tagging and isotope dilution high-pressure liquid chromatography-inductively coupled plasma mass spectrometry determination*, Anal. Chem., 2012, *84*, 2769-2775.

[162] Moreno-Gordaliza, E.; Esteban-Fernandez, D.; Giesen, C.; Lehmann, K.; Lazaro, A.; Tejedor, A.; Scheler, C.; Canas, B.; Jakubowski, N.; Linscheid, M. W.; Gomez-Gomez, M. M. *LA-ICP-MS and nHPLC-ESI-LTQ-FT-MS/MS for the analysis of cisplatin-protein complexes separated by two dimensional gel electrophoresis in biological samples*, J. Anal. At. Spectrom., 2012, *27*, 1474-1483.

[163] Yang, M. W.; Wang, Z. W.; Fang, L.; Zheng, J. P.; Xu, L. J.; Fu, F. F. *Simultaneous and ultra-sensitive quantification of multiple peptides by using europium chelate labeling and capillary electrophoresis-inductively coupled plasma mass spectrometry*, J. Anal. At. Spectrom., 2012, *27*, 946-951.

[164] Yoon, S. Y.; Lim, H. B. *Preparation of Metal-p-aminobenzyl-DOTA complex using magnetic particles for bio-tagging in laser ablation ICP-MS*, Bulletin of the Korean Chemical Society, 2012, *33*, 3665-3670.

[165] Christopher, S. J.; Kilpatrick, E. L.; Yu, L. L.; Davis, W. C.; Adair, B. M. *Preliminary evaluation of a microwave-assisted metal-labeling strategy for quantification of peptides via RPLC-ICP-MS and the method of standard additions*, Talanta, 2012, *88*, 749-758.

[166] de Bang, T. C.; Pedas, P.; Schjoerring, J. K.; Jensen, P. E.; Husted, S. r. *Multiplexed Quantification of Plant Thylakoid Proteins on Western Blots Using Lanthanide-Labeled Antibodies and Laser Ablation Inductively Coupled Plasma Mass Spectrometry (LA-ICP-MS)*, Anal. Chem., 2013, *85*, 5047-5054.

[167] Konz, T.; Alonso-García, J.; Montes-Bayón, M.; Sanz-Medel, A. *Comparison of copper labeling followed by liquid chromatography-inductively coupled plasma mass spectrometry and immunochemical assays for serum hepcidin-25 determination*, Anal. Chim. Acta, 2013, *799*, 1-7.

[168] Liu, R.; Hou, X.; Lv, Y.; McCooeye, M.; Yang, L.; Mester, Z. *Absolute quantification of peptides by isotope dilution liquid chromatography-inductively coupled plasma mass spectrometry and gas chromatography/mass spectrometry*, Anal. Chem., 2013, *85*, 4087-4093.

[169] Schwarz, G.; Beck, S.; Benda, D.; Linscheid, M. W. *MeCAT - comparing relative quantification of alpha lactalbumin using both molecular and elemental mass spectrometry*, Analyst, 2013, *138*, 2449-2455.

[170] Waentig, L.; Techritz, S.; Jakubowski, N.; Roos, P. H. *A multi-parametric microarray for protein profiling: simultaneous analysis of 8 different cytochromes via differentially element tagged antibodies and laser ablation ICP-MS*, Analyst, 2013, *138*, 6309-6315.

[171] Goebel-Stengel, M.; Stengel, A.; Taché, Y.; Reeve Jr, J. R. *The importance of using the optimal plasticware and glassware in studies involving peptides*, Analytical Biochemistry, 2011, *414*, 38-46.

[172] *BMSL - UWO Biological Mass Spectrometry Laboratory - Protocols - In-Solution Digestion*; http://www.biochem.uwo.ca/wits/bmsl/in-solution_digestion.html; accessed 23.10.2013

[173] Pierce Biotechnology *NHS and Sulfo-NHS Instructions*; Thermo Scientific: Rockford, IL 61105 USA, 2011.

[174] Pécheyran, C.; Cany, S.; Chabassier, P.; Mottay, E.; Donard, O. F. X. *High repetition rate and low energy femtosecond laser ablation coupled to ICPMS detection: a new analytical approach for trace element determination in solid samples* J. Phys. Conf. Ser., 2007, *59*, 122.

[175] Yan, X. W.; Xu, M.; Yang, L. M.; Wang, Q. Q. *Absolute Quantification of Intact Proteins via 1,4,7,10-Tetraazacyclododecane-1,4,7-trisacetic acid-10-Maleimidoethylacetamide-Europium Labeling and HPLC Coupled with Species-Unspecific Isotope Dilution ICPMS*, Anal. Chem., 2010, *82*, 1261-1269.

[176] Millipore, *User Guide for Reversed-Phase ZipTip*; http://www.millipore.com/userguides.nsf/a73664f9f981af8c852569b9005b4eee/55fe75ff9addc81385256b3e006a4f10/$FILE/PR02358A.pdf; accessed 07.11.2013

[177] Cai, B.; Li, J. *Evaluation of trifluoroacetic acid as an ion-pair reagent in the separation of small ionizable molecules by reversed-phase liquid chromatography*, Anal. Chim. Acta, 1999, *399*, 249-258.

[178] Tholey, A.; Toll, H.; Huber, C. G. *Separation and detection of phosphorylated and nonphosphorylated peptides in liquid chromatography-mass spectrometry using monolithic columns and acidic or alkaline mobile phases*, Anal. Chem., 2005, *77*, 4618-4625.

[179] Ahrends, R. *MeCAT - Neue Wege in der Peptid- und Proteinquantifizierung*,MeCAT - Neue Wege in der Peptid- und Proteinquantifizierung. PhD Thesis, Humboldt University Berlin, 2009.

[180] *WebElements Periodic Table of the Elements | Periodicity | Ionization energy: 1st | periodicity*; http://www.webelements.com/periodicity/ionisation_energy_1/; accessed 13.12.2013

[181] Nič, M.; Jirát, J.; Košata, B.; Jenkins, A.; McNaught, A. In *IUPAC Compendium of Chemical Terminology*; IUPAC: Research Triagle Park, NC, 2012.

[182] Tholey, A. *Ionic liquid matrices with phosphoric acid as matrix additive for the facilitated analysis of phosphopeptides by matrix-assisted laser desorption/ionization mass spectrometry*, Rapid Communications in Mass Spectrometry, 2006, *20*, 1761-1768.

[183] Park, S.-G.; Murray, K. K. *Infrared laser ablation sample transfer for on-line liquid chromatography electrospray ionization mass spectrometry*, Journal of Mass Spectrometry, 2012, *47*, 1322-1326.

[184] Park, S.-G.; Murray, K. K. *Infrared Laser Ablation Sample Transfer for MALDI Imaging*, Anal. Chem., 2012, *84*, 3240-3245.

[185] Ardini, F.; Soggia, F.; Rugi, F.; Udisti, R.; Grotti, M. *Conversion of rare earth elements to molecular oxide ions in a dynamic reaction cell and consequences on their determination*

by inductively coupled plasma mass spectrometry, Journal of Analytical Atomic Spectrometry, 2010, *25*, 1588-1597.

[186] Du, Z.; Houk, R. S. *Attenuation of metal oxide ions in inductively coupled plasma mass spectrometry with hydrogen in a hexapole collision cell*, Journal of Analytical Atomic Spectrometry, 2000, *15*, 383-388.

[187] *Union College Geology Department, Kurt Hollocher, ICP-MS facilities, Oxide and hydroxide corrections*; http://minerva.union.edu/hollochk/icp-ms/ree_corrections.htm; accessed 15.12.2013

[188] Eilers, P. H. C. *Parametric Time Warping*, Anal. Chem., 2003, *76*, 404-411.

[189] Bloemberg, T. G.; Gerretzen, J.; Wouters, H. J. P.; Gloerich, J.; van Dael, M.; Wessels, H. J. C. T.; van den Heuvel, L. P.; Eilers, P. H. C.; Buydens, L. M. C.; Wehrens, R. *Improved parametric time warping for proteomics*, Chemometrics and Intelligent Laboratory Systems, 2010, *104*, 65-74.

[190] Johnson, K. J.; Wright, B. W.; Jarman, K. H.; Synovec, R. E. *High-speed peak matching algorithm for retention time alignment of gas chromatographic data for chemometric analysis*, Journal of Chromatography A, 2003, *996*, 141-155.

[191] *www.gravy-calculator.de*; accessed 07.10.2013

VII Appendix I: Indices

7.1 Abbreviations

µ	micro (10^{-6})
2D	Two-dimensional
Å	Angström (10^{-10}m)
a	atto (10^{-18})
AA	Amino acid
AB	Antibody
ABC	Ammoniumbicarbonate
ACN	Acetonitrile
AcOH	Acetic acid
APEX	Absolute protein expression profiling
APS	Ammonium Persulfate
AQUA	Absolute quantification
AUC	Area Under Curve
BSA	Bovine serum albumin
C	Cysteine
ca.	Circa, approximately
CAE	capillary array electrophoresis
Cal	Calibration spot
CE	Capillary electrophoresis
CEC	capillary electro chromatography
CGE	capillary gel electrophoresis
CHAPS	3-[(3-Cholamidopropyl)dimethylammonio]-1-propanesulfonate hydrate
CHCA	α-cyano-4-hydroxycinnamic acid
CID	Collision induced dissociation/decomposition
cps	Counts per Second
Cys	Cysteine
CZE	Capillary zone electrophoresis
Da	Dalton
DIGE	Differential gel electrophoresis
DNA	Deoxyribonucleic acid
DOTA	1,4,7,10-tetraazacyclododecane-1,4,7,10-tetraacetic acid
DRC	Dynamic reaction cell

DTPA	Diethylenetriamine pentaacetic acid
DTPAA	Diethylenetriamine pentaacetic acid anhydride
EC	Electro chemical
ECD	Electron capture dissociation
EDTA	Ethylenediaminetetraacetic acid
emPAI	Exponentially modified protein abundance index
ESI	Electrospray ionisation
ETD	Electron transfer dissociation
EtOH	Ethanol
eV	electron volt
f	femto (10^{-15})
FFF	Field flow fractionation
FIA	Flow-injection analysis
FT	Fourier transform
FWHM	Full width at Half Maximum
g	gram
GC	Gas Chromatography
GluFib	Glu1-fibrinopeptide B (EGVNDNEEGFFSAR)
GRAVY	Grand average of hydropathicity
HCD	High energy CID
HCl	hydrochloric acid or hydrochloride
HEPES	4-(2-hydroxyethyl)-1-piperazineethanesulfonic acid
HFBA	Heptafluorobutyric acid (2,2,3,3,4,4,4-heptafluorobutanoic acid)
HIC	Hydrophobic interaction chromatography
HILIC	Hydrophilic interaction liquid chromatography
HPLC	High performance liquid chromatography
HSA	Human serum albumin
Hz	Hertz (s^{-1})
I.D.	Inner diameter
IA	Iodoacetamide
ICAT	Isotope-coded affinity tag
ICP	Inductively coupled plasma
ICPL	Isotope-coded protein label
ICR	ion cyclotron resonance

ID	intentity/identification
IDA	Isotope dilution analysis
IEF	Isoelectric focussing
IEX	Ion exchange chromatography
IgG	Immunoglobulin G
IP	Ion-pairing
IR	Infrared
IRMPD	Infrared multiphoton dissociation
iTRAQ	Isobaric tag for relative and absolute quantification
IUPAC	International Union of Pure and Applied Chemistry
K	Kelvin
k	kilo (10^3)
K	Lysine
L	Liter
LA	Laser ablation
LC	Liquid chromatography
LeuEnk	Leu-enkephalin (YGGFL)
LIF	Laser induced fluorescence
Ln	Lanthanide
LOD	Limit of detection
Lys	Lysine
m	metre
M	molar (mol/L)
m	prefix: milli (10^{-3})
m/z	Mass to charge ratio
Mal	maleinimido-(monoamide)
MALDI	Matrix assisted laser desorption/ionisation
max.	maximum
MC	Missed Cleavage(s)
MeCAT	Metal-coded affintity tag
MEKC	micellar electrokinetic chromatography
MeOH	Methanol
MeThio	methylthio-
min.	minimum

MMTS	Methyl methanethiosulfonate
Mr(calc)	Relative molecular mass calculated from matched peptide sequence
Mr(expt)	Experimental m/z transformed to a relative molecular mass
MRM	Multiple reaction monitoring
MS	Mass spectrometry
MS^2	Tandem mass spectrometry
MΩ	Electrical resistance (megaohm)
n	nano (10^{-9})
Nd:YAG	Neodymium-doped yttrium aluminium garnet ($Nd:Y_3Al_5O_{12}$)
NHS	N-Hydroxysuccinimide
N-term	N-Terminus
O.D.	outer diameter
p	pico (10^{-12})
PAGE	Polyacrylamide gel electrophoresis
PDMS	Polysimethylsiloxane
Ppm	parts-per-million
PTM	Post translational modification
Q	Quadrupole
QIT	Quadrupole ion trap
RP	Reverse phase
RT	room temperature (20°C)
RTM	Retention time marker
s	second
S/N	Signal to noise ratio
SCN	Isothiocyanate
SCX	Strong cation exchange
SDS	Sodium docecyl sulfate
SEC	Size-exclusion chromatography
SI units	Units of the International System of Units
SI	Signal Intensity
SILAC	Stable isotope labelling with amino acids in cell culture
SPE	Solid phase extraction
TEMED	Tetramethylethylenediamine
TFA	Trifluoroacetic acid

TMT	Tandem mass tag
TOF	time of flight
TRIS	tris(hydroxymethyl)aminomethane
ULB	Urea lysis buffer
uPLC	ultra performance liquid chromatography
UV	ultraviolet
v/v	volume concentration
W	Watt
w/v	mass concentration
z	zepto (10^{-21})

7.2 Tables

Table 29: Identified peptides for a Lu-NHS-DOTA labelled cytochrome C digest, after MALDI-MS and MS^2 on a cut target for consecutive measurement with fsLA-ICP-MS. Corresponding to section 4.5.3. For the Mascot search parameters see section 3.8.1..163

7.3 Figures

VIII Appendix II: Material

8.1.1 Apparatus

Table 20: List of apparatus and instruments

Apparatus / Instrument	Company	Type
Absorbance microplate reader	Biotek	ELx800NB
Bench centrifuge	vwr	Galaxy ministar
Centrifuge (0.5 - 2 mL)	Heraeus	Biofuge Fresco 21
Centrifuge (Falcon size)	Heraeus	Biofuge stratos
Fraction collector	LC Packings	Probot
fs Laser Ablation System	Novalase	Alfamet
ICP-MS 1	Agilent	7500ce
ICP-MS 2	Perkin Elmer	Elan II
Lyophiliser	Scanvac	Coolsafe 110-4
Magnetic stirrer	Heidolph	MR Hei-Standard
MALDI-MS	ABSCIEX	TOF/TOF 5800
Microscope	Leica	Leica dfc 280
nanoHPLC 1	Dionex	Ultimate 3000
nanoHPLC 2	LC Packings	Famos Switchos Ultimate
pH-Meter	Metler-Toledo	SevenEasy, Benchtop, S20
Pipettes (2.5 µL to 1 mL)	Eppendorf	Research
Pipettes (2.5 µL to 1 mL)	Eppendorf	Reference
Special accuracy weighing machine	Sartorius Mechatronics	Sartorius ME
Speedvac	Eppendorf	Concentrator plus
Thermomixer	Eppendorf	comfort
Ultra sonic bath	Elma	Elmasonic S40H
Ultrapure Water filter	Sartorius stedim	Arium 611VF
Vortex mixer	Neolab	VM-300 Vortex Mixer

8.1.2 Chemicals

Table 21: List of Chemicals

Compound	Company	Ordering Info
2-(4-(2-Hydroxyethyl)-1-piperazinyl) ethansulfonic acid (HEPES)	Sigma-Aldrich	H3375-100G
2-Mercaptoethanol	Sigma-Aldrich	63689-25ML-F
4700 Mass Standards Kit	ABSCIEX	4333604
Acetic acid	Sigma-Aldrich	45726-1L-F
Aceton	Fluka	00585-2.5L
Acetonitrile - CHROMASOLV® gradient grade, for HPLC, ≥99.9%	Sigma-Aldrich	34851-2,5L
Ammoniumhydrogencarbonat	Fluka	09830-1KG
Ammoniumpersulfate	Sigma-Aldrich	A9164-25G
Bromophenol blue	Sigma-Aldrich	80126
Cerium(III) chloride heptahydrate	Sigma-Aldrich	202983
CHAPS	Sigma-Aldrich	C3023-1G
CHCA	Sigma-Aldrich	C2020-10G

Table 21, continued: list of chemicals

Compound	Company	Ordering Info
CHCA	Laserbio Labs *	M001 - aCHCA
Coomassie G250	Sigma-Aldrich	27815-25G-F
Coomassie R250	Sigma-Aldrich	27816-25G
Dimethyl sulfoxide, >=99,7%, Hybri-Max/ DMSO	Sigma-Aldrich	D2650-5X5ML
Dithiothreitol	Sigma-Aldrich	43815-1G
EDTA Di-Na-Salz	Sigma-Aldrich	E5134-50G
Erbium(III) chloride hexahydrate	Sigma-Aldrich	289256
EthOH	Sigma-Aldrich	34963-1L
Europium(III) chloride hexahydrate 1g	Sigma-Aldrich	203254
Helium	Linde	
Heptafluoro butyric acid	Fluka	52411-25ML-F
Holmium(III) chloride hexahydrate	Sigma-Aldrich	289213
Iodoacetamide	Sigma-Aldrich	I1149-5G
Isopropanole	Sigma-Aldrich	24137
Lutetium(III) chloride hexahydrate	Sigma-Aldrich	542075
Maleimido-mono-amide-DOTA	macrocyclics	B-272-100
MeOH	Sigma-Aldrich	34966-2.5L
NaOH	Sigma-Aldrich	30620-1KG-R
Neodymium(III) nitrate hexahydrate 25g	Sigma-Aldrich	289175
NHS DOTA	Chematech	DOTA-NHS ester
Praseodymium(III) nitrate hexahydrate	Sigma-Aldrich	205133
Proteaseinhibitor complete mini	Roche	11836170001
Rare Earth element mix for ICP	Sigma Aldrich	67349
SDS ultra pure	C.Roth	2326.2
S-Methyl-methanthiosulfonat	Fluka	64306-1ML
TCEP (tris(2-carboxyethyl)phosphine)	Merck	580560-1GM
Terbium(III) chloride hexahydrate	Sigma-Aldrich	212903
Thulium(III) chloride hexahydrate	Sigma-Aldrich	204668
Triethylamine - ≥99%	Sigma-Aldrich	T0886-500ML
Triethylammonium acetate buffer	Sigma-Aldrich	90358-100ML
Triethylammonium bicarbonate buffer - puriss. p.a., for HPLC, volatile buffer, 1 M	Sigma-Aldrich	17902-100ml
Trifluoroacetic acid - ReagentPlus®, 99%	Sigma-Aldrich	T62200-100ML
Tris base	C.Roth	4855.2

8.1.3 Consumables

Table 22: List of consumables

consumable	Company	Ordering Info
Acclaim PepMap100, C18, 3 µm, 100 Å, 75 µm i.d. x 15 cm	Dionex/Thermo fisher scientific	160321
Acclaim PepMap100, C18, 3 µm, 100 Å, 75 µm i.d. x 25 cm	Dionex/Thermo fisher scientific	164569
ZipTip w/ 0.6µL C18 resin 96/Pk	millipore	ZTC18S096
Universal indicator paper 1-14	vwr	1109620003
Micro-Precolumn 300µmi.d.x5mm, packed with Acclaim PepMap100 C18	Dionex	160454
Cutter for fused silica tubing	Dionex	P/N 160483
LLG glass sample vials N9-1	Macherey-Nagel	702282
Sample vial Inserts 15mm tip	Macherey-Nagel	702813
Caps for sample vial N9	Macherey-Nagel	702285.1
Pipette tips 100-1000µl	vwr/ axygen	613-0669
Pipette tips 1-200µl	vwr/ axygen	613-0652
Pipette tips 0.5-10µl	vwr/ axygen	613-0643
Eppendorf Tubes 0.5mL, lobind	Eppendorf	0030 108.094
Eppendorf Tubes 1.5mL, lobind	Eppendorf	0030 108.116
Eppendorf Tubes 2mL, lobind	Eppendorf	0030 108.132
PCR Tubes, 200 µL lobind	Eppendorf	0030 124.359
Falcons 50mL	Greiner bioOne	7.380 421
Falcons 15mL	Greiner bioOne	7.380 423
Amicon Ultra-0.5 3kDa Ultracel-PL memb 24/Pk	millipore	UFC500324
Glas beads 0.10 – 0.25 mm Ø	Retsch	22.222.0001
Glas beads 0.25 – 0.50 mm Ø	Retsch	22.222.0002
MALDI Targets LC	ABSCIEX	1018469
MALDI Targets spot based	ABSCIEX	1016629
MALDI Target plate holder	ABSCIEX	1016492
Scalpel	pfm medical	200130010
Parafilm	Neolab	3-1011
Nickel Skimmer cone	Agilent	G3270-65024
Nickel sampling cone	Agilent	G1820-65238
Standard-Mikrotiterplatten F- Boden	vwr	735-2002

8.1.4 Peptides, Proteins, Enzymes

Table 23: List of standard proteins and enzymes

Protein / Enzyme	Company	Ordering Info
Cytochrome c Digest	Dionex	P/N 161089
α-Lactalbumin	Sigma-Aldrich	L5385-100MG
β-Lactoglobulin B	Sigma-Aldrich	L8005-100MG
Lysozyme	Sigma-Aldrich	L6876-1G
Trypsin	promega	V511A
BSA	Sigma-Aldrich	A7511-1G
Chymotrypsin	promega	V1061

Table 24: Synthetic peptides (including GRAVY index[191] as classification of their hydrophobicity)

Peptide	Sequence	Manufacturer	GRAVY Index
S36 (peptide C)	GACLLPK	R. Pipkorn (DKFZ, Germany)	+0.857
S22 (peptide B)	LRRACLG	R. Pipkorn (DKFZ, Germany)	+0.357
T3 (peptide A)	EGHIARNCRA	R. Pipkorn (DKFZ, Germany)	-0.900
S17	RPQYAEASWNAR	R. Pipkorn (DKFZ, Germany)	-1.558
S19	RPQYACASWNAR	R. Pipkorn (DKFZ, Germany)	-1.058
S27	LRRASpLGERRASLGE	R. Pipkorn (DKFZ, Germany)	(-0.827)
Leu-Enkephalin (LeuEnk)	YGGFL	Waters (70000 3276)	+0.900
[Glu1]-Fibrinopeptid B human (GluFib)	EGVNDNEEGFFSAR	Sigma-Aldrich (F3261-1MG)	-1.107
Hy	ESLSSSEE	A. Tholey	-1.238
PP A	ASQDGTPALR	Biosyntan, Germany	-0.760
PP L	LSVYDPYR	Biosyntan, Germany	-0.625
PP Q	QDYLQYR	Biosyntan, Germany	-1.971

IX Appendix III: Additional Data

9.1 Identified Labelled Peptides for MALDI-MS Analysis of a Labelled Lysozyme Digest

Corresponding to section 4.3, starting on page 81.

Table 25: Tryptic digest of chicken lysozyme (LYSC_CHICK) labeled with ^{141}Pr Mal-DOTA. Labeled peptides found by Mascot Search after LC-MALDI MS/MS. (only ion scores above the identity threshold of p<0.05 are listed), original data from Holste et al. 2013[4]

Observed mass	Mr (expt)	Mr (calc)	MC	Score	Peptide	labels
1500.5123	1499.5051	1499.5161	0	32.45	CELAAAMK	Mal-DOTA Pr (C)
1500.5148	1499.5075	1499.5161	0	27.33	CELAAAMK	Mal-DOTA Pr (C)
1516.4982	1515.4909	1515.5110	0	19.16	CELAAAMK	Mal-DOTA Pr (C)
1600.4925	1599.4853	1599.4937	0	7.95	WWCNDGR	Mal-DOTA Pr (C)
1656.6218	1655.6146	1655.6172	1	11.60	CELAAAMKR	Mal-DOTA Pr (C)
1656.6239	1655.6166	1655.6172	1	42.83	CELAAAMKR	Mal-DOTA Pr (C)
1932.7096	1931.7023	1931.7248	0	26.78	GYSLGNWVCAAK	Mal-DOTA Pr (C)
1932.7100	1931.7027	1931.7248	0	30.43	GYSLGNWVCAAK	Mal-DOTA Pr (C)
1932.7240	1931.7167	1931.7248	0	27.24	GYSLGNWVCAAK	Mal-DOTA Pr (C)
1932.7352	1931.7280	1931.7248	0	17.86	GYSLGNWVCAAK	Mal-DOTA Pr (C)
1940.7644	1939.7571	1939.7623	1	25.38	CKGTDVQAWIR	Mal-DOTA Pr (C)

Table 26: Tryptic digest of chicken lysozyme (LYSC_CHICK) labeled with ^{169}Tm NHS-DOTA. Labeled peptides found by Mascot Search after LC-MALDI MS/MS. (only ion scores above the identity threshold of p<0.05 are listed), original data from Holste et al. 2013[4]

Observed mass	Mr (expt)	Mr (calc)	MC	Score	Peptide	labels		
1426.4923	1425.4850	1425.5002	0	21.63	HGLDNYR	NHS-DOTA Tm (N-term)		
1426.5044	1425.4971	1425.5002	0	32.19	HGLDNYR	NHS-DOTA Tm (N-term)		
1426.5062	1425.4990	1425.5002	0	23.58	HGLDNYR	NHS-DOTA Tm (N-term)		
1488.4667	1487.4594	1487.4617	0	18.42	WWCNDGR	NHS-DOTA Tm (N-term)		
1534.4539	1533.4466	1533.4494	0	35.88	WWCNDGR	NHS-DOTA Tm (N-term)		Methylthio (C)
1582.6000	1581.5927	1581.6013	1	23.57	RHGLDNYR	NHS-DOTA Tm (N-term)		
1590.5790	1589.5717	1589.5729	1	35.68	CELAAAMKR	NHS-DOTA Tm (K)		Methylthio (C)
1597.6145	1596.6072	1596.6261	0	34.42	GTDVQAWIR	NHS-DOTA Tm (N-term)		
1597.6222	1596.6149	1596.6261	0	20.01	GTDVQAWIR	NHS-DOTA Tm (N-term)		
1597.6293	1596.6220	1596.6261	0	61.44	GTDVQAWIR	NHS-DOTA Tm (N-term)		
1828.7402	1827.7330	1827.7303	1	6.28	CKGTDVQAWIR	NHS-DOTA Tm (K)		
1866.6766	1865.6694	1865.6805	0	59.33	GYSLGNWVCAAK	NHS-DOTA Tm (N-term)		Methylthio (C)
1874.7269	1873.7197	1873.7180	1	47.42	CKGTDVQAWIR	NHS-DOTA Tm (K)		Methylthio (C)
1980.7288	1979.7215	1979.7338	0	37.45	FESNFNTQATNR	NHS-DOTA Tm (N-term)		
1980.7328	1979.7255	1979.7338	0	21.53	FESNFNTQATNR	NHS-DOTA Tm (N-term)		
1980.7332	1979.7259	1979.7338	0	29.88	FESNFNTQATNR	NHS-DOTA Tm (N-term)		
1980.7494	1979.7421	1979.7338	0	87.43	FESNFNTQATNR	NHS-DOTA Tm (N-term)		
1986.5608	1985.5535	1985.5626	0	23.34	CELAAAMK	NHS-DOTA Tm (K)	NHS-DOTA Tm (N-term)	Methylthio (C)
2032.7117	2031.7044	2031.7045	1	10.65	WWCNDGRTPGSR	NHS-DOTA Tm (N-term)		Methylthio (C)
2142.6738	2141.6666	2141.6637	1	26.76	CELAAAMKR	NHS-DOTA Tm (K)	NHS-DOTA Tm (N-term)	Methylthio (C)
2227.8767	2226.8694	2226.8845	0	25.3	IVSDGNGMNAWVAWR	NHS-DOTA Tm (N-term)		
2227.8826	2226.8753	2226.8845	0	12.97	IVSDGNGMNAWVAWR	NHS-DOTA Tm (N-term)		
2227.8933	2226.8860	2226.8845	0	17.01	IVSDGNGMNAWVAWR	NHS-DOTA Tm (N-term)		
2227.9021	2226.8948	2226.8845	0	84.61	IVSDGNGMNAWVAWR	NHS-DOTA Tm (N-term)		
2305.9153	2304.9080	2304.9187	0	60.67	NTDGSTDYGILQINSR	NHS-DOTA Tm (N-term)		
2305.9221	2304.9148	2304.9187	0	25.3	NTDGSTDYGILQINSR	NHS-DOTA Tm (N-term)		
2305.9231	2304.9158	2304.9187	0	24.46	NTDGSTDYGILQINSR	NHS-DOTA Tm (N-term)		
2305.9314	2304.9241	2304.9187	0	119.64	NTDGSTDYGILQINSR	NHS-DOTA Tm (N-term)		
2418.7852	2417.7779	2417.7714	0	39.47	GYSLGNWVCAAK	NHS-DOTA Tm (K)	NHS-DOTA Tm (N-term)	Methylthio (C)
2426.8272	2425.8199	2425.8089	1	18.75	CKGTDVQAWIR	NHS-DOTA Tm (K)	NHS-DOTA Tm (N-term)	Methylthio (C)
2908.0889	2907.0816	2907.0704	1	24.23	KIVSDGNGMNAWVAWR	NHS-DOTA Tm (K)	NHS-DOTA Tm (N-term)	

9.2 Analysis of Labelled Digests

Corresponding to section 4.3.1.

For the following sequences: **Green**: Labelled. **Red**: not detected.

Black: no target for the reagent. Labelling site underlined.

9.2.1 Sequence Coverage for Chicken Lysozyme (LYSC_CHICK)

^{141}Pr Mal-DOTA labelled tryptic digest of lysozyme:

```
        10         20         30         40         50         60
MRSLLILVLC FLPLAALGKV FGRCELAAAM KRHGLDNYRG YSLGNWVCAA KFESNFNTQA

        70         80         90        100        110        120
TNRNTDGSTD YGILQINSRW WCNDGRTPGS RNLCNIPCSA LLSSDITASV NCAKKIVSDG

       130        140
NGMNAWVAWR NRCKGTDVQA WIRGCRL
```

^{169}Tm NHS-DOTA labelled tryptic digest of lysozyme:

```
        10         20         30         40         50         60
MRSLLILVLC FLPLAALGKV FGRCELAAAM KRHGLDNYRG YSLGNWVCAA KFESNFNTQA

        70         80         90        100        110        120
TNRNTDGSTD YGILQINSRW WCNDGRTPGS RNLCNIPCSA LLSSDITASV NCAKKIVSDG

       130        140
NGMNAWVAWR NRCKGTDVQA WIRGCRL
```

9.2.2 Sequence Coverage for α-Lactalbumin (LALBA_BOVIN)

^{165}Ho Mal-DOTA labelled tryptic digest of α-lactalbumin:

```
        10         20         30         40         50         60
MMSFVSLLLV GILFHATQAE QLTKCEVFRE LKDLKGYGGV SLPEWVCTTF HTSGYDTQAI

        70         80         90        100        110        120
VQNNDSTEYG LFQINNKIWC KDDQNPHSSN ICNISCDKFL DDDLTDDIMC VKKILDKVGI

       130        140
NYWLAHKALC SEKLDQWLCE KL
```

^{169}Tm NHS DOTA labelled tryptic digest of α-lactalbumin:

```
        10         20         30         40         50         60
MMSFVSLLLV GILFHATQAE QLTKCEVFRE LKDLKGYGGV SLPEWVCTTF HTSGYDTQAI

        70         80         90        100        110        120
VQNNDSTEYG LFQINNKIWC KDDQNPHSSN ICNISCDKFL DDDLTDDIMC VKKILDKVGI

       130        140
NYWLAHKALC SEKLDQWLCE KL
```

9.2.3 Sequence Coverage for β-Lactoglobulin (LACB_BOVIN)

^{141}Pr NHS-DOTA labelled tryptic digest of β-lactoglobulin:

```
        10         20         30         40         50         60
MKCLLLALAL TCGAQALIVT QTMKGLDIQK VAGTWYSLAM AASDISLLDA QSAPLRVYVE

        70         80         90        100        110        120
ELKPTPEGDL EILLQKWENG ECAQKKIIAE KTKIPAVFKI DALNENKVLV LDTDYKKYLL

       130        140        150        160        170
FCMENSAEPE QSLACQCLVR TPEVDDEALE KFDKALKALP MHIRLSFNPT QLEEQCHI
```

^{169}Tm Mal-DOTA labelled tryptic digest of β-lactoglobulin:

```
        10         20         30         40         50         60
MKCLLLALAL TCGAQALIVT QTMKGLDIQK VAGTWYSLAM AASDISLLDA QSAPLRVYVE

        70         80         90        100        110        120
ELKPTPEGDL EILLQKWENG ECAQKKIIAE KTKIPAVFKI DALNENKVLV LDTDYKKYLL

       130        140        150        160        170
FCMENSAEPE QSLACQCLVR TPEVDDEALE KFDKALKALP MHIRLSFNPT QLEEQCHI
```

9.2.4 Sequence coverage for cytochrome C (CYC_BOVIN)

^{165}Ho NHS-DOTA labelled tryptic digest of cytochrome C (Dionex standard):

```
        10         20         30         40         50         60
MGDVEKGKKI FVQKCAQCHT VEKGGKHKTG PNLHGLFGRK TGQAPGFSYT DANKNKGITW

        70         80         90        100
GEETLMEYLE NPKKYIPGTK MIFAGIKKKG EREDLIAYLK KATNE
```

9.2.5 nanoHPLC-ICP-MS Chromatograms of the Digests above

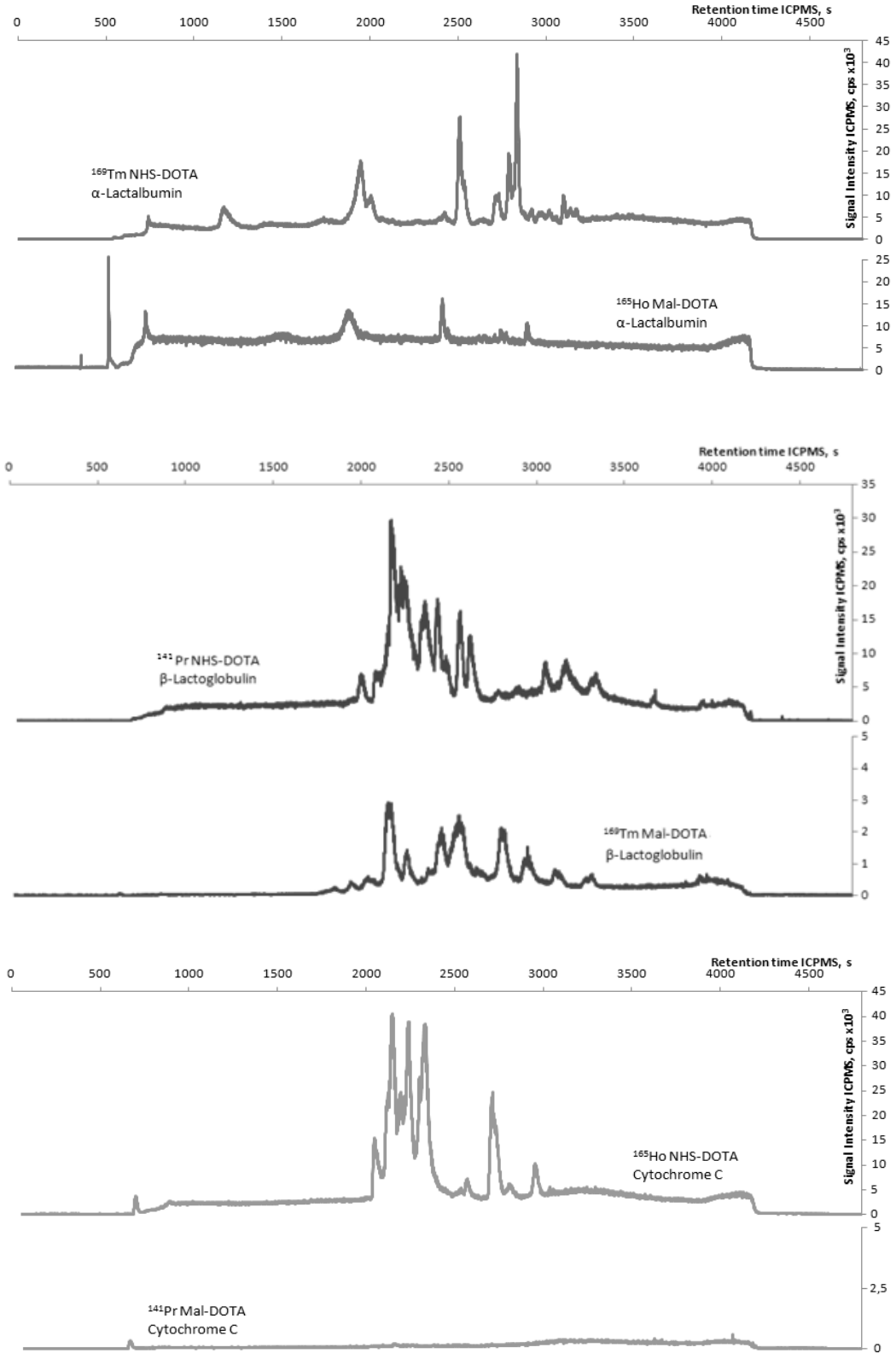

9.3 Quantification of Labelled Cytochrome C via nanoHPLC ICP-MS using Standard Peptides

Table 27 and Table 28 are complementary data to section 4.4.2 on the quantification of a labelled cytochrome C digest after treatment with C18 ZipTips. Labelled standard peptides were applied with an amount of 1 pmol each. The Cyt C eluate and remnant solution were both dried after ZipTip treatment and reconstituted in exactly the same way prior to analysis. Both solutions were employed as if they contained the same amount of digest peptides. Employed amounts equalled 1 pmol at 100 % recovery.

Sample 1 in Table 27 shows quantification data matching the chromatogram shown in Figure 28 b in section 4.1.1.

Table 27: Quantification of a labelled Cytochrome C (Cyt C) digest after treatment with ZipTip C[18], samples 1 and 2. Peak areas of the respective peaks were acquired by integration with the software TST (LCABIE, Pau). Eluate Peptide A to D correspond to four representative peptide peaks in the digest.

Continued in Table 28. Complementary data to section 4.4.2

Sample 1	Analyte	Lanthanide Label NHS-DOTA	Peak area in total counts	Average of standard peptides total counts	Average of digest peptides A, B, C,D total counts	equals total amount in pmol	Sum of all digest peaks total counts
Standard peptides (1pmol each)	LeuEnk	Pr141	21 484 248	29 232 339		1.000	
	GluFib	Tb159	13 893 131				
	S17	Tm169	52 319 637				
Cyt C Lu ZipTip Eluate versus **Cyt C Ho ZipTip Remnant** (equivalent of 1 pmol each)	Cyt C (all peptide peaks together)	Lu175	29 340 022			1.004	29 340 022
	CytC eluate peptide A	Lu175	5 680 561		4 210 955	0,144	
	CytC eluate peptide B	Lu175	3 912 211				
	CytC eluate peptide C	Lu175	4 584 757				
	CytC eluate peptide D	Lu175	2 666 291				
	Cyt C remnant peaks 1	Ho165	232 883 165			10.233	299 133 135
	Cyt C remnant peaks 2	Ho165	10 931 788				
	Cyt C remnant peaks 3	Ho165	11 703 504				
	Cyt C remnnnt peaks 4	Ho165	7 936 926				
	Cyt C remnant peaks 5	Ho165	24 288 048				
	Cyt C remnant peaks 6	Ho165	3 298 952				
	Cyt C remnant peaks 7	Ho165	8 090 752				

Sample 2	Analyte	Label	Peak area	Average standard	Average digest	Amount in pmol	Sum digest
Standard peptides (1pmol each)	S27	Pr141	17 020 695	29 281 094		1.000	
	LeuEnk	Tb159	27 166 125				
	Glufib	Ho165	22 718 320				
	S17	Tm169	50 219 234				
Cyt C Lu ZipTip Eluate (equivalent of 1 pmol)	Cyt C (all peptide peaks together)	Lu175	40 956 518			1.399	40 956 518
	CytC eluate peptide A	Lu175	7 346 000		5 739 159	0.196	
	CytC eluate peptide B	Lu175	5 491 844				
	CytC eluate peptide C	Lu175	6 387 829				
	CytC eluate peptide D	Lu175	3 730 962				

Table 28: continued from Table 27. Quantification of a labelled Cytochrome C (Cyt C) digest after treatment with ZipTip C[18]. Sample 3 is a 1:10 dilution of sample two. Sample 4 and 5 have the same composition as sample 1 to 3, with switched metal labels.

Complementary data to section 4.4.2.

	Analyte	Lanthanide Label NHS-DOTA	Peak area in total counts	Average of standard peptides total counts	Average of digest peptides A, B, C,D total counts	equals total amount in pmol	Sum of all digest peaks total counts
Sample 3							
Standard peptides (0,1 pmol each)	S27	Pr141	1 742 509	3 094 313		0.100	
	LeuEnk	Tb159	2 839 255				
	Glufib	Ho165	2 450 553				
	S17	Tm169	5 344 934				
Cyt C Lu ZipTip Eluate (equivalent of 0,1 pmol)	Cyt C (all peptide peaks together)	Lu175	4 324 644			0.1398	4 324 644
	CytC eluate peptide A	Lu175	785 882		605 571	0.0196	
	CytC eluate peptide B	Lu175	573 237				
	CytC eluate peptide C	Lu175	673 805				
	CytC eluate peptide D	Lu175	389 360				
Sample 4	**Analyte**	**Label**	**Peak area**	**Average standard**	**Average digest**	**Amount in pmol**	**Sum digest**
Standard peptides (1pmol each)	S17	Pr141	20 887 885	22 878 001		1.000	
	GluFib	Tb159	19 593 216				
	S27	Tm169	34 522 735				
	LeuEnk	Lu175	16 508 168				
Cyt C Ho ZipTip Eluate (equivalent of 2 pmol)	Cyt C (all peptide peaks together)	Ho165	58 068 758			2.538	58 068 758
	CytC eluate peptide A	Ho165	7 085 552		6 847 302	0.299	
	CytC eluate peptide B	Ho165	3 618 488				
	CytC eluate peptide C	Ho165	11 424 426				
	CytC eluate peptide D	Ho165	5 260 740				
Sample 5	**Analyte**	**Label**	**Peak area**	**Average standard**	**Average digest**	**Amount in pmol**	**Sum digest**
Standard peptides (1pmol each)	S17	Pr141	20 842 756	23 325 815		1.000	
	GluFib	Tb159	20 217 700				
	S27	Tm169	35 431 493				
	LeuEnk	Lu175	16 811 312				
Cyt C Ho ZipTip Eluate (equivalent of 2 pmol)	Cyt C (all peptide peaks together)	Ho165	56 174 067			2.408	56 174 067
	CytC eluate peptide A	Ho165	7 345 715		6 841 767	0.293	
	CytC eluate peptide B	Ho165	3 759 012				
	CytC eluate peptide C	Ho165	11 091 823				
	CytC eluate peptide D	Ho165	5 170 517				

9.4 Identified Cytochrome C Peptides in MALDI-MS (Modified Target)

Table 29: Identified peptides for a Lu-NHS-DOTA labelled cytochrome C digest, after MALDI-MS and MS^2 on a cut target for consecutive measurement with fsLA-ICP-MS. Corresponding to section 4.5.3. For the Mascot search parameters see section 3.8.1

Observed mass	Mr (expt)	Mr (calc)	MC	Score	Peptide and labels/modifications
964.5226	963.5153	963.5277	0	65	EDLIAYLK
1168.5897	1167.5824	1167.6149	0	92.44	TGPNLHGLFGR
1168.6108	1167.6036	1167.6149	0	37.19	TGPNLHGLFGR
1168.6218	1167.6146	1167.6149	0	49.2	TGPNLHGLFGR
1168.6278	1167.6205	1167.6149	0	101.5	TGPNLHGLFGR
1192.4579	1191.4506	1191.5085	0	12	IFVQK + NHS-DOTA Lu (K)
1192.4689	1191.4616	1191.5085	0	22.56	IFVQK + NHS-DOTA Lu (K)
1236.4263	1235.419	1235.4983	0	22.65	YIPGTK + NHS-DOTA Lu (K)
1236.4651	1235.4578	1235.4983	0	13.42	YIPGTK + NHS-DOTA Lu (N-term)
1306.6885	1305.6812	1305.6928	1	1.61	GEREDLIAYLK
1320.5663	1319.5590	1319.6034	1	24.46	KIFVQK + NHS-DOTA Lu (N-term)
1320.5770	1319.5698	1319.6034	1	20.6	KIFVQK + NHS-DOTA Lu (N-term)
1337.5222	1336.5149	1336.5646	0	0.82	MIFAGIK + NHS-DOTA Lu (N-term)
1337.5264	1336.5191	1336.5646	0	37.1	MIFAGIK + NHS-DOTA Lu (N-term)
1337.5394	1336.5322	1336.5646	0	7.58	MIFAGIK + NHS-DOTA Lu (N-term)
1353.4764	1352.4692	1352.5595	0	22.25	MIFAGIK + NHS-DOTA Lu (K) + Ox(M)
1353.5127	1352.5054	1352.5595	0	28.89	MIFAGIK + NHS-DOTA Lu (K) + Ox(M)
1353.5198	1352.5125	1352.5595	0	23.24	MIFAGIK + NHS-DOTA Lu (N-term) + Ox(M)
1364.4362	1363.4289	1363.5932	1	16.52	KYIPGTK + NHS-DOTA Lu (N-term)
1456.6360	1455.6287	1455.663	0	99.03	TGQAPGFSYTDANK
1465.6250	1464.6177	1464.6595	1	14.49	MIFAGIKK + NHS-DOTA Lu (N-term)
1465.6349	1464.6276	1464.6595	1	23.92	MIFAGIKK + NHS-DOTA Lu (K)
1522.6111	1521.6038	1521.6511	0	37.51	EDLIAYLK + NHS-DOTA Lu (N-term)
1633.6299	1632.6226	1632.8116	1	21.36	IFVQKCAQCHTVEK
1650.7046	1649.6973	1649.7461	1	34.56	EDLIAYLKK + NHS-DOTA Lu (K)
1726.7002	1725.6929	1725.7384	0	57.2	TGPNLHGLFGR + NHS-DOTA Lu (N-term)
1726.7063	1725.6990	1725.7384	0	41.92	TGPNLHGLFGR + NHS-DOTA Lu (N-term)
1726.7229	1725.7156	1725.7384	0	30.5	TGPNLHGLFGR + NHS-DOTA Lu (N-term)
1794.4746	1793.4673	1793.6218	0	8.68	YIPGTK + **2** NHS-DOTA Lu (K + N-term)
1794.4873	1793.4800	1793.6218	0	14.6	YIPGTK + **2** NHS-DOTA Lu (K + N-term)
1864.7815	1863.7742	1863.8163	1	18.28	GEREDLIAYLK + NHS-DOTA Lu (N-term)
1878.6011	1877.5938	1877.7269	1	22.49	KIFVQK + **2** NHS-DOTA Lu (K + N-term)
1878.6751	1877.6678	1877.7269	1	17.89	KIFVQK + **2** NHS-DOTA Lu (K + N-term)
1895.5641	1894.5568	1894.6881	0	20.23	MIFAGIK + **2** NHS-DOTA Lu (K + N-term)
1911.5608	1910.5535	1910.6830	0	17.45	MIFAGIK + **2** NHS-DOTA Lu (K + N-term) + Ox(M)
1911.5749	1910.5677	1910.6830	0	5.75	MIFAGIK + **2** NHS-DOTA Lu (K + N-term) + Ox(M)
1922.6397	1921.6324	1921.7167	1	21.34	KYIPGTK + **2** NHS-DOTA Lu (K + N-term)

Table 29, continued

Observed mass	Mr (expt)	Mr (calc)	MC	Score	Peptide and labels/modifications
1922.6440	1921.6368	1921.7167	1	17.2	KYIPGTK + **2** NHS-DOTA Lu (K + N-term)
1992.8680	1991.8608	1991.9113	2	48.15	KGEREDLIAYLK + NHS-DOTA Lu (N-term)
2023.6942	2022.6869	2022.783	1	31.64	MIFAGIKK + **2** NHS-DOTA Lu (K + N-term)
2039.6796	2038.6723	2038.7779	1	19.97	MIFAGIKK + **2** NHS-DOTA Lu (K +N-term) + Ox(M)
2080.5879	2079.5806	2079.7746	0	28.54	EDLIAYLK + **2** NHS-DOTA Lu (K + N-term)
2142.7869	2141.7796	2141.8815	1	55.57	KTGQAPGFSYTDANK + NHS-DOTA Lu (N-term)
2142.7949	2141.7876	2141.8815	1	1.05	KTGQAPGFSYTDANK + NHS-DOTA Lu (N-term)
2191.7659	2190.7586	2190.9351	1	30.58	IFVQKCAQCHTVEK + NHS-DOTA Lu (K)
2208.7468	2207.7396	2207.8696	1	53.2	EDLIAYLKK + **2** NHS-DOTA Lu (K + N-term)
2422.9031	2421.8958	2421.9398	1	40.54	GEREDLIAYLK + **2** NHS-DOTA Lu (K + N-term)
2436.7031	2435.6959	2435.8504	1	14.53	KIFVQK +**3** NHS-DOTA Lu (2xK + N-term)
2480.6589	2479.6517	2479.8402	1	13.18	KYIPGTK + **3** NHS-DOTA Lu (2xK + N-term)
2550.9131	2549.9058	2550.0347	2	34.24	KGEREDLIAYLK + **2** NHS-DOTA Lu (K + N-term)
2567.9688	2566.9615	2567.0686	0	51.25	GITWGEETLMEYLENPK + NHS-DOTA Lu (N-term)
2572.7271	2571.7198	2571.9100	0	50.91	TGQAPGFSYTDANK + **2** NHS-DOTA Lu (K+ N-term)
2581.7607	2580.7535	2580.9065	1	24.82	MIFAGIKK + 2 NHS-DOTA Lu (K)
2583.9690	2582.9617	2583.0636	0	11.61	GITWGEETLMEYLENPK + NHS-DOTA Lu (N-term)
2700.9038	2699.8965	2700.0049	1	25.08	KTGQAPGFSYTDANK + **2** NHS-DOTA Lu (K + N-term)
3109.0786	3108.0713	3108.1582	2	13.21	KGEREDLIAYLK + **2** NHS-DOTA Lu (K + N-term)
3254.1060	3253.0987	3253.2871	1	101.17	GITWGEETLMEYLENPKK + **2** NHS-DOTA Lu (K + N-term)
3270.2024	3269.1951	3269.2820	1	50.21	GITWGEETLMEYLENPKK + **2** NHS-DOTA Lu (K + N-term)

9.5 Reactions

9.5.1 Reaction of Maleimido-mono-amide DOTA with Cysteine Peptides

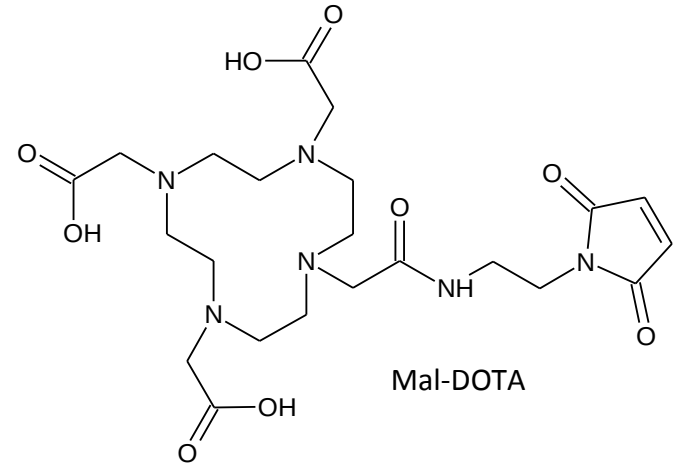

Mal-DOTA

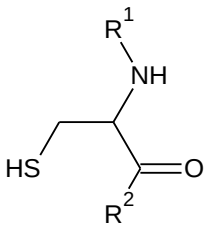

Cysteine peptide

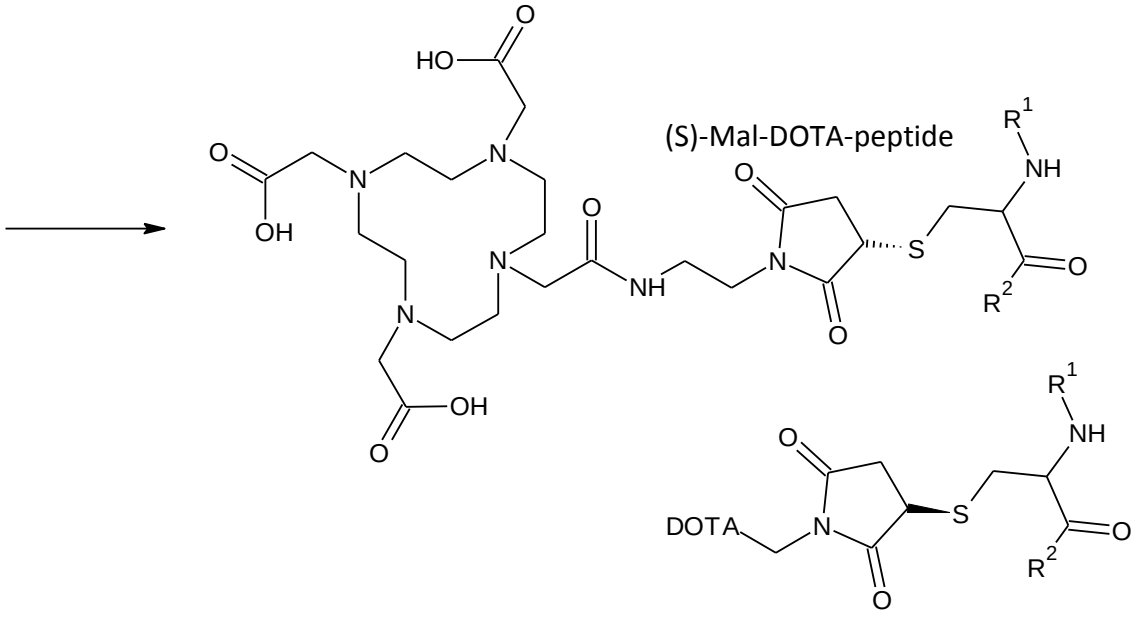

(S)-Mal-DOTA-peptide

(R)-Mal-DOTA-peptide

After Complexation:

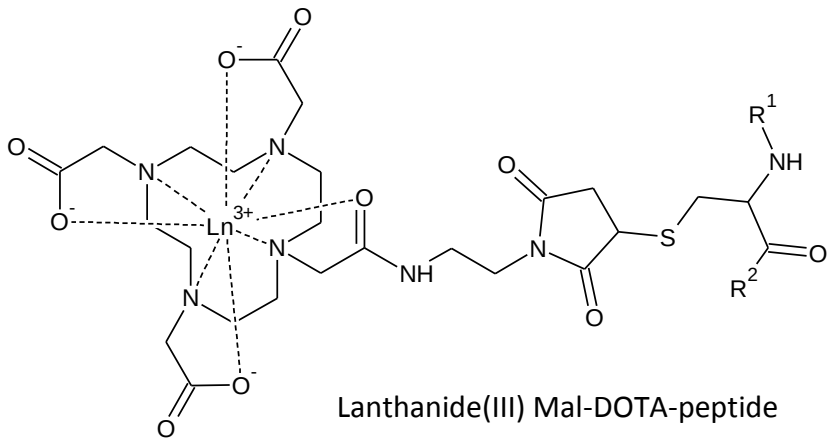

Lanthanide(III) Mal-DOTA-peptide

9.5.2 Reaction of NHS-DOTA with Amino Groups in Lysine

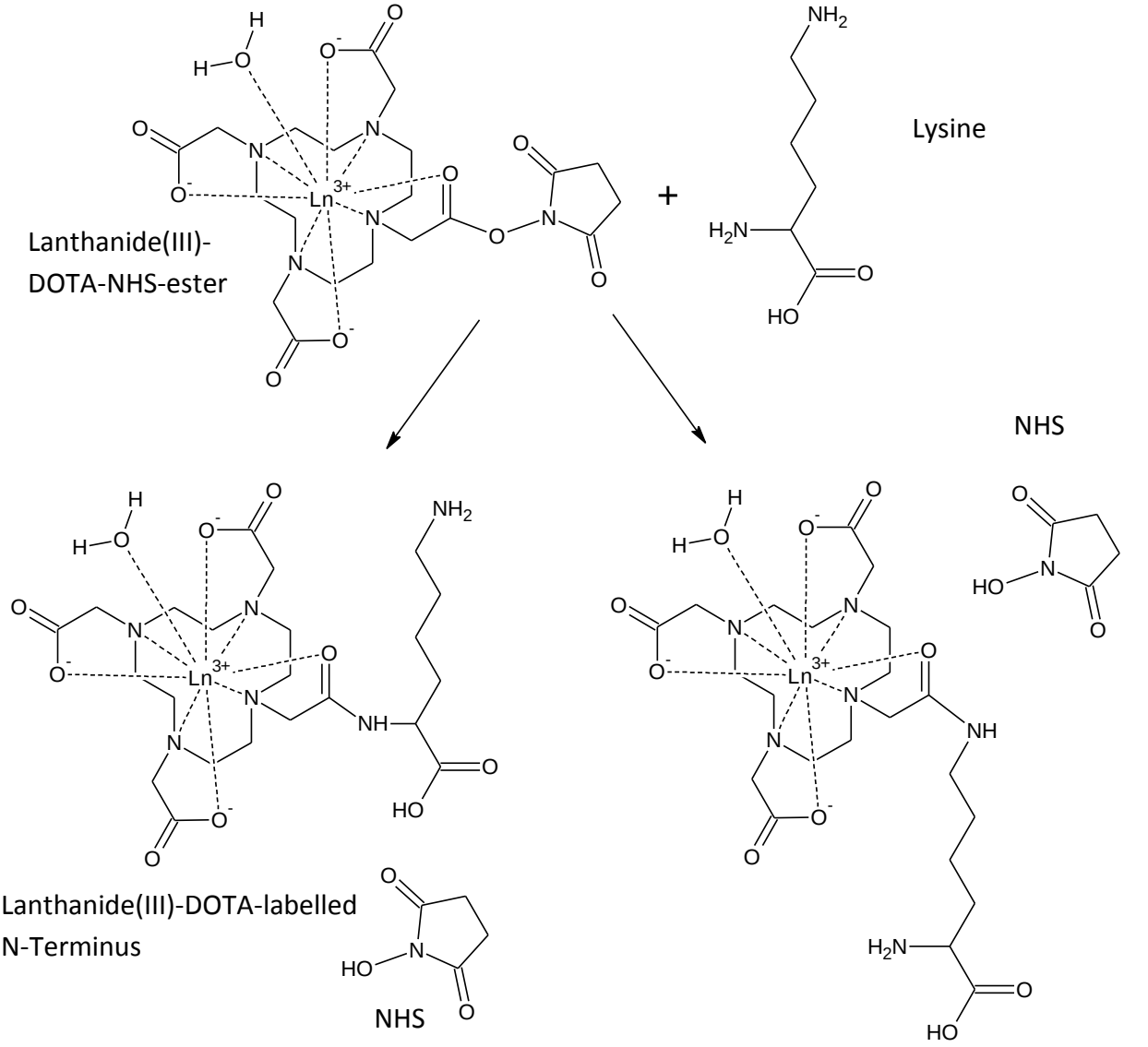

The reaction on lysine is an example. Reaction is also possible on all free amino-groups in a peptide, so all unmodified N-termini of other AA are targets as well.

9.6 Microscopic Examinations of Matrix Crystal Sizes and Distributions

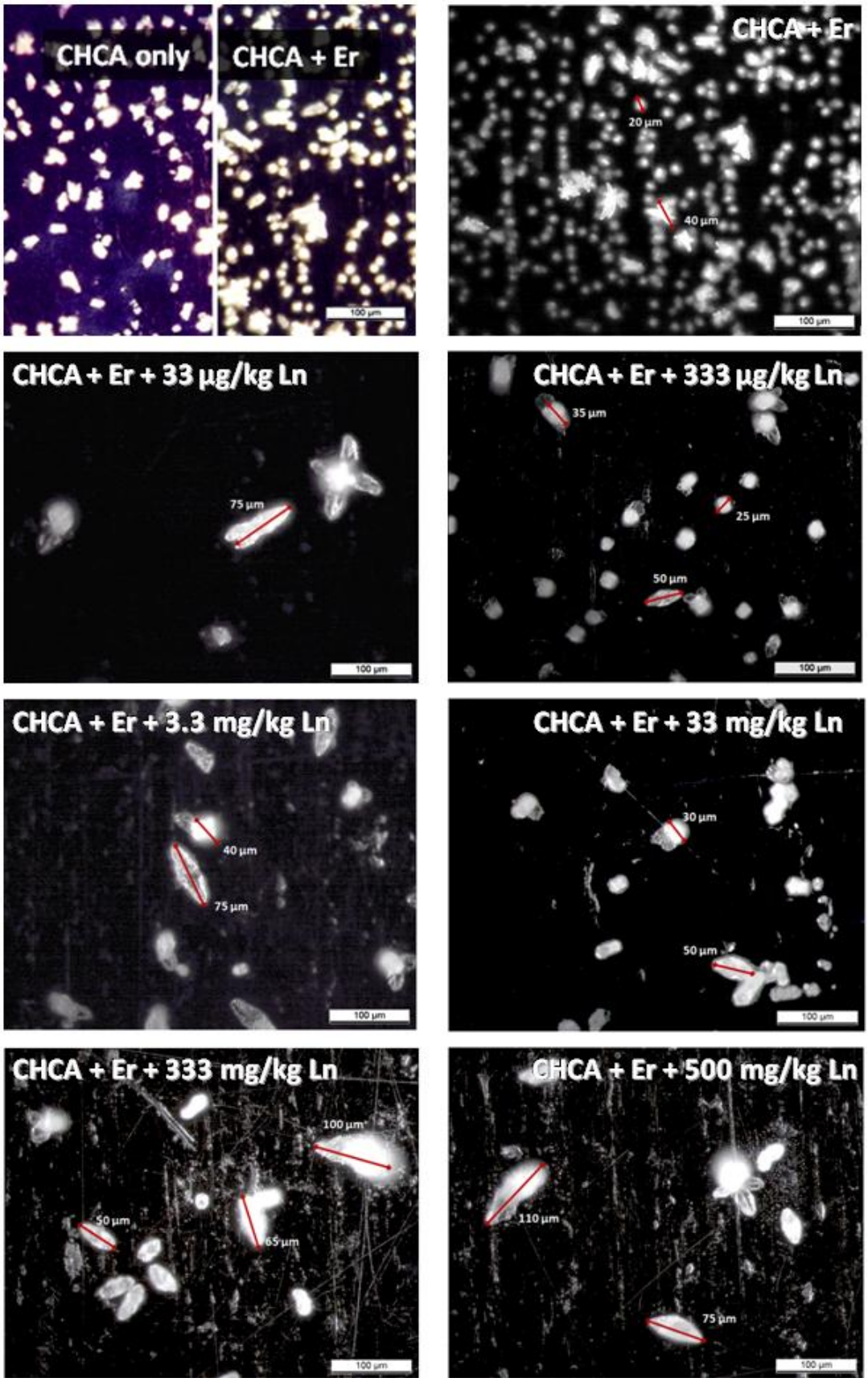

Figure 51: Microscopic observations of matrix crystal sizes and distributions for different lanthanide salt contents. (Er stands for 40 µg/L erbium standard; Ln stands for the mixture of the five lanthanides ^{141}Pr, ^{159}Tb, ^{169}Tm, ^{165}Ho and ^{175}Lu)

9.7 Sample Transportation

For transportation in between the two laboratories, several possibilities were tested. It was made sure, that no sample degradation occurred in between transports.

In general the tubes containing the samples were sealed additionally using Parafilm®. Tubes were placed in plastic bags, which were closed firmly.
The samples themselves were usually transported in lyophilised form. If transportation took less than 24 hours, no additional cooling was necessary. For longer transports, by e.g. postal services or for samples in solution, a Styrofoam box was filled with dry ice, to ensure a temperature lower than -20 °C.

Spotted MALDI-targets were put in their black transport box and fixated using foam material and sticky tape on the target corners. It was made sure that the surface was not touched during this process. Fixation was done in a way that ensured no movement of the target during transportation and that no friction of any kind was applied to the target surface. The transportation box was sealed with tape and put in an airtight transportation bag. No cooling was applied, to avoid attraction of moisture. Targets were generally measured within less than 48 hours of spotting. Good signal intensities and identification efficiencies were achieved using the transported targets.

For targets that were cut by a guillotine, double-sided adhesive tape was used to fix them on a MALDI- target plate holder. The cut targets were transported on the plate holder, which was fixated in its transport box in a similar way to the normal targets. The transport box was sealed with parafilm and put into an airtight plastic bag, away from light, without cooling.

9.8 Publications and Conferences

9.8.1 Publications

Nano-High-Performance Liquid Chromatography with Online Precleaning Coupled to Inductively Coupled Plasma Mass Spectrometry for the Analysis of Lanthanide-Labeled Peptides in Tryptic Protein Digests

Angela Holste †‡, Andreas Tholey ‡, Chien-Wen Hung ‡, and Dirk Schaumlöffel *†

† Université de Pau et des Pays de l'Adour/CNRS UMR 5254, Laboratoire de Chimie Analytique Bio-Inorganique et Environnement/IPREM, 64053 Pau, France
‡ Institute for Experimental Medicine−Div. Systematic Proteome Research, Christian-Albrechts-Universität, 24105 Kiel, Germany

Anal. Chem., 2013, 85 (6), pp 3064–3070
DOI: 10.1021/ac303618v
Publication Date (Web): February 1, 2013

Laser Ablation ICPMS on MALDI-MS Target Plates for the Quantitative Analysis of Peptides and Protein Digests (working title)

Angela Holste †‡, Julien Malherbe†, Christophe Pécheyran†, Andreas Tholey ‡, Chien-Wen Hung ‡, Thomas Jakoby‡, and Dirk Schaumlöffel *†

† Université de Pau et des Pays de l'Adour/CNRS UMR 5254, Laboratoire de Chimie Analytique Bio-Inorganique et Environnement/IPREM, 64053 Pau, France
‡ Institute for Experimental Medicine−Div. Systematic Proteome Research, Christian-Albrechts-Universität, 24105 Kiel, Germany

In preparation

9.8.2 Conferences

Spectr'Atom 2012

19-22 June, Pau France

Poster Presentation:
NanoLC-ICP-MS et MALDI-MS pour l'analyse de peptides marqués avec des lanthanides[1]

European Winter Conference on Plasma Spectrochemistry (EWCPS) 2013

10-15 February 2013, Krakow, Poland

Poster Presentation:

Analysis of lanthanide labelled protein digests via RP-IP-nanoHPLC coupled to ICP-MS and MALDI-MS

[1] Awarded with the 1st prize for the best poster, provided by Bruker Daltonique, France

Acknowledgements

Firstly I would like to express my deep gratitude to my two thesis directors Prof. Dr. Dirk Schaumlöffel and Prof. Dr. Andreas Tholey for entrusting me with the topic and giving me the opportunity to work in this international one-of-a-kind project. Their patient guidance and encouragement, as well as the useful critique were greatly appreciated.

I also want to express my very great appreciation to my referees and members of the jury, Prof. Dr. Lehmann, Prof. Dr. Lindhorst, Prof. Dr. Dreisewerd, Prof. Dr. Sönnichsen, Prof. Dr. Röder, Prof. Dr. Braulke, Prof. Dr. Sotiropoulos, Prof. Dr. Gutsmann and Prof. Dr. Leippe, especially for taking up the task in such short notice.

I wish to thank everyone from my German laboratory at the IEM in Kiel, especially Dr. Chien-Wen Hung, the southern hemisphere Post-Docs, Thomas Jakoby, Barbara Gregorius and Jana Schlenk for their helpful discussions and assistance.

At the LCABIE in Pau, I would like to thank the other PhD students for their greatly appreciated advice not only in the laboratory, but also regarding my stay in a foreign country. I would like to especially mention Ariane Donard, Guillaume Bucher, Magali Perez, Carolina Lyrio, Pamela Di Tullo and Dr. Juliusz Bianga for the constructive discussions. I also want to thank the permanent staff, in particular Eric Normandin for the technical assistance and Eddy Lasseur for cutting the MALDI targets. Additionally I would like to thank Dr. Christophe Pécheyran and Dr. Julien Malherbe for giving me the opportunity to work with Laser Ablation.

My grateful thanks are also extended to Prof. Dr. Olivier Donard for the financial support from ADERA.

Mes remerciements vont également à mon professeur de français M. Anthony Rouy pour m'aider à avancer avec mon français dans si peu de temps.

Besonderer Dank gilt meiner Familie, insbesondere Inge, Hans und Volker Conrath für all die Geduld und Unterstützung.

The thesis project was funded by the German BMBF (project 'Sweepro'), by the German DAAD (project 'Procope'), by the UPPA (project BQR) and ADERA.